

Treatment of benzene and ammonium contaminated  
groundwater using microbial electrochemical  
technology and constructed wetlands

**Dissertation for Obtaining the Doctoral Degree  
of Natural Sciences (Dr. rer. nat.)**

**Faculty of Natural Sciences  
University of Hohenheim**

Institute of Animal Science, Jun.-Prof. Dr. Jana Seifert,  
Institute of Plant Physiology and Biotechnology, Prof. Waltraud Schulze

Submitted by

Diplom-Microbiologin Manman Wei

Born in Shandong, China

Leipzig

2018

Dean: Prof. Dr. Heinz Breer

1st reviewer: Jun.-Prof. Dr. Jana Seifert

2nd reviewer: Prof. Waltraud Schulze

Submitted on: 25.10.2017

Oral examination on: 05.02.2018

This work was accepted by the Faculty of Natural Sciences at the University of Hohenheim on (27.12.2017) as “Dissertation for Obtaining the Doctoral Degree of Natural Sciences”.

## TABLE OF CONTENTS

<b>LIST OF FIGURES</b> .....	<b>V</b>
<b>LIST OF TABLES</b> .....	<b>VII</b>
<b>ABBREVIATIONS</b> .....	<b>VIII</b>
<b>SUMMARY</b> .....	<b>X</b>
<b>ZUSAMMENFASSUNG</b> .....	<b>XII</b>
<b>CHAPTER 1 Introduction</b> .....	<b>1</b>
1.1 Global groundwater contamination.....	1
1.1.1 Benzene and ammonium in contaminated groundwater .....	1
1.1.2 Contaminated field site-Leuna, Germany .....	3
1.2 Remediation technologies for contaminated groundwater.....	4
1.2.1 Constructed wetland.....	5
1.2.2 Microbial electrochemical technology .....	10
1.3 Microbial processes involved in benzene degradation and nitrogen transformation.....	11
1.3.1 Benzene degradation mechanisms .....	11
1.3.2 Microbial nitrogen transformation and removal .....	15
1.4 Methods for analyzing microbial process .....	20
1.4.1 Stable isotope fractionation analysis .....	20
1.4.2 Protein-based stable isotope probing (Protein-SIP) .....	22
1.5 Objectives and outlines of the thesis .....	23
1.5.1 Harvesting electricity from benzene and ammonium-contaminated groundwater using a microbial fuel cell with an aerated cathode.....	23
1.5.2 Enhancement and monitoring of pollutant removal in a constructed wetland by microbial electrochemical technology .....	24
1.5.3 Isotopic and proteomic evidence for microbial nitrogen transformation process in a microbial electrochemical technology-constructed wetland (MET-CW) treating contaminated groundwater .....	24
<b>CHAPTER 2 Harvesting electricity from benzene and ammonium-contaminated     groundwater using a microbial fuel cell with an aerated cathode</b> .....	<b>26</b>

2.1	Introduction .....	27
2.2	Materials and Methods .....	29
2.2.1	Reactor construction.....	29
2.2.2	Start-up and reactor operation.....	31
2.2.3	Chemical analysis.....	32
2.2.4	Electrochemical measurements and calculations .....	32
2.2.5	Compound-specific stable isotope analysis (CSIA).....	33
2.2.6	MiSeq Illumina sequencing.....	33
2.2.7	Statistical analysis .....	34
2.3	Results and discussion.....	34
2.3.1	Overall treatment performance during continuous operation .....	34
2.3.2	Mechanisms of benzene and ammonium removal .....	37
2.3.3	Effect of the flow rate on the performance of the MFC.....	39
2.3.4	Detection of electrochemical reaction in the MFC .....	42
2.3.5	Analysis of microbial communities in the MFC and Control .....	44
2.4	Supporting information .....	48
	<b>CHAPTER 3 Enhancement and monitoring of pollutant removal in a constructed wetland by microbial electrochemical technology .....</b>	<b>51</b>
3.1	Introduction .....	52
3.2	Materials and methods .....	53
3.2.1	Reactor construction and set-up.....	53
3.2.2	Setup and operation of the MET-CW system .....	54
3.2.3	Electrochemical measurements and calculations .....	55
3.2.4	Sampling procedure .....	56
3.2.5	Chemical analysis and calculations.....	56
3.2.6	Compound-specific stable isotope analysis .....	58
3.2.7	Statistical analysis .....	58
3.3	Results and discussion.....	58
3.3.1	Removal efficiencies of benzene and $\text{NH}_4^+\text{-N}$ .....	58
3.3.2	Electricity recovery in the MET-CW.....	64

3.3.3	Correlations between pollutant removal and electricity generation.....	68
3.3.4	Electron donors for the anode modules.....	68
3.3.5	Implications for the mechanism of benzene activation.....	70
3.4	Supporting information .....	72
<b>CHAPTER 4 Isotopic and proteomic evidence for microbial nitrogen transformation processes in the MET-CW .....</b>		<b>75</b>
4.1	Introduction .....	77
4.2	Materials and Methods .....	79
4.2.1	N isotopic analysis of $\text{NH}_4^+$ .....	79
4.2.2	<i>In situ</i> $^{15}\text{N}$ labelling experiment .....	80
4.2.3	Protein-SIP and metaproteomic analysis .....	80
4.2.4	Potential ammonia oxidation rates .....	82
4.2.5	Measuring anammox and denitrification rates using $^{15}\text{N}$ isotope tracing method. ....	82
4.2.6	Statistical analysis .....	83
4.3	Results and discussion.....	83
4.3.1	Microbial ammonia oxidation confirmed by N- $\text{NH}_4^+$ isotope fractionation ( $\delta^{15}\text{N-NH}_4^+$ ) .....	83
4.3.2	Identification of functional proteins and active species involved in microbial nitrogen transformation .....	86
4.3.3	Functional and phylogenetic distributions of identified proteins.....	89
4.3.4	Potential nitrification, anammox and denitrification rates .....	92
4.3.5	Implications for nitrogen transformation and removal .....	94
4.4	Supporting information .....	97
<b>CHAPTER 5 Conclusions and outlook.....</b>		<b>98</b>
5.1	Treatment of benzene and ammonium contaminated groundwater using a MFC ..	98
5.2	The integration of MET and CWs.....	100
5.3	Investigation of microbial nitrogen transformation processes .....	102
<b>REFERENCES.....</b>		<b>104</b>
<b>ACKNOWLEDGEMENTS .....</b>		<b>123</b>

**LIST OF PUBLICATIONS ..... 124**

## LIST OF FIGURES

Figure 1-1 A schematic view of the Leuna site.....	4
Figure 1-2 Main types of constructed wetlands.....	7
Figure 1-3 Initial benzene activation mechanisms under aerobic (A) and anoxic (B) conditions .....	14
Figure 1-4 Major microbial nitrogen transformation processes.....	15
Figure 2-1 Schematic (A) and picture (B) of the MFC and the control used in this study.....	30
Figure 2-2 Benzene and $\text{NH}_4^+$ -N removal in the MFC (A) and the Control (B) during continuous treatment of contaminated groundwater.....	35
Figure 2-3 Current generation in the MFC during continuous treatment of contaminated groundwater.....	36
Figure 2-4 Two-dimensional isotope plot of $\Delta\delta^{13}\text{C}$ versus $\Delta\delta^2\text{H}$ values of benzene measured at the anode of the MFC (red symbol) and pseudo-anode of the Control (black symbol) during continuous treatment.....	38
Figure 2-5 Effect of flow rate on benzene and ammonium removal (A), power generation (B), and electrode potentials (C) in the MFC.....	40
Figure 2-6 Effect of benzene and ammonium additions, and oxygen interruption on current generation in the MFC.....	42
Figure 2-7 Phylogenetic distribution of 16S rRNA genes based on the order of bacteria (A) and archaea (B) detected in the MFC and Control.....	45
Figure 3-1 Schematic diagram of the MET-CW used in this study.....	55
Figure 3-2 Removal efficiencies of benzene and $\text{NH}_4^+$ in the MET-CW and the control CW within 400 days.....	59
Figure 3-3 Pollutant removal efficiencies along the flow path in the MET-CW at the 95 <sup>th</sup> day and the control CW at the 97 <sup>th</sup> day.....	61
Figure 3-4 Electricity generation performance of the anode modules in the MET-CW.....	65
Figure 3-5 Linear relationship between benzene loading removal by the anode modules and current generation in the MET-CW.....	67

Figure 3-6 Two-dimensional isotope plot of $\Delta\delta^{13}\text{C}$ versus $\Delta\delta^2\text{H}$ values of benzene measured from pore water samples of the MET-CW at the 95 <sup>th</sup> day.....	70
Figure 4-1 Change of $\text{NH}_4^+$ -N loads (A) and $\delta^{15}\text{N-NH}_4^+$ values (B) at the deep layers along the flow path in the MET-CW.....	84
Figure 4-2 Mass spectra of the peptide VTHANYDVPGR (m/z 410.2071) from ammonia monooxygenase subunit B, which showed a high degree of $^{15}\text{N}$ incorporation.....	87
Figure 4-3 The numbers of $^{15}\text{N}$ -labelled peptides, relative isotope abundance (RIA), labelling ratio (lr) and their respective phylogenetic assignment obtained from <i>in situ</i> protein-SIP analysis.....	88
Figure 4-4 Phylogenetic distribution of microbial orders based on the numbers of all identified proteins by the metaproteomic analysis.....	90
Figure 4-5 Schematic illustrations of microbial nitrogen transformation processes and $^{15}\text{N}$ incorporated proteins identified in the MET-CW.....	94

## LIST OF TABLES

Table 1-1 Terminal electron acceptors and reaction stoichiometry used by bacteria for benzene degradation.....	12
Table 2-1 Physico-chemical properties of contaminated groundwater used in this study...	31
Table 3-1 Physico-chemical parameters along the flow path and the depth in the MET-CW and the control CW. Values are the average measured during the whole operation of 400 days.....	62
Table 3-2 Investigated pollutants, used loading rates, and gained electrochemical parameter in this and other constructed wetland systems combined with microbial electrochemical technology.....	67
Table 3-3 Comparison of possible half-cell reactions and thermodynamic cell potential (Eh) for benzene and $\text{NH}_4^+$ in this study.....	69
Table 4-1 Calculated rates of potential nitrification, anammox and denitrification ( $\text{nmol N}_2 \text{g}^{-1} \text{h}^{-1}$ ) at the deep layers along the flow path.....	92

## ABBREVIATIONS

AMO	Ammonia monooxygenase
Anammox	Anaerobic ammonia oxidation
AOA	Ammonia oxidizing archaea
AOB	Ammonia oxidizing bacteria
BOD	Biochemical oxygen demand
BTEX	Benzene, toluene, ethylbenzene and xylene
CANON	Completely autotrophic nitrogen removal over nitrite
CE	Coulombic efficiency
COD	Chemical oxygen demand
CSIA	Compound-specific stable isotope analysis
CW	Constructed wetland
DO	Dissolved oxygen
Eh	Redox potential
EU	European Union
FWF CWs	Free water surface constructed wetlands
HAO	Hydroxylamine oxidoreductase
HDH	Hydrazine dehydrogenase
HRT	Hydraulic retention time
HSSF CWs	Horizontal subsurface flow constructed wetlands
HZS	Hydrazine synthase
lr	Labelling ratio
MEC	Microbial electrolysis cell
MET	Microbial electrochemical technology
MFC	Microbial fuel cell
N <sub>2</sub> H <sub>4</sub>	Hydrazine
N <sub>2</sub> OR	Nitrous oxide reductase
NAC	Net anode compartment volume

NAR	Nitrate reductase
NH <sub>2</sub> OH	Hydroxylamine
NIR	Nitrite reductase
NO	Nitric oxide
NOB	Nitrite oxidizing bacteria
NOR	Nitric oxide reductase
NXR	Nitrite oxidoreductase
OCP	Open circuit potential
OLAND	Oxygen-limited autotrophic nitrification-denitrification
Protein-SIP	Protein-based stable isotope probing
RIA	Relative isotope abundance
SHARON	High-activity ammonium removal over nitrite
SND	Short-cut nitrification and denitrification
SSF CWs	Subsurface flow constructed wetlands
TCA cycle	Tricarboxylic acid cycle
TN	Total nitrogen
VSSF CWs	Vertical subsurface flow constructed wetlands
WHO	World Health Organization

## SUMMARY

With the rapid development of modern industry, energy shortage and environmental pollution are getting more and more serious. Groundwater pollution is one of the most important problems. A multitude of remediation techniques *in situ* or *ex situ* have been used to treat contaminated groundwater. This thesis was to investigate whether groundwater contaminated mainly by benzene and ammonium can be remediated by constructed wetlands in combination with microbial electrochemical technology. The objectives of this thesis are (i) to develop and test systems for removing pollutants and simultaneously recovering energy from contaminated groundwater, (ii) to maximize the benefits of both constructed wetland and microbial electrochemical technology while treating contaminated groundwater, (iii) to elucidate the underlying electrochemical reactions and pollutant degradation pathways, and (iv) to investigate microbial active species and functional proteins involved in benzene degradation and ammonium removal.

A microbial fuel cell (MFC) equipped with an aerated cathode and a control without aeration at the cathode were designed to remove benzene and ammonium from contaminated groundwater collected in the Leuna site (Saxony-Anhalt, Germany). The performance of pollutant removal and electricity generation was investigated and compared in the two reactors. Electrochemical processes occurring in the MFC were determined by benzene and ammonium spiking experiments as well as oxygen interruption experiments. Additionally, the biodegradation pathways and dominant organisms were elucidated by compound specific stable isotope analysis (CSIA) and Illumina sequencing. The results indicated the principal feasibility of treating benzene and ammonium contaminated groundwater by a MFC equipped with an aerated cathode. Benzene (~15 mg/L) was completely removed in the MFC, of which 80% disappeared already at the anoxic anode. Ammonium (~20 mg/L) was oxidized to nitrate at the cathode; this reaction was not directly linked to electricity generation. The maximum power density was 316 mW/m<sup>3</sup> net anoxic compartment (NAC) at a current density of 0.99 A/m<sup>3</sup> NAC. Coulombic and energy efficiencies of 14% and 4% were obtained based on the anodic benzene degradation. Benzene was initially activated by enzymatic monohydroxylation at the oxygen-limited anode; the further anaerobic oxidation of the intermediate metabolites released electrons accompanied by electrons transfer to the anode. Dominant phylotypes at the MFC anode revealed by 16S rRNA Illumina sequencing were affiliated to the *Chlorobiaceae*, *Rhodocyclaceae* and *Comamonadaceae*, presumably associated with benzene degradation. Nitrification took place at the aerated cathode of the MFC and was catalyzed by phylotypes

belonging to the *Nitrosomonadales* and *Nitrospirales*. The control reactor failed to generate electricity, although phylotypes affiliated to the *Chlorobiaceae*, *Rhodocyclaceae* and *Comamonadaceae* were dominant as well; the control reactor can be thus regarded as a mesocosm in which granular graphite was colonized by benzene degraders, but showed a lower benzene removal efficiency compared to the MFC.

In order to enhance benzene and ammonium removal while simultaneously harvesting energy, a constructed wetland integrated with microbial electrochemical technology (MET-CW) was established by embedding four anode modules into the sand bed and connecting it to a cathode placed in the open pond inside a bench-scale horizontal subsurface flow constructed wetland (HSSF-CW). Compared with the control CW, enhanced benzene and ammonium removal efficiencies were found in the MET-CW. The electrochemical performances of anode modules located at the four different depths were compared; the results showed that anode modules located in the deep layer (Module 3 and 4) had the relatively high power densities whereas the power densities located in the upper layer (modules 1 and 2) were extremely low. The initial activity mechanism of benzene degradation was analyzed by CSIA. Ammonium removal processes were assessed using nitrogen isotope fractionation of ammonium. Functional proteins and active microbial species involved in nitrogen transformation processes were detected using protein-based stable isotope probing (protein-SIP) with *in situ* feeding of  $^{15}\text{N-NH}_4^+$ . Additionally, potential denitrification and anammox rates were measured using Nitrogen isotope tracing. The results demonstrated that benzene and ammonium removal in a CW can be improved by combination with microbial electrochemical technology. The enhanced benzene removal was linked to the use of the anode modules as electron acceptor, whereas efficient ammonium removal was probably attributed to the elimination of inhibition effects by the co-contaminant benzene. Benzene was initially activated by monohydroxylation, forming intermediates which were subsequently oxidized accompanied by extracellular electron transfer, leading to current production. Partial nitrification accompanied by either heterotrophic denitrification or nitrifier-denitrification was mainly responsible for  $\text{NH}_4^+\text{-N}$  removal in the MET-CW, whereas anammox played a minor role. However, the contribution of anammox was markedly increased at the location near to the anode modules.

In summary, this research indicated that microbial electrochemical technology can be used to improve the performance of pollutant removal while simultaneously harvesting energy from contaminated groundwater. Especially, the combination of MET with other traditional treatment approaches (e.g. constructed wetland) is a promising alternative to treat contaminated water.

## ZUSAMMENFASSUNG

Die rasante Entwicklung der modernen Industrie ist begleitet von einer größer werdenden Problematik des Energiemangels und der Umweltverschmutzung. Verschmutztes Grundwasser ist eines der größten Probleme. Eine Vielzahl von *in situ* oder *ex situ*-Sanierungstechniken zur Reinigung von kontaminiertem Grundwasser sind bekannt. In dieser vorliegenden Arbeit wurde untersucht, wie hauptsächlich durch Benzol und Ammonium verunreinigtes Grundwasser in Pflanzenkläranlagen kombiniert mit mikrobieller elektrochemischer Technologie gereinigt werden kann. Die Ziele dieser Arbeit waren (i) ein System zu entwickeln und auszutesten, mit dem Benzol und Ammonium aus dem Grundwasser entfernt und gleichzeitig Energie gewonnen werden kann und, (ii) die Vorteile der Kombination Pflanzenkläranlage – mikrobieller elektrochemischer Technologie bei der Behandlung von kontaminiertem Grundwasser zu maximieren, (iii) die verantwortlichen elektrochemischen Reaktionen und Schadstoffabbauwege aufzuklären und (iv) die Benzol- und Ammonium-abbauenden mikrobiellen Gemeinschaften zu charakterisieren.

Eine mikrobielle Brennstoffzelle (MFC) mit einer belüfteten Kathode und einer Kontrolle ohne Belüftung an der Kathode wurde entwickelt, um Benzol und Ammonium aus verunreinigtem Grundwasser vom Standort Leuna (Sachsen-Anhalt, Deutschland) zu entfernen. Die Effizienz der Schadstoffentfernung und Stromerzeugung wurde für beide Reaktoren bestimmt und miteinander verglichen. Die elektrochemischen Prozesse in der mit Benzol betriebenen MFC wurden durch Zugaben von Ammonium sowie durch Unterbrechung der Sauerstoffzufuhr experimentell bestimmt. Darüber hinaus wurden die mikrobiellen Abbauwege und dominanten Organismen durch komponentenspezifische Analyse stabiler Isotope und Illumina-Sequenzierung aufgeklärt. Die Ergebnisse zeigen die grundsätzliche Durchführbarkeit der Behandlung von mit Benzol und Ammonium verunreinigtem Grundwasser durch eine mit einer belüfteten Kathode ausgestatteten MFC. Benzol (~15 mg/L) wurde in der MFC vollständig entfernt; 80% waren bereits in der anoxischen Anode verschwunden. Ammonium (~20 mg/L) wurde an der Kathode zu Nitrat oxidiert; dieser Prozess war nicht direkt mit der Stromerzeugung gekoppelt. Die maximale Leistungsdichte betrug 316 mW/m<sup>3</sup> NAC bei einer Stromdichte von 0,99 A/m<sup>3</sup>. Coulomb- und Energieeffizienzen von 14% und 4% wurden für den anodischen Benzolabbau bestimmt. Benzol wurde durch enzymatische Monohydroxylierung an der sauerstofflimitierten Anode aktiviert; die weitere Oxidation von Metaboliten verlief anaerob, wobei die freigesetzten Elektronen auf die Anode übertragen wurden. An der MFC-Anode dominierten Phylotypen, die den Familien *Chlorobiaceae*, *Rhodocyclaceae*

und *Comamonadaceae* angehören und die vermutlich am Abbau von Benzol beteiligt waren. An der belüfteten Kathode der MFC traten Phylotypen der *Nitrosomonadales* und *Nitrospirales* gehäuft auf, die vermutlich die dort ablaufende Nitrifikation durchführten. Der Kontrollreaktor erzeugte keine Elektrizität, war aber ebenfalls mit Phylotypen der *Chlorobiaceen*, *Rhodocyclaceen* und *Comamonadaceen* besiedelt. Der Kontrollreaktor kann daher als Mesokosmos angesehen werden, bei dem körniger Graphit durch Organismen besiedelt wurde, die Benzol in geringerer Rate abbauten als in der MFC

Darüber hinaus wurde im Labormaßstab eine Pflanzenkläranlage kombiniert mit mikrobieller elektrochemischer Technologie (MET-CW) durch Einbetten von vier Anodenmodulen in das Sandbett und Verbinden mit einer in der offenen Wasserschale platzierten Kathode (HSSF-CW); es sollte überprüft werden, ob es in dem System zu erhöhten Schadstoffabbauraten bei gleichzeitiger Produktion von elektrischer Energie kommt. Die Leistungen der Anodenmodule, die sich in vier verschiedenen Tiefen befanden, wurden verglichen. Der Benzolabbauweg wurde durch komponentenspezifische Analyse stabiler Isotopen analysiert. Der mikrobielle Abbau von Ammonium wurde mittels Stickstoffisotopenfraktionierung, einer Isotopenverfolgungstechnik sowie nach *in situ*-Zugabe von <sup>15</sup>N-markierten Ammoniums mittels proteinbasierten *stable isotope probing* (Protein-SIP) untersucht. Es konnte gezeigt werden, dass die Kombination von Pflanzenkläranlage und mikrobieller elektrochemischer Technologie den Abbau von Benzol und Ammonium stimuliert. Die Ergebnisse weisen darauf hin, dass die erhöhten Abbauleistungen für Benzol durch die Verwendung der Anodenmodule als Elektronenakzeptor ermöglicht wurde, während die effizientere Entfernung von Ammonium wahrscheinlich auf die Aufhebung von Inhibitionseffekten durch die Co-Kontaminante Benzol zurückzuführen war. Benzol wurde initial durch Monohydroxylierung aktiviert, wobei vermutlich Zwischenprodukte gebildet wurden; diese wurden über die Anodenmodule oxidiert, was zur Stromproduktion führte. Ammonium wurde hauptsächlich über partielle Nitrifikation, begleitet von heterotropher Denitrifikation oder Nitrifizierer-Denitrifikation, aus dem MET-CW entfernt. Anammox spielte eine untergeordnete Rolle, der Anammox-Prozess wurde aber in Nähe der Anodenmodule deutlich stimuliert.

Zusammenfassend konnte festgestellt werden, dass mittels mikrobieller elektrochemischer Technologie Grundwasserschadstoffe effizienter abgebaut werden können, bei gleichzeitiger Produktion von elektrischer Energie. Insbesondere die Kombination von MET mit traditionellen Technologien (z. B. Pflanzenkläranlagen) ist eine vielversprechende Alternative zur Behandlung von kontaminiertem Wasser.

## CHAPTER 1 Introduction

### 1.1 Global groundwater contamination

Groundwater is the largest reservoir of freshwater in the world, accounting for about 97% of all accessible freshwater on earth (Gleick 2014). Groundwater is usually the primary source not only for drinking water but also for agriculture and industry in most areas over the world. For example, about 75% of drinking water supply comes from groundwater in the European Union (EU). Therefore, groundwater plays an essential role in the survival of humans and the development of society. Nowadays, groundwater contamination is mainly caused by industry, agriculture and human activities and become more and more serious with the rapidly development of economy and society. Numerous potentially contaminated sites are found worldwide. For example, a total of 2.5 million potentially polluted sites are estimated in the EU, of which 340,000 are expected to likely require remediation. A variety of contaminants have been detected in groundwater, such as arsenic, nitrate, heavy metals and organic compounds (Burmester 2013). The most frequently observed contaminants in groundwater include heavy metals, mineral oil, nitrate and BTEX (benzene, toluene, ethylbenzene and xylene) (Panagos et al. 2013). Due to the multitude of polluted sites and various pollutants, remediating groundwater sustainably and efficiently is still challenging.

#### 1.1.1 Benzene and ammonium in contaminated groundwater

##### *Benzene contamination*

Benzene is a main aromatic hydrocarbon contaminant in groundwater and also often recalcitrant under anoxic conditions. Benzene is often derived from fossil fuels, particularly gasoline, and has been extensively used as solvent or chemical intermediate for the manufacture of plastics, resins, nylon, lubricants and pesticides. Benzene is also highly toxic and highly water-soluble ( $1.8 \text{ g L}^{-1}$  at  $25 \text{ }^\circ\text{C}$ ); it usually enters groundwater by the discharge of industrial wastewater, gasoline leakage of underground storage tanks or pipelines or accidental spills during transportation (Ghattas et al. 2017). According to SPBI

(2012), if benzene-concentration in groundwater is above  $50 \mu\text{g L}^{-1}$ , the risk of vapors in buildings will increase; the concentration of above  $500 \mu\text{g L}^{-1}$  will constitute a threat to surface water. The guideline value for benzene concentration in drinking water is set at  $1 \mu\text{g L}^{-1}$  in Germany (USEPA, 2005; DVGW, 2001). In 2012, global benzene production stood at approximately 42.9 million tons and the global benzene consumption exceeded 42.89 million tons, with increase by more than 1.29 million tons compared to the previous year (Merchant Research and Consulting Ltd.). In 2017, the global benzene production will follow an upward trend and is forecast to go beyond 50.95 million tons. The large amount of production and consumption resulted in serious environmental problems for water, air and soil. Nowadays, benzene contaminated groundwater has becoming a widespread problem and attracts much attentions due to its persistence and toxicity. The degradation of benzene in groundwater primarily depends on microbial activity. Benzene is readily degraded under aerobic conditions (Chiang et al. 1989). However, in the underground, oxygen is rapidly depleted by microbial respiration (Lovley 1997), leading to anoxic conditions, thus anaerobic biodegradation is more important for remediation of benzene contaminated groundwater. Benzene biodegradation under anaerobic conditions often is slow. When oxygen is not available, an alternative electron acceptor such as nitrate, carbonate or iron (II) as well as benzene-degrading microorganisms are needed (Vogt et al. 2011). Benzene degradation mechanisms are given in a detailed description in 1.3.1.

#### *Ammonium pollution*

Inorganic nitrogen in the forms of ammonia ( $\text{NH}_3$ ) or ammonium ( $\text{NH}_4^+$ ) is one of most common contaminant in groundwater, probably arising from waste disposal, fertilizer use and sewage leakage (Mulder 2003). In general, the natural concentration of  $\text{NH}_4^+$  is below  $0.2 \text{ mg L}^{-1}$  in surface water and  $0.3 \text{ mg L}^{-1}$  in groundwater. The high level of  $\text{NH}_4^+$  in water is usually caused by anthropogenic activities. For example, the extensive use of nitrogen fertilizers in regions of intensive agriculture and factory farming result in excessive nitrogen leaching into groundwater bodies. In 2016, the world nitrogen fertilizer consumption was approximately 115 million tons, with 15 million tons in Europe (Heffer and Prud'homme 2016). In Europe, up to 18% of N loss from fertilizers enters in water bodies (Mulder 2003), resulting in high levels of  $\text{NH}_4^+$  in aquatic ecosystems. While the

usual level of  $\text{NH}_4^+$  does not pose an immediate risk to human health, a high  $\text{NH}_4^+$  concentration suggests the presence of more serious residential or agricultural contaminants, such as pathogens or pesticides. In drinking water,  $\text{NH}_4^+$  can reduce disinfection efficiency, produce nitrite and nitrate, and result in taste and odour problems at the concentrations above 35 and 1.5  $\text{mg L}^{-1}$  respectively (World Health Organization 2003a). In surface water, ammonia is toxic to fish and often causes eutrophication at a low concentration (Environment agency 1998). The World Health Organization (WHO) and European Union standards set a recommended level of 0.05  $\text{mg L}^{-1}$  and a maximum level of 0.5  $\text{mg L}^{-1}$  of  $\text{NH}_4^+$  for drinking water quality (European Council 1998, World Health Organization 2003a). Another important form of N compounds is nitrate ( $\text{NO}_3^-$ ), which is converted to nitrite ( $\text{NO}_2^-$ ) under anaerobic conditions and thus causes methaemoglobinaemia particularly in infants. The WHO established the maximum limit with 10  $\text{mg L}^{-1}$   $\text{NO}_3^-$  and 1  $\text{mg L}^{-1}$   $\text{NO}_2^-$  in drinking water (World Health Organization 2003b).

### 1.1.2 Contaminated field site-Leuna, Germany

Large-scale groundwater contamination is a wide-spread problem especially at industrial sites throughout the developed world. Leuna located in Saxony-Anhalt, Germany, is one example, which is a center of chemical industry for about 100 years. Synthesis of ammonia in Leuna started in 1916 to produce nitrogen-based fertilizers and explosives. The site was rapidly expanded with plants producing methanol, synthetic petrol and mineral oil, becoming one of the biggest chemical industrial complexes in Germany in the last century. During world war II, more than 80% of the facilities were destroyed, resulting in massive local contamination of the saturated and unsaturated zone (Martienssen et al. 2006). Between 1949 and 1990, the Leuna site was gradually rebuilt and expanded for an oil refinery, producing a large amount of gasoline, diesel fuel, syngas and methanol. Nowadays, Leuna is still one of the largest and modern gas production centers in Europe. During the production period, a large amount of gasoline was introduced into the subsurface due to accidental spills and leakages from underground storage tanks, resulting in serious pollution of groundwater and soil nearby. The subsurface at the former refinery is contaminated with different gasoline components, particularly benzene and ammonia

released into the groundwater (Seeger et al. 2011). From 2007 to 2015, a pilot plant was operated by the Helmholtz Centre for Environmental Research within the project Compartment Transfer (CoTra), located at the site “Old Refinery Leuna”, supporting the development of near natural groundwater remediation techniques for large scale contaminated sites, which is called megasites (Figure 1-1). The groundwater used in this study was collected from the Leuna site with benzene ( $>10 \text{ mg L}^{-1}$ ) and ammonium ( $>20 \text{ mg L}^{-1}$ ) as main contaminants.

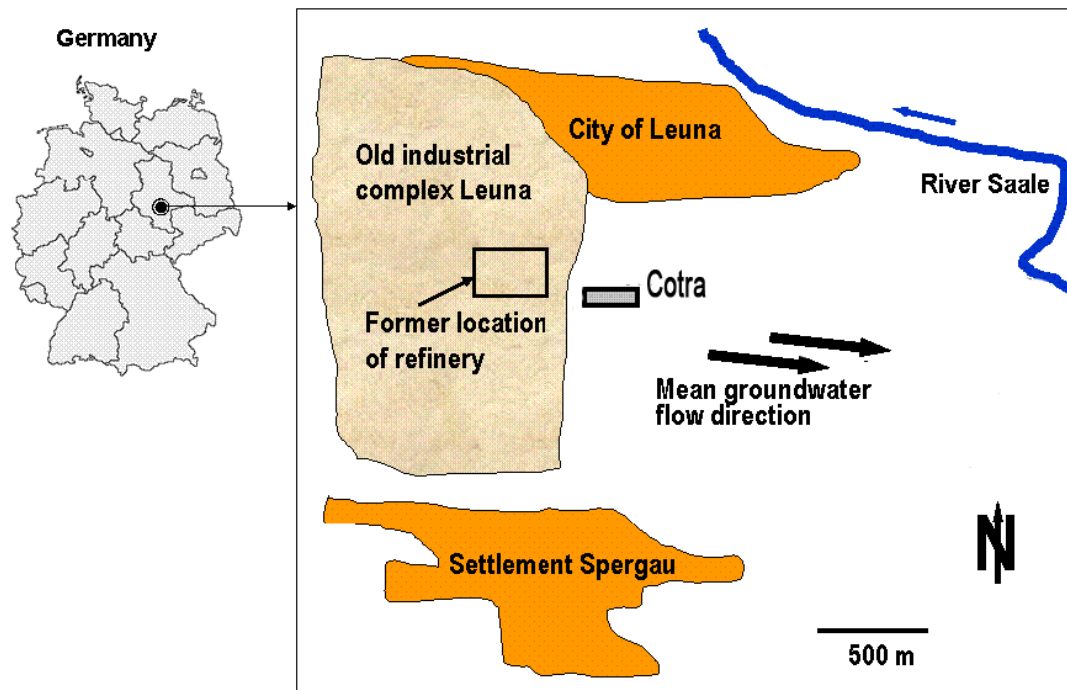


Figure 1-1 A schematic view of the Leuna site (Schirmer and Niemes 2010).

## 1.2 Remediation technologies for contaminated groundwater

Over the past few decades, different remediation technologies were developed and applied to treat contaminated groundwater, such as physical treatment technologies (air sparging, adsorption, filtration), chemical technologies (chemical oxidation/reduction, photo catalysis), and biological technologies (bioremediation, bioaugmentation, phytoremediation, wetlands) (Hashim et al. 2011). These methods are usually divided into *in situ* and *ex situ* remediation technologies, which can be applied alone or in combination (Hashim et al. 2011). Contaminants in groundwater are often multi-component and are dispersed underground in plumes with large areas, making conventional treatment

technologies difficult to apply. *In situ* technologies based on physical, chemical and biological principles were developed to treat contaminated groundwater, accounting for around 63% of the contaminated groundwater treatments due to their low cost and easy maintenance compared to ex-situ physical and/or chemical remediation techniques (Farhadian et al. 2008). Especially, *in situ* bioremediation appears to be an efficient, economical and environment-friendly approach, because it takes advantage of the natural potential of microorganisms or plants for detoxifying polluted waters. Therefore, much interest is focused on *in situ* bioremediation for contaminated groundwater. Constructed wetland is a passive *in situ* bioremediation approach, and is potentially applicable for eliminating a variety of pollutants, including petroleum hydrocarbons, chlorinated solvents, metals, and nitrogen (Saeed and Sun 2012). Microbial electrochemical technology (MET) is a rapidly developing technology platform at the nexus of microbiology and electrochemistry (Schröder et al. 2015), which was reported to be able to remove organic and nitrogen pollutants from various types of wastewater (Zhang and He 2012a). In this thesis, constructed wetlands and microbial electrochemical technology were applied to treat benzene and ammonium contaminated groundwater from the Leuna site.

### 1.2.1 Constructed wetland

Constructed wetlands (CWs) are known as a promising technology for wastewater treatment due to their low cost, easy operation and maintenance (Garcia et al. 2010, Imfeld et al. 2009). The CW systems have rapidly developed over the last three decades, and have been established worldwide as an ecological technology for wastewater treatment (Wu et al. 2014). CWs were initially used to treat traditional tertiary and secondary municipal wastewater, but during the last two decades, their usage has been expanded to treat various types of wastewater including domestic sewage, agricultural wastewater, industrial effluents, mine drainage, landfill leachate, storm water, polluted river water, and urban runoff (Saeed and Sun 2012, Vymazal 2014). A wide variety of pollutants have been successfully removed from these wastewaters, such as organic compounds, suspended solids, pathogens, metals, and nitrogen, phosphorus (Jiang et al. 2016, Saeed and Sun 2012). CWs have become an attractive alternative for wastewater treatment due to high removal efficiency, low cost and simple operation (Zhang et al. 2014).

The removal of contaminants in CWs is complex and a variety of removal mechanisms, including sedimentation, filtration, precipitation, adsorption, volatilization and plant uptake, are involved in (Imfeld et al. 2009, Wu et al. 2014). It has been recognized that the removal of most pollutants in CWs is primarily due to microbial activity (Faulwetter et al. 2009). In CWs, the biodegradation of chemicals often involves a complex series of biochemical reactions and usually varies with the microorganisms involved and the surrounding redox conditions (Faulwetter et al. 2009, Imfeld et al. 2009). The availability of oxygen is very important for the degradation of many contaminants as oxygen is often used for activation reactions by mono- and dioxygenases; the produced activated compounds are often degradable under oxic and anoxic conditions (Faulwetter et al. 2009). Nitrogen removal is attributed to microbial metabolism such as ammonification, nitrification-denitrification or anammox processes. In addition, microorganisms play a vital role in sulfur transformations, and the removal of phosphorous and heavy metal (Garcia et al. 2010). While plant uptake generally plays a minor role in pollutant removal, it has been reported that microbial density, activity, and diversity are enhanced in planted CWs compared to unplanted CWs (Faulwetter et al. 2009). Plants in CWs transfer oxygen to their root system and release a fraction of oxygen into the rhizosphere, promoting the formation of an oxidized layer around the root and creating a redox gradient (Faulwetter et al. 2009). Therefore, the rhizosphere exhibits a strong oxygen and redox gradient enabling the formation of many ecological niches that promote microbial processes and further enhance pollution removal (Garcia et al. 2010).

The performance of CWs are generally directly and/or indirectly influenced by the different loading rates, temperatures, soil types, operation strategies and redox conditions in the wetland bed (Saeed and Sun 2012). There are two basic types of constructed wetlands: free water surface (FWF) CWs, and subsurface flow (SSF) CWs. SSF CWs are further divided into vertical subsurface flow (VSSF) CWs and horizontal subsurface flow (HSSF) CWs according to the flow direction. In addition, hybrid systems have been developed by combining different types of constructed wetlands with each other to utilize their specific advantages, such as VF-HF CWs, HF-VF CWs, HF-FWS CWs and FWS-HF CWs (Vymazal 2013). The schematic diagrams of these CW systems are shown in Figure 1-2.

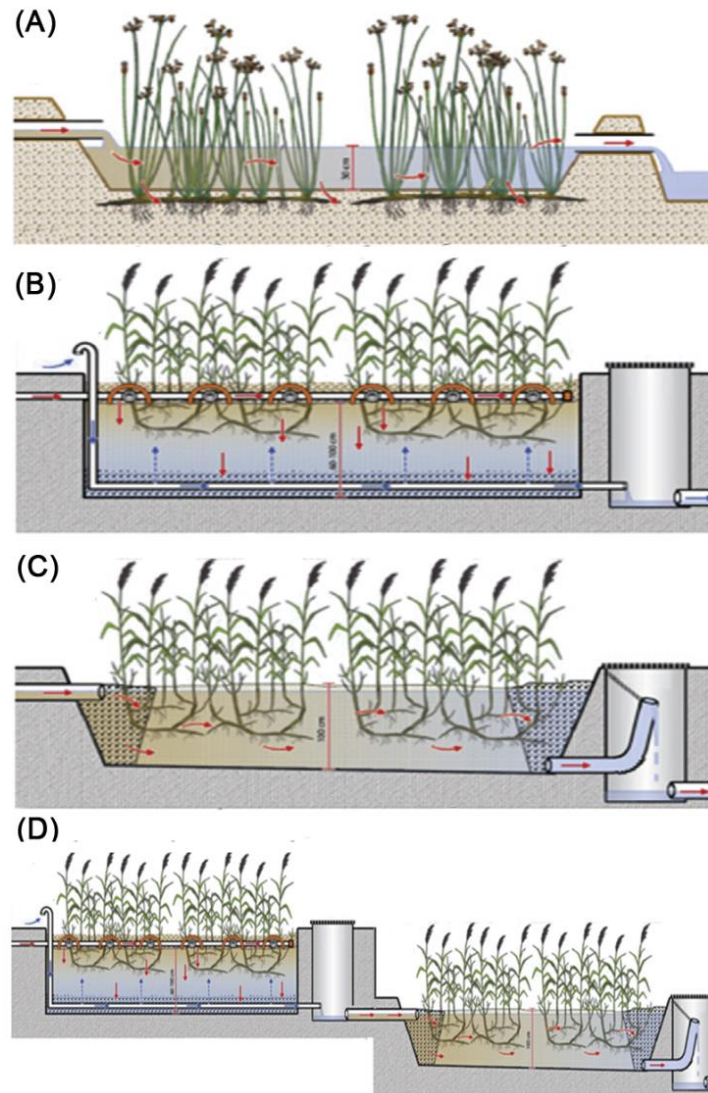


Figure 1-2 Main types of constructed wetlands modified from Wu et al. (2015b). A: FWF CW; B: VSSF CW; C: HSSF CW; D: hybrid VF-HF CW.

### *Free water surface CWs*

SWF CWs are similar to natural wetlands and have a thin aerobic layer at the surface attributed to passive aeration of water. SWF CWs mostly employ gravel or soil as the main media to support the growth of plants, with water at a relatively shallow depth (usually <60 cm), allowing wastewater flows vertically or horizontally through the media where it comes into contact with microorganisms especially in the rhizosphere, resulting in pollutant removal from wastewater (Faulwetter et al. 2009). The aerobic near-surface water

layer and the anaerobic deeper water layer are usually formed in the FWS CWs. The removal of organics and suspended solids are more efficient in FWS CWs, compared with nitrogen and phosphorus removal (Kadlec and Wallace, 2009). However, their treatment performance and sustainable application are usually restricted in the colder climate or after the plant decay (Vymazal 2014). The major removal mechanisms for organics are microbial degradation and that for suspended solids is through filtration and sedimentation (Kadlec and Wallace 2009). In FWS CWs, above 70% of biodegradable organic matter, particulate organic matter and pathogens can be removed (Vymazal 2014). Additionally, FWS CWs were found to be efficient in removing nitrogen with an efficiency of typically 40-50% depending on inflow concentration, water temperature, season, organic carbon availability, and dissolved oxygen (DO) concentration (Kadlec and Wallace 2009).

#### *Vertical subsurface flow CWs*

In the VSSF CW systems, the wastewater is fed through the whole surface area via a distribution system and passes through the media vertically, which generally have a bed depth of less than 0.6 m (Vymazal 2014). The feeding mode of the VSSF CW system allows wastewater drains vertically through the planted bed, leading to unsaturated flow conditions and excellent oxygen transfer, and thus VSSF CWs are generally considered as aerobic systems as the high DO and redox potential generally favor aerobic microbial processes. Thus, the removal of organic matter and nitrification were significantly higher in VSSF CWs compared to FWS and HSSF CWs, but denitrification was low (Faulwetter et al. 2009). In a review, Zhang et al. (2014) summarized the previous studies and found that VSSF CWs exhibits the better removal performance for biodegradable organic matter (89.29%) compared to HSSF CWs (75.1%). In addition, the higher oxygenation in VSSF beds can enhance nitrification and thus a higher  $\text{NH}_4^+$ -N removal efficiency was generally found in VSSF compared to HSSF CWs. But for total nitrogen (TN) removal, both of HSSF (51.97%) and VSSF (50.55%) CW systems were reported to be moderately efficient (Dan et al. 2011).

#### *Horizontal subsurface flow CWs*

In HSSF CWs, the wastewater flows slowly through the wetland bed under the surface in a more or less horizontal path; these systems are generally considered as

anoxic/anaerobic systems. However, the aerobic zones occur in the surface zone (5-20 cm) due to passive oxygen diffusion from the atmosphere or around roots and rhizomes due to plant oxygen release, which support aerobic microbial processes; thus, anoxic/anaerobic processes prevail in the wetland bed while aerobic processes are restricted to a small zone around the rhizosphere or to the thin surface layer where oxygen diffusion from the atmosphere may occur. The redox potentials in HSSF CWs usually decrease from the surface to deep layer, creating a redox gradient in the range of +700 mV to -300 mV (Meng et al. 2014). Organic compounds are decomposed in HSSF CWs by both aerobic and anaerobic microbial processes as well as by sedimentation and filtration of particulate organic matter (Vymazal 2014). Nitrogen can be removed in HSSF CWs primarily by nitrification and denitrification. In general, HSSF CWs can provide suitable anoxic or microoxic conditions for denitrification, but nitrification is typically limited due to the low DO concentration. It is generally reported that HSSF CWs show low removal efficiencies for  $\text{NH}_4^+$ -N and high removal efficiencies for  $\text{NO}_3^-$ -N (Saeed and Sun 2012).

#### *Hybrid constructed wetlands*

The hybrid CW systems were firstly introduced in the 1960s and were extensively developed since the late 1990s (Vymazal 2013). As most of wastewater are complex and may be difficult to be treated in a single-stage system, hybrid systems can combine various types of constructed wetlands to complement each other. Considering that the VSSF CW is intended to remove organics and suspended solids and to favor nitrification while HSSF CW favors denitrification and further removal of organics and suspend solids, the hybrid systems of VSSF and HSSF CWs were developed to enhance organic and nitrogen removal efficiencies (Vymazal 2013). The hybrid VF-HF CWs are the most frequently used systems and have been successfully demonstrated to be able to treat both of sewage and industrial wastewater (Dan et al. 2011). A system consisted of FWS CWs and multistage CWs have been recently developed as well and these hybrid CWs were reported to be more efficient in total nitrogen removal than single HF or VF CWs (Vymazal 2013). Besides hybrid systems consisting of different CWs types, the combination of constructed wetlands with other treatment processes such as membrane bioreactors, anaerobic processes, electrolysis, and biofilm reactors are also developed (Liu et al. 2015). The combinations of CWs with other

wastewater treatment processes can achieve a “win–win” performance and also offer a new alternative for widespread application of CWs (Liu et al. 2015).

### 1.2.2 Microbial electrochemical technology

Microbial electrochemical technology (MET) is a rapidly growing environmental technology, which combines the disciplines of microbiology, electrochemistry, materials science and engineering. MET can be applied for a range of environmental challenges, such as wastewater treatment, bioremediation, environmental monitoring, synthesis of valuable and novel chemicals, and clean energy generation (Logan and Rabaey 2012). In general, microbial electrochemical reactors are engineered systems that use microorganisms to convert the chemical energy stored in biodegradable organic or inorganic matter into electric current or chemicals (Zhang and Angelidaki 2016). Microbial electrochemical systems consist of two chambers, i.e. anode and cathode chambers, separated by a membrane. In the anode chamber, biodegradable substrates, such as organic matter in wastewater, are oxidized by microorganisms. Using the electrons released from biodegradable materials, many functions have been developed based on the MET platform (Wang and Ren 2013). In brief, the electrons can be captured directly for electricity generation (microbial fuel cells, MFCs), or be used to produce H<sub>2</sub> and other valuable chemicals (microbial electrolysis cells, MECs). The electrons can also be used in the cathode chamber to synthesize organic compounds (microbial electrosynthesis, MES) or remediate contaminants (microbial remediation cells, MRCs). The potential across the electrodes can also drive desalination (microbial desalination cells, MDCs).

MFCs are a typical microbial electrochemical system which can convert chemical energy of organic or inorganic compounds directly into electrical power. In general, MFCs consist of an anode, a cathode, a separator and an external circuit. In MFC, substrates are oxidized by electrochemically active bacteria, releasing electrons and protons. The electrons are transferred to the anode and through the external circuit to the cathode, thus generating a current. The protons simultaneously pass through a proton exchange membrane (PEM) into the cathode chamber where the reduction of the terminal electron acceptor takes place (Logan 2008). When used for wastewater treatment, organic matter or nutrients in wastewater can be used as anodic substrate, resulting in pollutant removal by

bacterial oxidation. MFCs are considered to be a very promising technology for wastewater treatment due to the combination of effective pollutants removal and electricity generation (Logan and Regan 2006). Recently, several MFCs have been developed for treating various types of wastewater, e.g., municipal wastewater (Feng et al. 2014) animal wastewater (Kim et al. 2008, Zhuang et al. 2012) and industrial wastewater (Cercado-Quezada et al. 2010, Ha et al. 2012).

The combination of MFC and CWs are recently developed in order to improve wastewater treatment capacity of wetlands while simultaneously producing electrical power (Doherty et al. 2015). Considering the fact that MFCs principally contain an anaerobic anode and a cathode exposed to oxygen while aerobic and anoxic zones can develop naturally in CWs, the combination of CWs with MFCs (CW-MFC) was first conducted by Yadav et al. (2012). In their study, a vertical flow CW was embedded with graphite plate electrodes and a glass wool separator to treat an azo dye synthetic wastewater, where a cathode electrode was placed in the upper near to the aerobic root zone and an anode was placed in the anoxic bottom of the CW (Yadav et al. 2012). In order to maximize the redox gradient, most CW-MFCs have been operated under upflow conditions with a buried anode and a cathode at the surface and/or in the plant rhizosphere (Doherty et al. 2015). The integration of MFC with HSSF CWs has been also reported for treating high strength wastewater (Villasenor et al. 2013). The integration of MFCs with CWs is a promising technique; however, there are still challenges to increasing the electrical output and overcoming the limited nitrification and denitrification in the CW-MFC system.

### **1.3 Microbial processes involved in benzene degradation and nitrogen transformation**

#### **1.3.1 Benzene degradation mechanisms**

Benzene is readily biodegradable under aerobic conditions (Chiang et al. 1989). However, once benzene reaches the groundwater, oxygen is usually depleted by microbial respiration. Consequently, anaerobic degradation is essential for benzene removal from such oxygen-depleted subsurface environments (Lovley 1997). Under both aerobic and anoxic conditions, a terminal electron acceptor is required to degrade benzene, which also

determines the energy balance and the metabolic reaction used by microorganisms (Ladino-Orjuela et al. 2016). When oxygen becomes unavailable, anaerobic benzene degradation occurs using other electron acceptors such as  $\text{NO}_3^-$ ,  $\text{Fe}^{3+}$ , and  $\text{SO}_4^{2-}$  (Table 1-1).

#### *Aerobic benzene degradation*

According to Gibbs free energy, bacteria will firstly use oxygen as the terminal electron acceptor to degrade benzene, followed by  $\text{NO}_3^-$ ,  $\text{Fe}^{3+}$ ,  $\text{SO}_4^{2-}$ , and finally methanogenesis or fermentation reactions (Vogt et al. 2011). Benzene is readily degraded under aerobic conditions by bacteria, such as *Pseudomonas* and *Rhodococcus* (Chiang et al. 1989). In a shaker flask experiment, aerobic degradation of benzene was performed using enrichment cultures from industrial wastewater treatment plant and the results showed that only 8% ( $4 \text{ mg L}^{-1}$ ) of initial dose of  $50 \text{ mg L}^{-1}$  benzene still remained after 6 h (Davis et al. 1981). Chiang et al. (1989) demonstrated that aerobic biodegradation was the major mechanism responsible for benzene removal in the groundwater at a field site. Davis et al. (1994) observed the rapid aerobic degradation of benzene in groundwater samples, with the time of 50% disappearance ranging from 4 to 14 days for different initial benzene concentration.

Table 1-1 Terminal electron acceptors and reaction stoichiometry used by bacteria for benzene degradation (modified from Vogt et al. (2011)).

Electron acceptors	Stoichiometric equation	$\Delta G^{0'}$
$\text{O}_2/\text{H}_2\text{O}$	$\text{C}_6\text{H}_6 + 7.5\text{O}_2 + 3\text{H}_2\text{O} \rightarrow 6\text{HCO}_3^- + 6\text{H}^+$	-3173 <sup>a</sup>
$\text{ClO}_3^-/\text{Cl}^-$	$\text{C}_6\text{H}_6 + 5\text{ClO}_3^- + 3\text{H}_2\text{O} \rightarrow 6\text{HCO}_3^- + 5\text{Cl}^- + 6\text{H}^+$	-3813 <sup>b</sup>
$\text{NO}_3^-/\text{NO}_2^-$	$\text{C}_6\text{H}_6 + 15\text{NO}_3^- + 3\text{H}_2\text{O} \rightarrow 6\text{HCO}_3^- + 15\text{NO}_2^- + 6\text{H}^+$	-2061 <sup>b</sup>
$\text{NO}_3^-/\text{N}_2$	$\text{C}_6\text{H}_6 + 6\text{NO}_3^- + 3\text{H}_2\text{O} \rightarrow 6\text{HCO}_3^- + 3\text{N}_2$	-2978 <sup>b</sup>
$\text{Fe}^{3+}/\text{Fe}^{2+}$	$\text{C}_6\text{H}_6 + 30\text{Fe}^{3+} + 18\text{H}_2\text{O} \rightarrow 6\text{HCO}_3^- + 30\text{Fe}^{2+} + 36\text{H}^+$	-3070 <sup>a</sup>
$\text{SO}_4^{2-}/\text{H}_2\text{S}$	$\text{C}_6\text{H}_6 + 3.75\text{SO}_4^{2-} + 3\text{H}_2\text{O} \rightarrow 6\text{HCO}_3^- + 1.875\text{H}_2\text{S}^{2-} + 1.875\text{HS}^- + 0.375\text{H}^+$	-185 <sup>c</sup>
$\text{CO}_2/\text{CH}_4$	$\text{C}_6\text{H}_6 + 6.75\text{H}_2\text{O} \rightarrow 2.25\text{HCO}_3^- + 3.75\text{CH}_4 + 2.25\text{H}^+$	-116 <sup>b</sup>

$\Delta G^{0'}$  is standard Gibbs free energy. Downward arrow indicates sequential order of terminal electron acceptors preferences according to decreasing redox potential. a: Burland and Edwards (1999), b: Weelink et al. (2007), c: Kleinstüber et al. (2008).

Benzene is structurally and chemically very stable due to the symmetric  $\pi$ -electron system of the aromatic ring and the lack of any potentially reactive substituents (Vogt et al. 2011). Therefore, the key for benzene degradation is an initial activation of the aromatic ring through reversible or irreversible chemical modifications (Diaz et al. 2013). Under aerobic conditions, benzene is initially activated by insertion of molecular oxygen to yield phenol or *cis*-benzene dihydrodiol, followed by further oxidization to catechol, which is catalyzed by monooxygenases or dioxygenases (Ladino-Orjuela et al. 2016). Catechol is then further transformed through ring cleavage, and then the metabolites are finally oxidized into CO<sub>2</sub> and H<sub>2</sub>O via the tricarboxylic acid cycle (TCA cycle) (Ladino-Orjuela et al. 2016). As shown in Figure 1-3, monooxygenases and dioxygenases are responsible for the initial step of aerobic benzene degradation. Monooxygenases attack aromatic rings by incorporating only a single oxygen atom, subsequently forming phenol and catechol in two enzymatic steps, while dioxygenases attack aromatic rings by incorporation of two oxygen atoms with the formation of *cis*-benzene dihydrodiol (Ladino-Orjuela et al. 2016). These two enzymes have been found e.g. in bacteria species of the genera *Pseudomonas*, *Rhodococcus* and *Burkholderia*, which were reported as benzene degraders in both enrichment cultures and contaminated field sites (Aburto-Medina and Ball 2015).

#### *Anaerobic benzene degradation*

Anaerobic benzene biodegradation has been most frequently observed in enrichment cultures as well as during remediation processes at anoxic field sites. The critical step of anaerobic benzene biodegradation is to destabilize the aromatic ring in the absence of molecular oxygen (Vogt et al. 2011). Nevertheless, in the past two decades it has shown that benzene can be anaerobically degraded under nitrate-reducing (van der Waals et al. 2017), sulfate-reducing (Abu Laban et al. 2009), iron-reducing (Abu Laban et al. 2010, Kunapuli et al. 2007), or methanogenic conditions (Weiner and Lovley 1998). Three mechanisms for the initial activation of anaerobic benzene degradation have been proposed: hydroxylation, carboxylation, or methylation, leading to the putative formation of phenol, benzoate, or toluene as the main first metabolites (Meckenstock et al. 2016, Vogt et al. 2011), followed by further transformation to benzoyl-coenzyme A (CoA) as central intermediate. Benzoyl-CoA can be further reduced by ATP-dependent or ATP-independent benzoyl-CoA reductases to CO<sub>2</sub> (Figure 1-3).

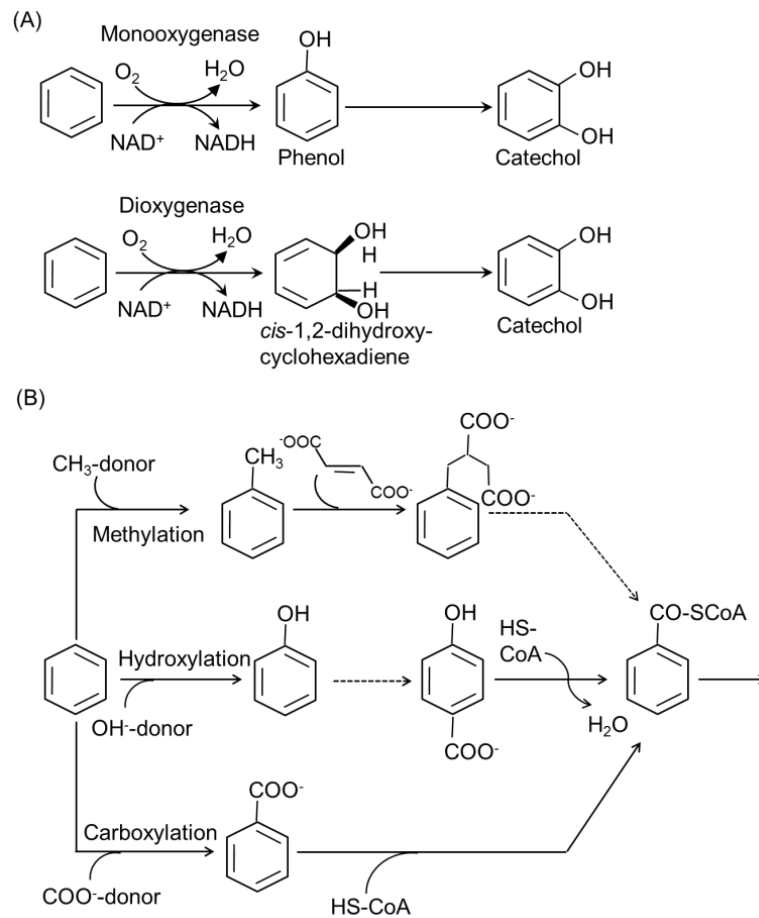


Figure 1-3 Initial benzene activation mechanisms under aerobic (A) and anoxic (B) conditions. Reactions under anoxic conditions are hypothesized.

A wide variety of bacteria were reported to participate in anaerobic benzene degradation. Members of *Peptococcaceae* within the class *Clostridia* have been identified as the dominant benzene degraders, which can switch from nitrate to sulfate or ferric iron as alternative electron acceptors (Aburto-Medina and Ball 2015, van der Zaan et al. 2012). Syntrophic associations are also found within the *Peptococcaceae*, suggesting that the same primary degraders are able to degrade benzene using different electron acceptors within the consortium (Gieg et al. 2014). *Rhodocyclaceae* and *Burkholderiaceae* were found to be associated with the anaerobic benzene degradation process. Members of the *Desulfobacteraceae* family have also been reported to be the dominant organisms in sulfate-reducing and methanogenic enrichments. In addition, other benzene-degrading microorganisms belonging to *Betaproteobacteria*, *Gammaproteobacteria* and

*Deltaproteobacteria* have been identified to be responsible for benzene degradation (Aburto-Medina and Ball 2015). Although the range of microorganisms capable of anaerobic benzene degradation has greatly expanded, the isolation of novel species and the understanding of their metagenomic and metaproteomic information remain critical in order to elucidate the degradation pathway of benzene in complex environments.

### 1.3.2 Microbial nitrogen transformation and removal

Nitrogen compounds are among the most important pollutants in aquifers, usually resulting in eutrophication and toxicity to aquatic species. Nitrogen compounds include a variety of organic and inorganic forms, of which the most important N compounds are  $\text{NH}_4^+$ ,  $\text{NO}_2^-$  and  $\text{NO}_3^-$  in polluted water. A variety of microbial transformation processes are known to remove nitrogen from contaminated water, including ammonification, nitrification, denitrification, nitrogen fixation, nitrogen assimilation and anaerobic ammonia oxidation (anammox) (Paredes et al. 2007). A general overview of microbial nitrogen transformation processes is presented in Figure 1-4.

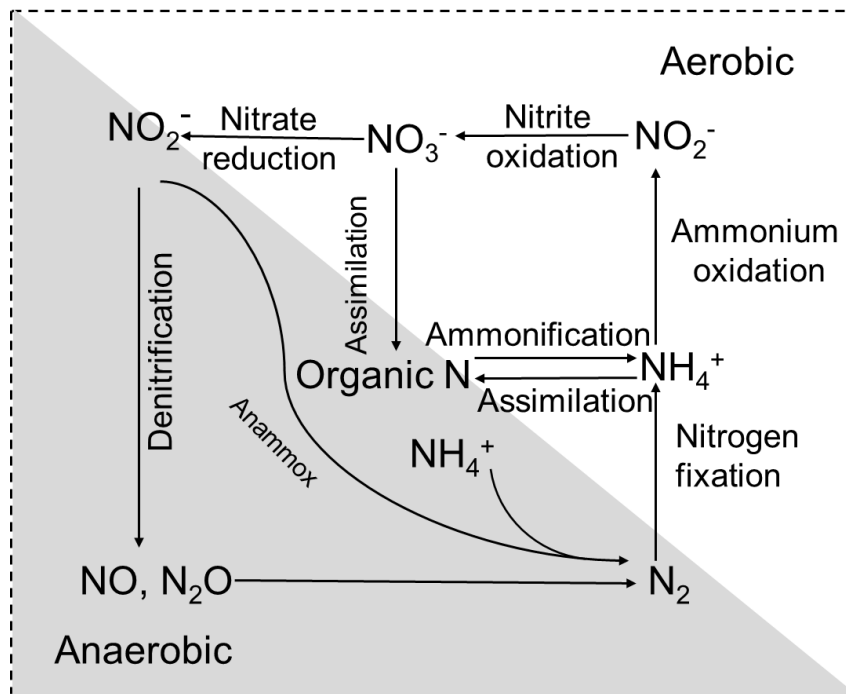


Figure 1-4 Major microbial nitrogen transformation processes.

Based on these nitrogen transformation processes, different nitrogen removal processes were developed. Conventional nitrification-denitrification was once thought to be

the main nitrogen removal process. However, this process usually requires an extra carbon source and large treatment areas, thus leading to high maintenance costs (Lee et al. 2009). Various novel biological nitrogen removal processes such as short-cut nitrification and denitrification (SND), high-activity ammonium removal over nitrite (SHARON), completely autotrophic nitrogen removal over nitrite (CANON) and oxygen-limited autotrophic nitrification-denitrification (OLAND), have been developed for wastewater treatment (Paredes et al. 2007). Recently, anammox was received considerable attention as an energy saving and cost-effective alternative, especially for nitrogen removal from wastewater at low oxygen levels and C/N ratios (Paredes et al. 2007).

### *Nitrification*

Nitrification is defined as biological oxidization of  $\text{NH}_4^+$  to  $\text{NO}_3^-$ , which is a two-step process, performed by different microorganisms. The first step is the oxidation of  $\text{NH}_4^+$  to  $\text{NO}_2^-$  (Eq. (1)) with hydroxylamine ( $\text{NH}_2\text{OH}$ ) as the intermediate product, which is the limiting step typically carried out by strictly chemolithotrophic ammonia oxidizing bacteria (AOB). Five genera of AOB, including clusters of *Nitrosomonas*, *Nitrosospira*, *Nitrosovibrio* and *Nitrosolobus* within the  $\beta$ -*Proteobacteria* and *Nitrosococcus* within the  $\gamma$ -*Proteobacteria* have been reported (Ge et al. 2015). *Nitrosomonas* and *Nitrosospira* were the most often detected. Two key enzymes, ammonia monooxygenase (AMO) and hydroxylamine oxidoreductase (HAO) are responsible for catalyzing ammonia oxidation to nitrite (Junier et al. 2010). Recently, ammonia oxidation organisms belonging to the archaeal domain have been discovered in terrestrial, marine, and geothermal habitats (Stahl and de la Torre 2012). The first isolated ammonia-oxidizing archaeon (AOA), *Nitrosopumilus maritimus* SMC1, is affiliated with group I *Crenarchaeota*, which contains putative genes for all three subunits (*amoA*, *amoB* and *amoC*) of ammonia monooxygenase. Members of this lineage are ubiquitously distributed in the open ocean and coastal water and have been demonstrated to represent 20% to 30% of marine microbes (Hatzenpichler 2012). Two thermophilic AOA species, “Ca. *Nitrososphaera gargensis*” (Hatzenpichler et al. 2008) and “Ca. *Nitrosocaldus yellowstonii*” (de la Torre et al. 2008), have been described. Besides these known AOA, sequence data suggest that more, as-yet-unidentified *amoA*-encoding and potentially ammonia-oxidizing groups might exist (Stahl and de la Torre 2012).

The second step of nitrification is the conversion of  $\text{NO}_2^-$  to  $\text{NO}_3^-$  by nitrite oxidizing bacteria (NOB) (Eq. (2)), which are facultative chemolithotrophic bacteria, including *Nitrococcus* within the  $\alpha$ -*Proteobacteria*, *Nitrobacter* within the  $\gamma$ -*Proteobacteria* and *Nitrospira* within the  $\delta$ -*Proteobacteria* (Ge et al. 2015). The key enzyme involved in nitrite oxidation is nitrite oxidoreductase (NXR) (Junier et al. 2010).



The overall nitrification reaction is given in Eq. (3):



Apart from autotrophic AOB and NOB, heterotrophic nitrifiers were also reported to be able to produce  $\text{NO}_3^+$ . A large number of bacteria and fungi, such as *Actinomyces*, *Arthrobacter*, *Bacillus*, *Thiosphaera* and *Pseudomonas*, can carry out heterotrophic nitrification using both  $\text{NH}_4^+$  and organic N compounds as substrates (Zhang et al. 2015). However, nitrification rates performed by *Nitrosomonas* and *Nitrobacter* groups are substantially higher, compared with other nitrifiers (Saeed and Sun 2012).

Recently, two *Nitrospira* species were reported to completely oxidize ammonium via nitrite to nitrate, which have phylogenetically distinct ammonia monooxygenases compared to the previous reported AMOs (van Kessel et al. 2015). This work demonstrated the existence of complete nitrification in a single organism, providing a competitive and energy-saving biogeochemical process for nitrogen cycle.

### *Denitrification*

Denitrification is a reductive pathway, by which  $\text{NO}_3^-$  is sequentially reduced to  $\text{NO}_2^-$ , NO and  $\text{N}_2\text{O}$ , and finally to  $\text{N}_2$  (Eqs. (4-7)):



The complete denitrification process can be expressed as a redox reaction (Eq. (8)):



This process is performed by diverse microorganisms, including bacteria, archaea and even fungi, which obtain energy through chemical reactions using organic compounds as electron donors and a source of cellular carbon and using nitrogen oxides as terminal electron acceptors (Vymazal 2007). Four enzymes are involved in a complete denitrification process, i.e. nitrate reductase (NAR), nitrite reductase (NIR), nitric oxide reductase (NOR) and nitrous oxide reductase (N<sub>2</sub>OR), reducing NO<sub>3</sub><sup>-</sup>, NO<sub>2</sub><sup>-</sup>, NO and N<sub>2</sub>O, respectively, and then releasing N<sub>2</sub> as the terminal product. However, not all denitrifiers possess these four types of enzymes and thus some of them are incapable of complete denitrification. For example, *Achromobacter* are NO<sub>2</sub><sup>-</sup> dependent and cannot reduce NO<sub>3</sub><sup>-</sup> due to the lack of NAR. Some genera, such as *Aerobacter* and *Flavobacterium* can only reduce NO<sub>3</sub><sup>-</sup> to NO<sub>2</sub><sup>-</sup> (Kumar and Lin 2010).

Denitrification was normally thought to be unable to take place in the presence of oxygen, since oxygen is thermodynamically more favorable as oxidizing agent compared to NO<sub>3</sub><sup>-</sup>. Thus, it is considered that the DO concentration should be maintained at <0.5 mg L<sup>-1</sup>, to accomplish nitrate reduction (Vymazal 2007). However, denitrifiers are primarily facultative anaerobic heterotrophs, which are capable of anaerobic respiration using NO<sub>3</sub><sup>-</sup>/NO<sub>2</sub><sup>-</sup> or aerobic respiration using O<sub>2</sub> as electron acceptors. Aerobic denitrification capable of the simultaneous use of both O<sub>2</sub> and NO<sub>3</sub><sup>-</sup> as oxidizing agents were reported in a broad range of microorganisms despite with lower productivity than that for aerobic respiration process (Ji et al. 2015). The reported aerobic denitrifiers mostly belong to *Actinobacteria*, *Bacillus* and *Pseudomonas*, of which ability to catalyze respiratory nitrate reduction under aerobic conditions has been shown to correlate with the activity of periplasmic nitrate reductase (Nap). In addition, some aerobic denitrifiers were reported to be capable of heterotrophic nitrification (He et al. 2016, Yao et al. 2013). *Nitrosomonas* was able to perform denitrification using H<sub>2</sub> as the electron donor and NO<sub>2</sub><sup>-</sup> as the electron acceptor, named as nitrifier denitrification; this process was detected during bioreactor operation upon coupling of aerobic and anaerobic ammonia oxidation (Su et al. 2017).

*Anammox*

Anammox is a newly discovered nitrogen removal process, where  $\text{NH}_4^+$  is directly oxidized to  $\text{N}_2$  with  $\text{NO}_2^-$  as the electron acceptor under anoxic conditions. Different intermediate products such as hydroxylamine and hydrazine ( $\text{N}_2\text{H}_4$ ) are formed during the anammox reaction. The overall reaction of the anammox process is provided in Eq. (9).



The anammox process is catalyzed by chemolithoautotrophic bacteria belonging to the phylum *Planctomycetes*. Currently, six anammox genera have been discovered, including *Brocadia*, *Kuenenia*, *Anammoxoglobus*, *Jettenia*, *Scalindua* and *Anammoximicrobium*. Although a large phylogenetic distance occurs between different anammox genera, the same anammox metabolism and cell structure are reported. The anammox bacteria have a membrane bound organelle, called anammoxosome, which is the locus of the anammox metabolism (Kartal et al. 2011). The anammox process includes the reduction of  $\text{NO}_2^-$  to nitric oxide (NO) by  $\text{cd}_1$  nitrite oxidoreductase (NirS), the reaction of  $\text{NH}_4^+$  and NO to hydrazine ( $\text{N}_2\text{H}_4$ ) by hydrazine synthase (HZS), and the oxidation of  $\text{N}_2\text{H}_4$  to  $\text{N}_2$  by hydrazine dehydrogenase (HDH) (Kartal et al. 2011).

Compared with conventional nitrification and denitrification processes, the anammox process has the obvious advantages, such as no requirement of external carbon sources, a lower oxygen demand and lower energy consumption.  $^{15}\text{N}$  tracing studies have shown that one N atom of  $\text{N}_2$  originate from  $\text{NO}_2^-$  and one from  $\text{NH}_4^+$ . A molar ratio of  $\text{NH}_4^+/\text{NO}_2^-$  of around 1:1.3 is used during wastewater treatment by anammox process (Jetten et al. 2001). The growth rate of anammox bacteria is extremely low, with doubling times varying from 7 to 22 days, which usually results in a slow start-up of the anammox reactor. Different levels of anammox inhibition by  $\text{NO}_2^-$  were reported, with 50 % inhibitory values ranging from 100 to 400 mg N  $\text{L}^{-1}$  (Lotti et al. 2012). Additionally, the anammox process is optimized at a pH range of 6.7 - 8.3 and a temperature range of 30 - 37 °C (Saeed and Sun 2012). Nevertheless, technologies based on anammox metabolism may provide a more sustainable alternative to wastewater treatment, due to the reduced requirement of aeration and external organic carbon.

## **1.4 Methods for analyzing microbial process**

Microbial transformation processes have been investigated using a variety of techniques, including physicochemical measurements, traditional microorganism cultivation techniques, molecular techniques and isotope tracing techniques.

Many molecular techniques have been used to analyze microbial processes and microbial communities, such as fluorescent in situ hybridization (FISH), polymerase chain reaction denaturing gradient gel electrophoresis (PCR-DGGE), real-time PCR (qPCR), and transmission electron microscopy (TEM). Compared to cultivation based methods, the culture-independent molecular approaches, are more sensitive and accurate, hence have been widely applied to characterize microbial communities and understand microbial community function, further supporting to analyze potential microbial processes (Faulwetter et al. 2009). In particular, molecular technologies based on functional genes, especially metagenomics, are used to understand possible functions of microbial communities and trace microbial transformation processes (Streit and Schmitz 2004). These techniques are generally believed to overcome the difficulties of selective cultivating and isolating bacteria from natural samples in traditional cultural methods. However, one of the drawbacks of these techniques is that they can only provide information on the functional potential rather than actually metabolic activities for microbial communities. In order to link specific microbes to specific ecological functions, labeling techniques with stable isotope probing (SIP) have been developed, including DNA-, RNA-, phospholipid fatty acids- and protein- SIP (Vogt et al. 2016). Especially, protein-SIP is a powerful method with a higher sensitivity in comparison with DNA- or RNA-SIP, which can not only provide taxonomic information similar to DNA or RNA analysis but also reflect the metabolic properties and actual activities of cells (von Bergen et al. 2013).

### **1.4.1 Stable isotope fractionation analysis**

Isotopes are atoms of the same element with different numbers of neutrons and therefore have different masses. Significant fractionation occurs naturally for elements of H, C, N, O, S, Cl (Meija et al. 2016). Isotope fractionation usually occurs during enzymatic catalyzed transformations in which chemical bonds are broken or formed due to different rate constants for molecules with variable isotope substitutions. Usually, molecules

containing the lighter isotope react faster than that containing the heavier isotope, resulting in that heavy isotopes are enriched in the residual substrate pool and the product becomes isotopically lighter (Meckenstock et al. 2004). In addition, isotope ratio variations can also occur during physical processes, such as sorption, evaporation and diffusion, but typically with a smaller extent compared to biotransformation. Therefore, by measuring changes in isotope ratios, stable isotope fractionation analysis can be used to assess biodegradation of contaminants in the environment.

Based on isotope fractionation concepts, compound-specific isotope analysis (CSIA) has been developed to characterize biodegradation pathways, identify contaminant sources and quantify the extent of biodegradation (Meckenstock et al. 2004). Currently, CSIA has been applied to assess biodegradation of most organic contaminants such as BTEX, chlorinated hydrocarbons and fuel oxygenates (Braeckevelt et al. 2012). Recent studies demonstrated that the initial activation mechanisms of benzene degradation were successfully elucidated using two-dimensional CSIA in benzene-contaminated field sites, model wetland systems and a MFC reactor (Fischer et al. 2009, Fischer et al. 2007, Rakoczy et al. 2011, Wei et al. 2015a). By using the Rayleigh equation, isotope enrichment factors ( $\epsilon$ ) can be calculated by quantifying the relationship between change of isotope signatures and concentrations, which can be compared with the previous reported references and thus allows to quantify degradation processes since isotope fractionation factors remarkably differ among different degradation pathway and even among different microorganisms using the same degradation pathway (Braeckevelt et al. 2012). Stable isotope fractionation analysis can also help to identify biochemical degradation pathways using the slope ( $\Lambda$ ) derived from a dual isotope plot of  $\delta^2\text{H}$  versus  $\delta^{13}\text{C}$  (Bergmann et al. 2011). Fischer and colleagues compared the specific  $\Lambda$  values among benzene-degrading enrichment and pure cultures using mono- or dioxygenase or anaerobic enzymatic pathways and found that  $\Lambda$  values could differentiate between aerobic (typically  $\Lambda < 10$ ) and anaerobic benzene degradation (typically  $\Lambda > 10$ ) (Fischer et al. 2008a).

The isotopic signature of N species can reflect their origin and allows to study nitrogen transformation processes (Casciotti et al. 2011). Microbial nitrogen transformations discriminate against the heavy N isotope, leaving the substrate enriched in  $^{15}\text{N}$  and the product depleted in  $^{15}\text{N}$ . N and O isotope fractionation of  $\text{NH}_4^+$  and  $\text{NO}_3^-$  has

been successfully used to characterize N sources and to identify nitrogen transformation processes such as nitrification or denitrification in aquifers (Clark et al. 2008, Ohte et al. 2007), lakes (Bartrons et al. 2009), marine environments (Robinson et al. 2012) and wetlands (Erler and Eyre 2010). Apparent isotope fractionation has been reported for microbial nitrogen transformation processes such as nitrification, denitrification and anammox (Brunner et al. 2013). For instance, the N isotope effects for bacterial nitrification was reported in the range of 14.2 - 38.2‰ and showed differences among the different nitrifying strains (Casciotti et al. 2003). The combination of  $\delta^{15}\text{N}$  and  $\delta^{18}\text{O}$  in  $\text{NO}_3^-$  was proved to be able to distinguish different nitrate origins and identify denitrification processes in the soil and water systems (Nisi et al. 2014). However, the quantitative assessment of denitrification based on simple measurements of the isotopic  $\text{NO}_3^-$  composition has mostly failed in wetlands, because additional fractionation processes were neglected or could not be assessed (Coban et al. 2015b).

#### **1.4.2 Protein-based stable isotope probing (Protein-SIP)**

Elucidating the metabolic activities of specific species within complex microbial communities is a difficult task. Protein-based stable isotope probing (protein-SIP) is a novel and powerful method which can link phylogenetic information and metabolic functions; the method is based on the metabolization of isotopically labelled substrates and subsequent analysis of the incorporation of heavy isotopes into proteins (Seifert et al. 2012). In brief, substrates labeled with heavy isotopes, such as  $^{13}\text{C}$ ,  $^{15}\text{N}$  or  $^{36}\text{S}$ , are assimilated by the metabolism, leading to the incorporation into biomolecules including proteins, which can be detected by mass spectrometry of peptides. From a peptide mass spectrum, the percentage of atoms replaced by heavy isotopes, referred to as relative isotope abundance (RIA), can be calculated, providing information about the incorporation of labelled substrate into biomass. Another important parameter, the labelling ratio (lr), describes the ratio of labelled to unlabeled peptides and allows the quantitation of the protein synthesis rate (von Bergen et al. 2013). The lr, together with the RIA, reflects the protein expression and substrate utilization pattern.

Recent studies have demonstrated the successful application of protein-SIP to detect metabolic activities in defined communities as well as in enrichment cultures

(Bastida et al. 2010, Jehmlich et al. 2008a, Jehmlich et al. 2008b). Protein-SIP was reported to trace benzene assimilation and detect the carbon flux in a sulfate-reducing, benzene-degrading microbial consortium (Taubert et al. 2012). Additionally, degradation pathways and metabolic key players were elucidated by *in situ* protein-SIP in a polycyclic aromatic hydrocarbon (PAH) contaminated aquifer (Herbst et al. 2013). More recently, the toluene degradation pathway and key degraders were identified by *in situ* protein-SIP in a constructed wetland (Lunsmann et al. 2016). These studies demonstrated that protein-SIP is applicable for detecting the key processes and identifying active species involved in the degradation of organic pollutants in complex ecosystems. However, protein-SIP studies of microbial communities need to be accompanied by metagenome sequencing for a reliable identification of proteins; if proteins with the incorporation of heavy isotope can be identified, the method allows to identify primary and secondary degraders and their respective metabolic pathways (von Bergen et al. 2013).

## 1.5 Objectives and outlines of the thesis

The objective of this work was to investigate the treatment performance and pollutant removal mechanisms while treating benzene and ammonium contaminated groundwater using microbial electrochemical technology and constructed wetlands. Therefore, a MFC with an aerated cathode was constructed to continuously treat benzene and ammonium contaminated groundwater from the Leuna site. Moreover, to improve benzene and ammonium removal, the integration of MET and a HSSF-CW was established to maximize the benefits of both constructed wetland and microbial electrochemical technology.

This thesis is written based on the following three scientific articles.

### 1.5.1 Harvesting electricity from benzene and ammonium-contaminated groundwater using a microbial fuel cell with an aerated cathode

Wei, M., Harnisch, F., Vogt, C., Ahlheim, J., Neue, T. R., Richnow, H. H. (2015)  
*RSC Advances*. 5(7): 5321-5330.

DOI: 10.1039/C4RA12144A

This work describes whether a MFC can be used to remediate real groundwater contaminated with benzene and ammonium and simultaneously recover energy. For that

purpose, a MFC with an aerated cathode and a control without aeration were compared for the removal performance of benzene and ammonium as well as electricity generation. Additionally, the effect of hydraulic retention time (HRT) on the performance of the MFC was investigated. To understand the electrochemical processes occurring in the MFC, benzene and ammonium spiking as well as oxygen interruption experiments were performed in the batch mode. Additionally, pollutant degradation pathways and key players in the MFC were investigated.

The work was completely finished by Manman Wei. Her own work includes experiments, data analysis, preparations of figures and tables, and manuscript writing.

### **1.5.2 Enhancement and monitoring of pollutant removal in a constructed wetland by microbial electrochemical technology**

Wei, M., Rakoczy, J., Vogt, C., Harnisch, F., Schumanna, R., Richnow, H. H. (2015) *Bioresource Technology* 196: 490-499.

DOI: 10.1016/j.biortech.2015.07.111

This work describes an integrated MET-CW which was established by embedding four anode modules into the sand bed and connecting it to a cathode placed in the open pond inside a bench-scale HSSF-CW. The objective was to evaluate whether MET can be used to (i) improve the biodegradation of the main contaminants and (ii) to monitor such degradation processes in the HSSF-CW. Furthermore, the performances of anode modules located at the different depths were compared in order to determine favorable depths for anodic reactions.

The work was completely finished by Manman Wei. Her own work includes experiments, data analysis, preparations of figures and tables, and manuscript writing.

### **1.5.3 Isotopic and proteomic evidence for microbial nitrogen transformation process in a microbial electrochemical technology-constructed wetland (MET-CW) treating contaminated groundwater**

Manman Wei, Carsten Vogt, Vanessa Lünsmann, Naomi Susan Wells, Jana Seifert, Nico Jehmlich, Kay Knödler, Hans H. Richnow. The manuscript is in preparation for publication in scientific journal.

This work describes the investigation of microbial nitrogen transformation processes in order to understand their importance for nitrogen removal in the MET-CW. In this study, the nitrogen transformation processes in the MET-CW were qualitatively and quantitatively analyzed by N stable isotope fractionation,  $^{15}\text{N}$  isotope tracing techniques and *in situ* protein-SIP. In addition, the effect of anode insertion on nitrogen transformation processes in the HSSF-CW was discussed.

The work was mainly finished by Manman Wei. Her own work includes experiments, preparations of figures and tables, and manuscript writing. The data for Protein-SIP and metaproteomics were analyzed by Vanessa L ünsmann.

## CHAPTER 2    **Harvesting electricity from benzene and ammonium-contaminated groundwater using a microbial fuel cell with an aerated cathode**

Wei, M., Harnisch, F., Vogt, C., Neue, T. R., & Richnow, H. H. (2015). Harvesting electricity from benzene and ammonium-contaminated groundwater using a microbial fuel cell with an aerated cathode. *RSC Advances*, 5(7): 5321-5330.

### **Abstract**

Groundwater contaminated with benzene and ammonium was continuously treated using a microbial fuel cell with aerated cathode and a control without cathode aeration. Benzene (~15 mg/L) was completely removed in the MFC; of which 80% disappeared already at the anoxic anode. Ammonium (~20 mg/L) was oxidized to nitrate at the cathode, which is not directly linked to electricity generation. The maximum power density was 316 mW/m<sup>3</sup> NAC at a current density of 0.99 A/m<sup>3</sup> normalized by the net anodic compartment (NAC). Coulombic and energy efficiencies of 14% and 4% were obtained for the anodic benzene degradation. The control reactor failed to generate electricity, and can be regarded as a mesocosm in which granular graphite was colonized by benzene degraders with a lower benzene removal efficiency 20% compared to the MFC. The dominance of phylotypes affiliated to the *Chlorobiaceae*, *Rhodocyclaceae* and *Comamonadaceae* was revealed by 16S rRNA Illumina sequencing in the control and the MFC anode, presumably associated with benzene degradation. Ammonium oxidation at the cathode of the MFC was mainly carried out by phylotypes belonging to the *Nitrosomonadales* and *Nitrospirales*. Compound specific isotope analysis (CSIA) indicated that benzene degradation was initially activated possibly by monohydroxylation with O<sub>2</sub>. The intermediates of benzene degradation pathway were then oxidized accompanied by transferring electrons to the anode, leading to current production. This study provided valuable insights into degradation mechanisms and microbial communities involved in the treatment of the anoxic wastewater contaminated with petroleum hydrocarbons (e.g. benzene) and ammonium using MFCs.

**Key words** benzene degradation; ammonium oxidation; microbial fuel cell; electricity recovery; compound-specific stable isotope analysis

## 2.1 Introduction

Remediation by microbial fuel cells (MFCs) is a very promising technology for wastewater treatment due to the combination of effective pollutants removal and electricity generation (Logan and Regan 2006). Recently, the practical application of MFCs has been widely developed to treat various wastewater including e.g., municipal wastewater (Feng et al. 2014), animal wastewater (Kim et al. 2008, Zhuang et al. 2012) and industrial wastewater (Cercado-Quezada et al. 2010, Ha et al. 2012). In a few cases, the effective removal of recalcitrant contaminants from wastewater, like petroleum constituents, coupled to electricity generation have been also achieved using MFC technology (Morris and Jin 2012, Wang et al. 2012). Many industrial activities such as oil refining and chemical industry produce wastewater containing ammonium, sulfide and petroleum hydrocarbons (e.g. BTEX, benzene, toluene, ethylbenzene, and xylene) (Olmos et al. 2004, van Afferden et al. 2011). For example, the Leuna site (Saxony-Anhalt, Germany) has been a center of chemical industry for about 100 years, leading to groundwater contaminated mainly by benzene and ammonium (Voyevoda et al. 2012). These pollutants have been reported to cause severe environmental and public health damage (Gibson 1968). A variety of remediation technologies, such as constructed wetlands (Seeger et al. 2011, Seeger et al. 2013), soil filter systems (Afferden et al. 2011) and aerated treatment pond technology with biofilm promoting mats (Jechalke et al. 2010) has been used to treat groundwater contaminated with benzene and ammonium from the Leuna site. However, oxygen was considered to be one of the limiting factors for efficient ammonium removal in these remediation systems (Jechalke et al. 2011, Seeger et al. 2011, Seeger et al. 2013). Heterotrophic bacteria were reported to potentially compete for oxygen and inorganic nitrogen with nitrifiers, possibly resulting in the low nitrification rate under oxygen-limited conditions (Ma et al. 2013a, Truu et al. 2005). Besides, the presence of BTEX and their metabolic intermediates (e.g. phenol) was described to inhibit nitrification process (Ben-Youssef et al. 2009, Lauchnor et al. 2011, Radniecki et al. 2008). The inhibitory effect of benzene on nitrification and probable competition between benzene degraders and nitrifiers

is an obstacle to simultaneously remove benzene and ammonium using the conventional treatment technologies.

It is already reported that the MFC technology has a practical potential for removing benzene at the anode during wastewater treatment. Zhang et al. (2010) observed benzene degradation in contaminated sediments by providing a graphite electrode as an electron acceptor, demonstrating the potential of electrode-based systems for degradation of aromatic hydrocarbons in anoxic environments. Luo et al. (2010) operated a packing-type MFC and found that 600 mg/L benzene was completely degraded within 24 h with simultaneous power generation when 1000 mg/L glucose was provided as the co-substrate. Simultaneous benzene biodegradation and electricity production with potassium ferricyanide as electron acceptor in a MFC was also reported by Wu et al. (2013). Due to the fast reaction kinetics, the aromatic ring of benzene was likely activated and cleaved by mono- and/or dioxygenases (Gibson 1968, Vaillancourt et al. 2006) in the studies of Luo et al. (2010) and Wu et al. (2013), indicating aerobic or microaerobic conditions; it has been reported previously that benzene can be effectively degraded under oxygen-limited conditions (Fahy et al. 2006, Yerushalmi et al. 2002). Nevertheless, the data indicate that benzene can be biodegraded under anoxic or oxygen-limited conditions in a MFC system, although the mentioned studies were performed under simulated and simplified conditions in the laboratory.

Ammonium removal at the cathode has been reported in the MFCs. He et al. (2009) reported that ammonium can be removed mainly by partial nitrification with nitrite production in a rotating-cathode MFC, although the process showed only a low coulombic efficiency ( $CE=0.34\%$ ). Subsequently, ammonium removal by simultaneous nitrification and denitrification was achieved in MFCs coupled with a nitrifying bioreactor (Viridis et al. 2008) or by introducing additional oxygen into the cathode (Viridis et al. 2010, Yan et al. 2012, Yu et al. 2011, Zhang and He 2012b). Notably, a denitrifying liter-scale MFCs has been successfully used to enhance the total nitrogen removal in a municipal wastewater treatment facility (Zhang et al. 2013a).

Therefore, MFCs are a good choice to sequentially remove benzene and ammonium due to the presence of separated anode and cathode compartments. Considering the complexity of real wastewater, the feasibility of MFCs for real wastewater treatment is

usually limited by high internal resistance, pH buffering, inhibition effect between co-contaminants and low efficiency of mixed culture biofilm on an electrode (Rozendal et al. 2008). The practical application of a MFC for benzene and ammonium-contaminated wastewater treatment is more complex and has not yet been studied so far. It is worthwhile to investigate the practical performance and bio-electrochemical processes using the MFC to treat real groundwater contaminated with benzene and ammonium, especially during a long-term operation.

The objective of this study was to investigate whether a MFC can be used to remediate real groundwater contaminated with benzene and ammonium and while simultaneously recovering energy. For that purpose, a MFC with an aerated cathode and a control without aeration were compared for the performance of benzene and ammonium removal as well as electricity generation. Additionally, the effect of hydraulic retention time (HRT) on the performance of the MFC was investigated. To understand the electrochemical processes occurring in the MFC, benzene and ammonium spiking as well as oxygen interruption experiments were performed in the batch mode. Additionally, the degradation pathways and key players were elucidated by compound specific isotope analysis (CSIA) and Illumina sequencing.

## **2.2 Materials and Methods**

### **2.2.1 Reactor construction**

Two reactors, MFC and control, were constructed as previously described by Rakoczy et al. (2013) with some modifications (Figure 2-1). Every reactor consisted of two cylindrical glass compartments having each a diameter of 6 cm which were separated by a Nafion-117 cation exchange membrane (CEM) (QuinTech, Göppingen, Germany). The cathode compartment (10 cm height, 330 mL total volume) was located on the top of the anode compartment (22 cm height, 680 mL total volume). Both compartments were completely filled with granular graphite of 1-6 mm diameter (Edelgraphit GmbH, Bonn, Germany) which served as electrodes. After filling with granular graphite, the anodic and cathodic compartment had a net liquid volume of 320 mL and 160 mL, respectively. A ring of stainless steel (304 SS, 2 cm length, 6 cm diameter) was used as electron collector for

granular graphite at each compartment and interfaced to the external resistor. A liquid loop between the anode and cathode compartment was added, allowing the anodic effluent flowing directly into the cathodic compartment. This loop configuration can eliminate proton mass transfer loss and solve the problem of membrane pH gradient. An air sparger linked to an air pump (EHEIM 100, Stuttgart, Germany) was installed in the cathodic compartment of the MFC to provide aeration. Continuous recirculation was generated using peristaltic pumps (Ismatec REGLO Analog MS-2/6, Wertheim, Germany) at a rate of 60 mL/min in both compartments in order to maintain well-mixed conditions. The reactors were completely covered with aluminum foil to avoid light exposure, hence inhibiting growth of phototrophic organisms. In the control reactor, pseudo-anode and cathode were defined as two separated compartments corresponding to anode and cathode of the MFC, as no efficiently electrochemical reactions occurred in the control.

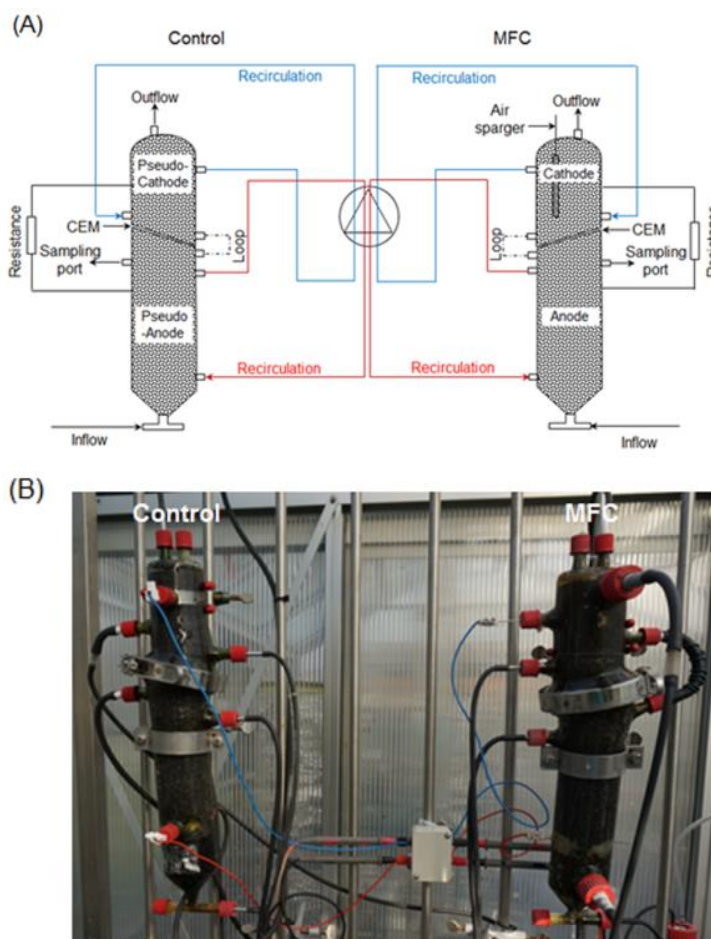


Figure 2-1 Schematic (A) and picture (B) of the MFC and the control used in this study.

### 2.2.2 Start-up and reactor operation

Both reactors were inoculated and continuously fed with contaminated groundwater from Leuna; the composition was listed in Table 2-1. The contaminated groundwater was periodically taken from a nearby groundwater well and stored in a 50 L tank which was kept at 0.5 bar N<sub>2</sub> pressure to maintain anoxic conditions and was also connected to a cooling system to keep temperature at 10-12 °C.

Table 2-1 Physico-chemical properties of contaminated groundwater used in this study.

Parameters	Means ±Stdv
NH <sub>4</sub> <sup>+</sup> (mg/L)	21.3±1.6
NO <sub>2</sub> <sup>-</sup> (mg/L)	<0.02
NO <sub>3</sub> <sup>-</sup> (mg/L)	<0.1
SO <sub>4</sub> <sup>2-</sup> (mg/L)	2.4±1.5
Total Fe (mg/L)	5.6±0.6
Fe <sup>2+</sup> (mg/L)	5.4±0.8
PO <sub>4</sub> <sup>3-</sup> (mg/L)	2.3±0.1
Cl <sup>-</sup> (mg/L)	95.2±5.6
Benzene (mg/L)	15.2±0.6
MTBE (mg/L)	1.1±0.1
COD (mg/L)	83.8±2.6
BOD <sub>5</sub> (mg/L)	36.8±4.7
TOC (mg/L)	29.0±7.2
IC (mg/L)	275.3±27.6
DO (mg/L)	0.05±0.01
Eh (mV)	-167±23
pH	7.5±0.3

Note: Contaminated groundwater was collected during September-December 2013 from the Leuna site.

The reactors were firstly operated in continuous treatment mode (day 0-134), using 1,000 Ω external resistance and a flow rate of 0.3 mL/min, resulting in a HRT of 27 h. These parameters were only changed for polarization measurements (see 2.2.4). Between day 134 and 160, the MFC was operated at the flow rates of 0.1, 0.5, 0.7, and 1.0 mL/min, corresponding to HRTs of 80, 16, 12, and 8 hours, in order to investigate the effect of

varying HRTs. Once changing to a new flow rate, the MFC was running for one week to reach a stable current output before further measurements. After running 160 days, benzene and ammonium spiking experiments were performed in the MFC. Briefly, 15, 30, and 50 mg/L of benzene were injected into the anode which was operated in a fed-batch mode, while the cathode was running in a continuous flow mode. Subsequently, 20, 50 and 100 mg/L of ammonium were injected to the cathode in a fed-batch mode, while the anode was operated in a continuous mode. Finally, through switching on or off the air pump, oxygen interruption was performed twice in the continuous flow mode in order to prove whether oxygen was the electron acceptor.

### 2.2.3 Chemical analysis

Benzene was analyzed using a gas chromatograph equipped with a flame ionization detector (Varian CP-3800 GC, Palo Alto, CA) described elsewhere (Fischer et al. 2008a).  $\text{NH}_4^+\text{-N}$ ,  $\text{NO}_2^-\text{-N}$  and  $\text{NO}_3^-\text{-N}$  were analyzed colorimetrically as described before (Bollmann et al. 2011); the detection limit was 10  $\mu\text{M}$  for each compound. The pH was monitored by a pH meter (Knick, Berlin, Germany). Dissolved oxygen (DO) was measured using an optical trace sensor system (PreSens sensor spot PSt6 and FIBOX-3 minisensor oxygen meter, Regensburg, Germany) described in more detail by Balcke et al. (2008). The redox potential (Eh) was measured with a pH/mV/Temp meter (Jenco Electronics 6230N, San Diego, USA). Samples for  $\text{Fe}^{2+}$  and total Fe measurements were acidified to pH 2 directly after the sampling and analyzed photometrically according to the guideline DIN 38405 D11.  $\text{PO}_4^{3-}$ ,  $\text{Cl}^-$ , and  $\text{SO}_4^{2-}$  were measured using the ion chromatograph (Dionex DX500, Idstein, Germany) following the guideline EN ISO 10304-2, DIN 38405-19. The total organic carbon (TOC), inorganic carbon (IC), 5-day biological oxygen demand (BOD), and chemical oxygen demand (COD) were analyzed according to the methods as previously described (Jechalke et al. 2010).

### 2.2.4 Electrochemical measurements and calculations

The Voltage (V) across a resistor (R) was recorded at 20 min intervals using a multimeter (Metrix MTX 3282, Paris, France). Current (I) was calculated by Ohm's law ( $I = V/R$ ) and power (P) was calculated as  $P = V \times I$ . Current and power density were

normalized by the net anode compartment volume (NAC). The coulombic efficiency ( $CE$ ) was calculated as the ratio of the number of electrons recovered as charge versus the number of released electrons by substrate removal. The energy efficiency ( $\eta$ ) was defined as the ratio of power produced by the cell to the heat of combustion of organic substrate, and was calculated as previously described (Logan et al. 2006). Polarization and power density curves presented in the Figure 2-5 were generated by varying the resistor from 56,000 to 100  $\Omega$  (forward). Backward polarizations were also recorded by varying resistance from 100 to 56,000  $\Omega$ ; the hysteresis was comparably low (Supporting information Figure S2-4). The reactor was initially disconnected with the external resistance and was running under open circuit for 5 h to produce a stable open circuit potential (OCP). Data for each resistor adjustment were recorded in intervals of 30 min or longer until the voltage change was less than 2 mV in 1 min. Individual anode and cathode potentials were measured using an Ag/AgCl reference electrode (Sensorteknik SE11, Meinsberg, Germany) and assumed to be +0.197 V against the standard hydrogen electrode (SHE).

### **2.2.5 Compound-specific stable isotope analysis (CSIA)**

Benzene-containing influent groundwater and water from the pseudo-/anodic compartments of two reactors were extracted with pentane. The carbon and hydrogen stable isotope compositions were determined using a gas chromatograph-combustion-isotope ratio mass spectrometer system (GC-IRMS). The detailed measurement and calculation were performed as previously described (Rakoczy et al. 2013). The benzene degradation pathways were analyzed by comparing measured isotope composition shifts with published isotope enrichment factors ( $\epsilon$ ) in a two-dimensional isotope plot (Fischer et al. 2008b, Mancini et al. 2008).

### **2.2.6 MiSeq Illumina sequencing**

Total DNA was extracted from graphite granules and cation exchange membranes using the FastDNA® spin Kit for soil (MP Biomedicals, Santa Ana, CA). PCR amplicons of bacterial and archaeal 16S rRNA genes were generated using the *Bacteria*-universal primers 341F (5'-TCCTACGGGNGGCWGCAG-3') and 785R (5'-TGACTACHVGGGTA

TCTAAKCC-3') and *Archaea*-universal primers 340F (5'-TCCCTAYGGGGYGCASCAG-3') and 915R (5'-TGTGCTCCCCCGCCAATTCCT-3'). Sequencing was performed using the Illumina MiSeq platform at a commercial laboratory (LGC Genomics GmbH, Berlin, Germany). Raw data were processed using Illumina CASAVA data analysis software and reads were demultiplexed according to index sequence. Overlapping regions within paired-end reads were then aligned to generate contigs. If a mismatch was discovered, the paired-end sequences involved in the assembly were discarded. OTU picking and taxonomical classification was performed at 97% identity level with Mothur 1.33. Sequence data were deposited in the Sequence Read Archive (SRA) of NCBI database under the accession number SRP044693.

### **2.2.7 Statistical analysis**

Statistical analyses were performed using SPSS 22.0 package (Chicago, IL, USA). The normality and homogeneity were assessed with a Shapiro-Wilk W test and a Levene test, respectively. Differences in benzene and ammonium removal efficiencies between the MFC and control reactor were compared with one-way ANOVA tests. The Tukey's post-hoc test was used to further evaluate the difference between the different flow rates when significant differences were found. Differences were considered to be statistically significant if  $p < 0.05$ . The linear relationship between removed pollutant loads and power generations were further analyzed by a regression analysis.

## **2.3 Results and discussion**

### **2.3.1 Overall treatment performance during continuous operation**

#### *Overall performance of the MFC with an aerated cathode*

The MFC was continuously fed for around 130 days with contaminated groundwater containing up to 15 mg/L for benzene and 20 mg/L for ammonium (Table 2-1), generating current and achieving a constant benzene and  $\text{NH}_4^+$ -N removal (Figure 2-2 and 2-3). During the initial stage, benzene and  $\text{NH}_4^+$ -N removal as well as current output gradually increased, probably due to the attachment and growth of ammonium- and benzene-metabolizing microorganisms from contaminated groundwater. After

approximately two months, benzene and  $\text{NH}_4^+\text{-N}$  removal became relatively stable, indicating that electrochemical active biofilms had been fully developed, reflected also by a stable current generation (Figure 2-3). In the anodic effluent of the MFC, roughly 80% of benzene was removed whereas  $\text{NH}_4^+\text{-N}$  concentrations decreased only slightly (~5%). The remaining 20% benzene was removed at the cathode, resulting in an overall benzene removal efficiency of 100% in the cathodic effluent. Ammonium disappeared completely in the cathodic effluent, showing finally 100% removal efficiency. In summary, benzene was removed mainly (80%) in the anodic compartment and  $\text{NH}_4^+\text{-N}$  was removed solely in the cathodic compartment of the MFC. Sequential removal of benzene and ammonium in the different compartments avoided putative negative effects of benzene and benzene degraders on the nitrification process which have been previously reported (2011, Jechalke et al. 2010). During steady stage, the MFC generated current between 200 and 250  $\mu\text{A}$  and a current density of 0.6~0.8  $\text{A m}^{-3}$  NAC was obtained (Figure 2-3) when being operated at 1,000  $\Omega$ .

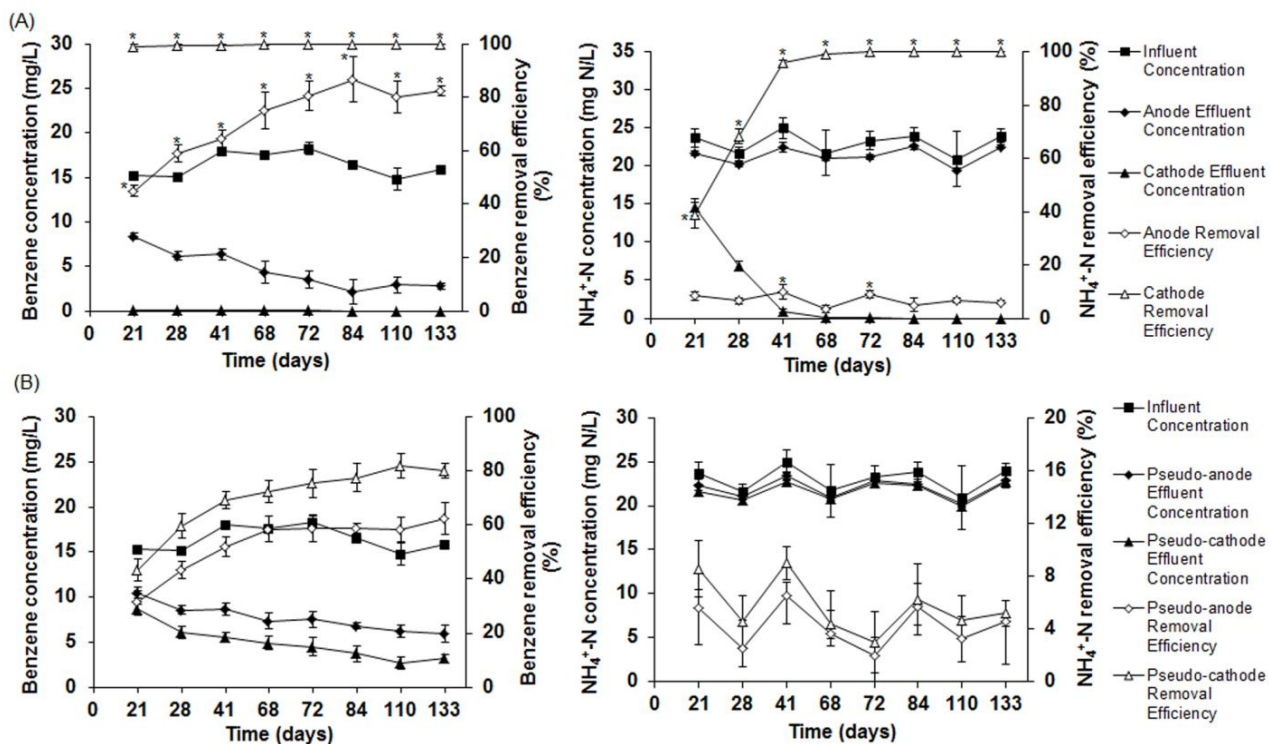


Figure 2-2 Benzene and  $\text{NH}_4^+\text{-N}$  removal in the MFC (A) and the Control (B) during continuous treatment of contaminated groundwater. \*represents significant higher removal efficiency (p<0.05) in the MFC compared to the control at the same sampling time.

The comparison with the field studies on the treatment of benzene and ammonium-contaminated groundwater with other remediation technologies, similar high percentage of benzene removal but far more  $\text{NH}_4^+\text{-N}$  concentration reduction were achieved in our MFC system, even only considering their best removal efficiencies achieved during summer. For example, Seeger et al. (2011) reported 81%-99% benzene removal and 40-50%  $\text{NH}_4^+\text{-N}$  removal in a planted constructed wetland. A novel aerated treatment pond exhibited approximately 100% benzene concentration reduction, whereas ammonium concentrations decreased only slightly from around 59 mg/L at the inflow to 56 mg/L in the outflow, indicating no significant  $\text{NH}_4^+\text{-N}$  removal during continuous operation (Jechalke et al. 2010). Therefore, sequential benzene degradation and nitrification eliminated the inhibition effect of benzene on nitrification in our MFC system.

Most studies on MFC operations using benzene as anodic substrates were performed under the simplified laboratory conditions using artificial wastewater. Thus, Current output in this study can be compared to these studies. Recently, Rakoczy et al. (2013) investigated the treatment of benzene and sulfide-contaminated groundwater using a MFC over a period of 770 days and obtained a maximum current output of approximately 250  $\mu\text{A}$  in a continuous flow mode, which was comparable with our study.

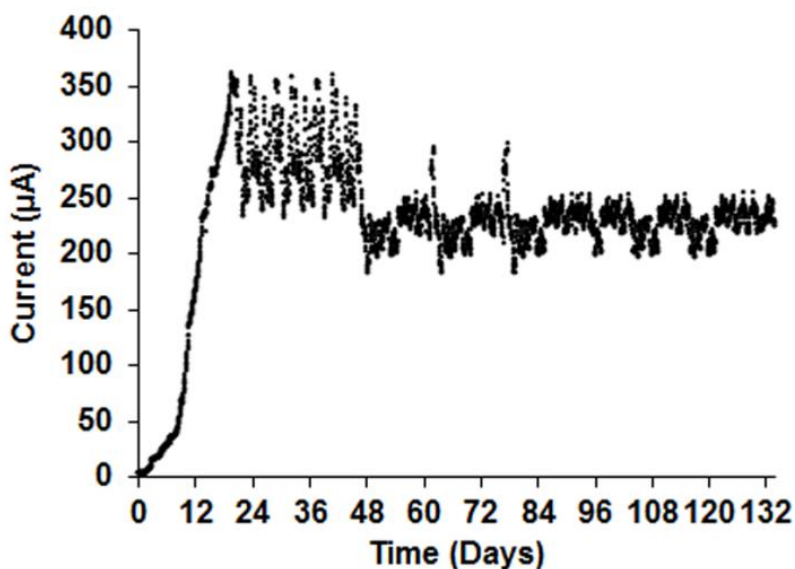


Figure 2-3 Current generation in the MFC during continuous treatment of contaminated groundwater.

*Overall performance of the control reactor without aeration*

In the control reactor, benzene removal in both pseudo-anodic and cathodic effluent gradually increased during the initial microbial enrichment, and then achieved steady removal efficiencies of 60% and 80%, respectively (Figure 2-2). Compared to the MFC, less benzene (20% lower) was removed in the control reactor ( $p < 0.05$ ), indicating enhanced benzene degradation in the anode compartment of the MFC. Ammonium was only slightly removed (<10%) in the control, similar to the anode of the MFC. A low noise current (< 5  $\mu\text{A}$ ) was observed in the control; hence current was not efficiently generated (Supporting information S2-2). In MFCs, the electrochemical potential difference of anode and cathode, depending on the redox potential of the electron donor and the terminal electron acceptor, determines the possibility and extent of generated current (Wrighton and Coates 2009). As nearly the same anode and cathode potentials were observed in the control, no electromotive force was obtained and thus no current generated. Therefore, the control reactor without aeration can be regarded as a benzene-degrading mesocosm in which granular graphite was colonized by benzene degraders but not served as electron donor or acceptor.

**2.3.2 Mechanisms of benzene and ammonium removal***Benzene removal mechanism*

CSIA was performed in order to identify the initial activation mechanisms of benzene degradation in the MFC and the control reactor. The initial attack on thermodynamically very stable benzene is critical for its degradation process. Combined carbon and hydrogen isotope fractionation has been proved to be a powerful tool for the characterization of initial metabolic reactions for benzene biodegradation (Fischer et al. 2008b, Mancini et al. 2008). Carbon and hydrogen isotope fractionations of benzene were significantly higher in the control compared to the MFC (Supporting information Figure S2-3). However, two dimensional plots of carbon versus hydrogen isotope fractionation were similar for both MFC and control (Figure 2-4), indicating that isotope fractionation was masked in the MFC. The detected values matched with those indicative for benzene monooxygenation to phenol catalyzed by a monooxygenase (Figure 2-4). The produced phenol might be further transformed into catechol by a second monooxygenation and also

the other possible intermediates after a possible *ortho* or *meta* ring cleavage of catechol (Yerushalmi et al. 2001, Zaki 2006). Monohydroxylation as benzene activation step was also identified in the anodic reaction of a MFC for treating benzene and sulfide-contaminated groundwater (Rakoczy et al. 2013). However, we cannot exclude that benzene was actually anaerobically activated and degraded by a mechanism producing similar carbon and hydrogen isotope fractionation as observed for aerobic monohydroxylation, as different anaerobic benzene activation mechanisms are currently proposed: an anaerobic hydroxylation to phenol (Zhang et al. 2013b) or a carboxylation to benzoate (Abu Laban et al. 2010, Luo et al. 2014). In any case, the intermediates of the initial benzene activation steps were probably further oxidized anaerobically and accelerate electricity generation by transferring the released electrons to the anode. This is also supported by our electrochemical results and the fact that no other electron donors except for benzene were provided.

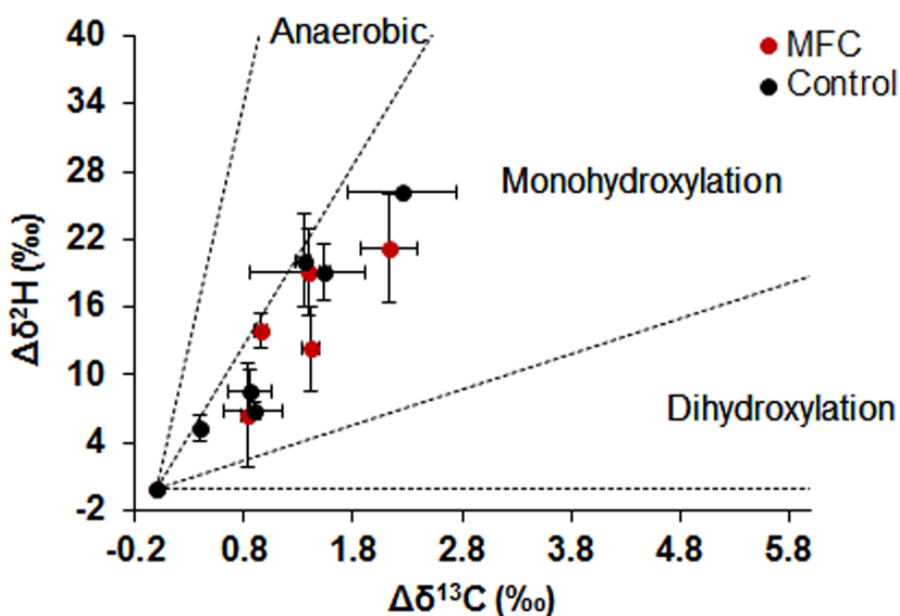


Figure 2-4 Two-dimensional isotope plot of  $\Delta\delta^{13}\text{C}$  versus  $\Delta\delta^2\text{H}$  values of benzene measured at the anode of the MFC (red symbol) and pseudo-anode of the Control (black symbol) during continuous treatment. Values of  $\Delta\delta$  were calculated by subtracting the measured isotopic value from the initial isotopic value determined at the influent.

*Ammonium removal mechanism*

At the cathode of the MFC, ammonium was mainly oxidized to nitrate by nitrification, as indicated by an increase of  $\text{NO}_3^-$ -N (Supporting information Figure S2-1). In the control and the anode of the MFC,  $\text{NO}_2^-$  and  $\text{NO}_3^-$  concentrations were extremely low (data not shown), showing that ammonium removal by nitrification activity was negligible; the oxygen concentrations were obviously too low for nitrification, as previously observed in an aerated treatment pond with biofilm promoting mats at the Leuna field site (Jechalke et al. 2011). The small ammonium losses in the control reactor and the anode compartment of the MFC might be due to physical-chemical processes, e.g. adsorption or volatilization (Kim et al. 2008, Yan and Regan 2013).

**2.3.3 Effect of the flow rate on the performance of the MFC**

To determine the effect of HRTs, different flow rates were used to study benzene and  $\text{NH}_4^+$ -N removal performance as well as power generation in the MFC. As shown in Figure 2-5A, benzene removal at the anode decreased from 80% at a flow rate of 0.3 mL/min (27 h HRT) to 40% at a flow rate of 1.0 mL/min (8 h HRT). At a flow rate of 0.1 mL/min (80 h HRT), benzene was completely removed already at the anode. However, 100% benzene removal efficiency was always obtained in the final cathodic effluent at the five studied HRTs. At the lower flow rate (0.1 and 0.3 mL/min), ammonium was completely removed (Figure 2-5A). At flow rates higher than 0.3 mL/min, the removal efficiencies decreased gradually to around 70% at a flow rate of 1.0 mL/min, implying that nitrification was limited at the shorter HRT.

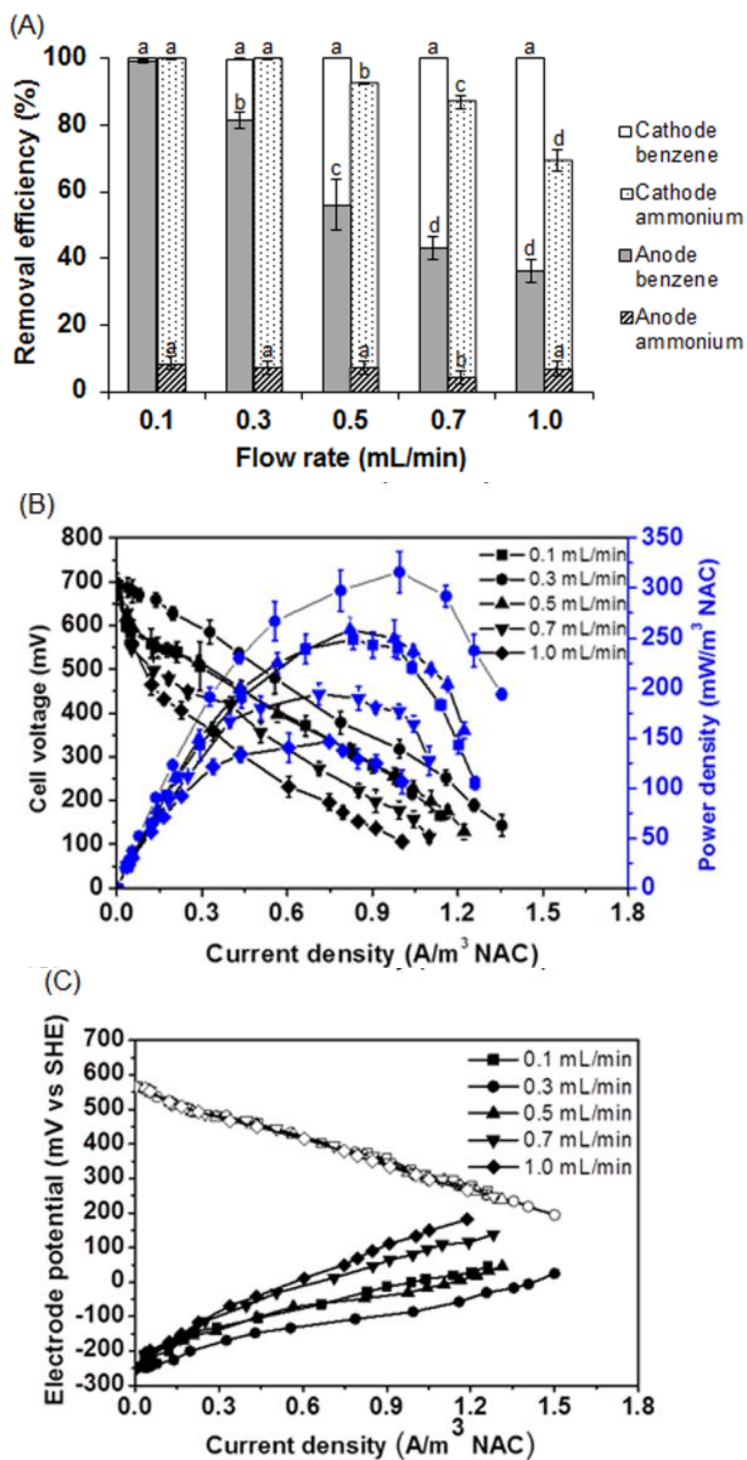


Figure 2-5 Effect of flow rate on benzene and ammonium removal (A), power generation (B), and electrode potentials (C) in the MFC. B: polarization curve (solid symbol) and power density curve (open symbol); C: anode potential (solid symbol) and cathode

potential (open symbol). Different letters (a, b, c, d) located above the bars indicate a significant difference between removal efficiencies at the different flow rates.

The maximum power density of 316 mW/m<sup>3</sup> NAC was achieved at a current of 0.99 A/m<sup>3</sup>, when the MFC was operated at the flow rate of 0.3 mL/min (Figure 2-5). As shown by the polarization and power density curves, lower performances were obtained at higher or lower flow rates. The electrode potentials as a function of current density were also examined at different flow rates (Figure 2-5C). As expected from the removal data, it was observed that the cathodic potentials were not affected by the different flow rates. The anodic OCP values shown at zero current density were also similar under the different flow rates, demonstrating an excellent stability of the system. The electrode polarization showed very different profiles for the anodic potentials at the different flow rates. Therefore, the difference of power density at the different flow rates was a result of the polarization behavior of the anodic potentials, indicating that anodic benzene oxidation was rate-limiting and thus determined electricity generation. In order to confirm this finding, subsequent benzene injection experiments were performed and also approved that benzene served as the main anodic electron donor in the MFC (Figure 2-6).

Coulombic efficiencies of 28±4.7%, 14±3.4%, 10±1.2%, 8±1.4% and 7±0.9% were obtained at the increased flow rates of 0.1, 0.3, 0.5, 0.7, and 1.0 mL/min, respectively; analogously, energy efficiencies of 8±1.3%, 4±0.9%, 3±0.3%, 2±0.3% and 1.2±0.2% were achieved. The lower coulombic and energy efficiencies at higher flow rates are indicative for incomplete benzene degradation, eventually resulting in a lower number of electrons transferred to the anode. The data also indicate that a substantial number of electrons were generally not transported to the anode, probably caused by the use of penetrating oxygen or alternative substances as electron acceptors (e.g. carbonate leading to methanogenesis or organic or inorganic metabolites upon fermentation processes). Notably, the MFC with aerated cathode was more efficient with regard to benzene degradation than the ferricyanide-based MFC described recently by Wu et al. (2013), which produced a power density of 2.1 mW/m<sup>2</sup> and showed a coulombic efficiency of 3.3%. In subsequent experiment, a flow rate of 0.3 mL/min was used due to the maximum power density and high pollutant removal performance achieved at this date.

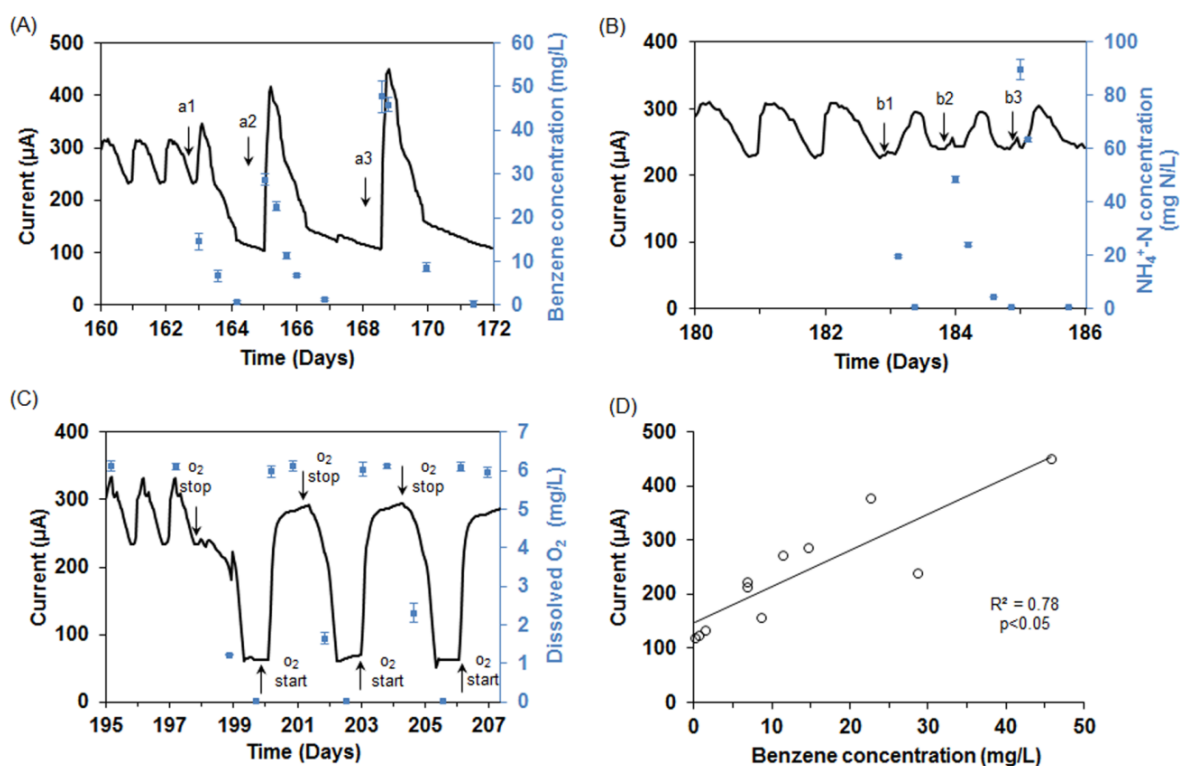


Figure 2-6 Effect of benzene and ammonium additions, and oxygen interruption on current generation in the MFC. (A): benzene injection of 15 mg/L (a1), 30 mg/L (a2), and : 50 mg/L (a3); (B):  $\text{NH}_4^+\text{-N}$  injection of 20 mg N/L (b1), 50 mg N/L (b2) and 100 mg N/L (b3); (C): Interruption of  $\text{O}_2$  supply at the cathode; (D): correlation between current generation and benzene concentration at the anode.

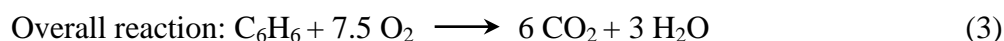
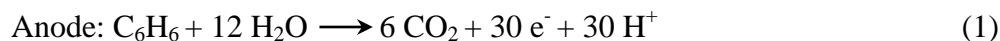
### 2.3.4 Detection of electrochemical reaction in the MFC

Although the complete degradation of benzene can theoretically release 30 electrons (Wu et al. 2013), current generation strongly depends on whether electrons from benzene oxidation can be efficiently transferred to the anode. In our study, when 15 mg/L benzene was injected into the anode, the current rapidly increased from around 240 to 350  $\mu\text{A}$  within 3 h; subsequently, the current gradually decreased corresponding to decreasing benzene concentrations (Figure 2-6A). Injecting higher benzene concentrations of 30 and 50 mg/L generated higher current maxima of 415 and 450  $\mu\text{A}$ , respectively. A linear correlation was obtained between the current and the concentration of benzene at the anode (Figure 2-6D), demonstrating that benzene oxidation was the main anodic reaction, and the

released electrons were efficiently delivered to the anode. In contrast, increasing ammonium concentrations by injection of 20, 50, 100 mg/L  $\text{NH}_4^+$ -N did not affect the current output (Figure 2-6B), indicating that cathodic ammonium oxidation did not limit electricity generation. Subsequently, the effects of varying oxygen concentrations at the cathode were investigated (Figure 2-6C). When the supply of oxygen at the cathode was stopped, the DO concentration gradually decreased from about 6 to 1 mg/L, and the current also decreased from about 300 to 60  $\mu\text{A}$ . The current generation immediately increased when oxygen was again supplied and the DO concentration increased. Hence, the DO concentration was coupled to current generation, suggesting that oxygen was the main terminal electron acceptor at the cathode.

As  $\text{NH}_4^+$ -N can release maximally eight electrons via oxidation to nitrate, ammonium can theoretically serve as an anodic electron donor (He et al. 2009). However, ammonium as a direct anodic fuel for electricity generation has not been demonstrated experimentally yet. In our study, ammonium was completely oxidized to nitrate at the cathode by nitrifying microorganisms (Supporting information Figure S2-1). Our results demonstrate that the released electrons were not involved in electrochemical reactions; probably, the electrons were directly respired by nitrifiers, explaining why ammonium consumption was not directly connected to electricity generation in the MFC. You et al. (2009) showed that additional protons produced from ammonium oxidation can reduce the ohmic resistance and maintain the pH balance in the absence of a phosphate buffer, which can contribute to the electricity generation process. Recently, it was also reported that the oxygen reduction relied on the nitrification activity at the biocathode, at least to some extent (Du et al. 2014). In this study, the contaminated groundwater from the Leuna site probably had a good buffer capacity, so that biological nitrification was not directly linked with current generation.

Based on these results, the anodic and cathodic reactions occurred in the MFC are described by the following equations, with the assumption of complete oxidation of benzene.



Coulombic and energy efficiencies at the different flow rate were calculated according to the above electrochemical reactions.

### 2.3.5 Analysis of microbial communities in the MFC and Control

#### *Bacterial community analysis*

The compositions of bacterial communities colonizing at the pseudo-/anode, CEM and pseudo-/cathode were analyzed (Figure 2-7A). The anode of the MFC and the control reactor were mainly colonized by bacterial phylotypes belonging to the *Chlorobiales*, *Rhodocyclales*, and *Burkholderiales*. The family *Chlorobiaceae* in the *Chlorobiales* accounted for ~15% and 41% of the pseudo-/anodic bacterial communities in the control and MFC, respectively. Although *Chlorobiales* were previously known as anaerobic photoautotrophs, several recent studies suggested that they were able to perform anaerobic dark respiration by the breakdown of organic substrates when sulfide is not used as electron donor (Badalamenti et al. 2013, Feng et al. 2010). *Chlorobiales* were also identified as the dominant phylotypes in benzene degrading enrichment cultures under nitrate-reducing conditions (Mancini et al. 2008, van der Zaan et al. 2012) which indicated that *Chlorobiales* can participate in degradation of benzene or its intermediate metabolites. Large percentages of *Rhodocyclaceae* of 43% and 21% (belonging to *Rhodocyclales*) were observed at the pseudo-/anode of the control and MFC respectively, indicating as well a role of these phylotypes upon benzene degradation; correspondingly, phylotypes of this family were shown to be associated with anaerobic benzene degradation either by DNA-stable isotope probing with <sup>13</sup>C-labelled benzene (Liou et al. 2008, van der Zaan et al. 2012) or by phylogenetic analysis of benzene-degrading enrichment cultures (Kasai et al. 2006). The *Comamonadaceae* within the order of *Burkholderiales*, accounting for 5% and 6% of bacterial communities at the pseudo-/anode of the control and MFC, were also shown to be involved in benzene degradation (Perez-Pantoja et al. 2012, van der Zaan et al. 2012). Overall, the dominance of these potential benzene degraders implies that those were actually related to benzene degradation in both MFC and control. The whole control reactor, including pseudo-anode, CEM and pseudo-cathode, were colonized by similar bacteria with slightly different abundances, again supporting the view that it is a homogenous mesocosm.

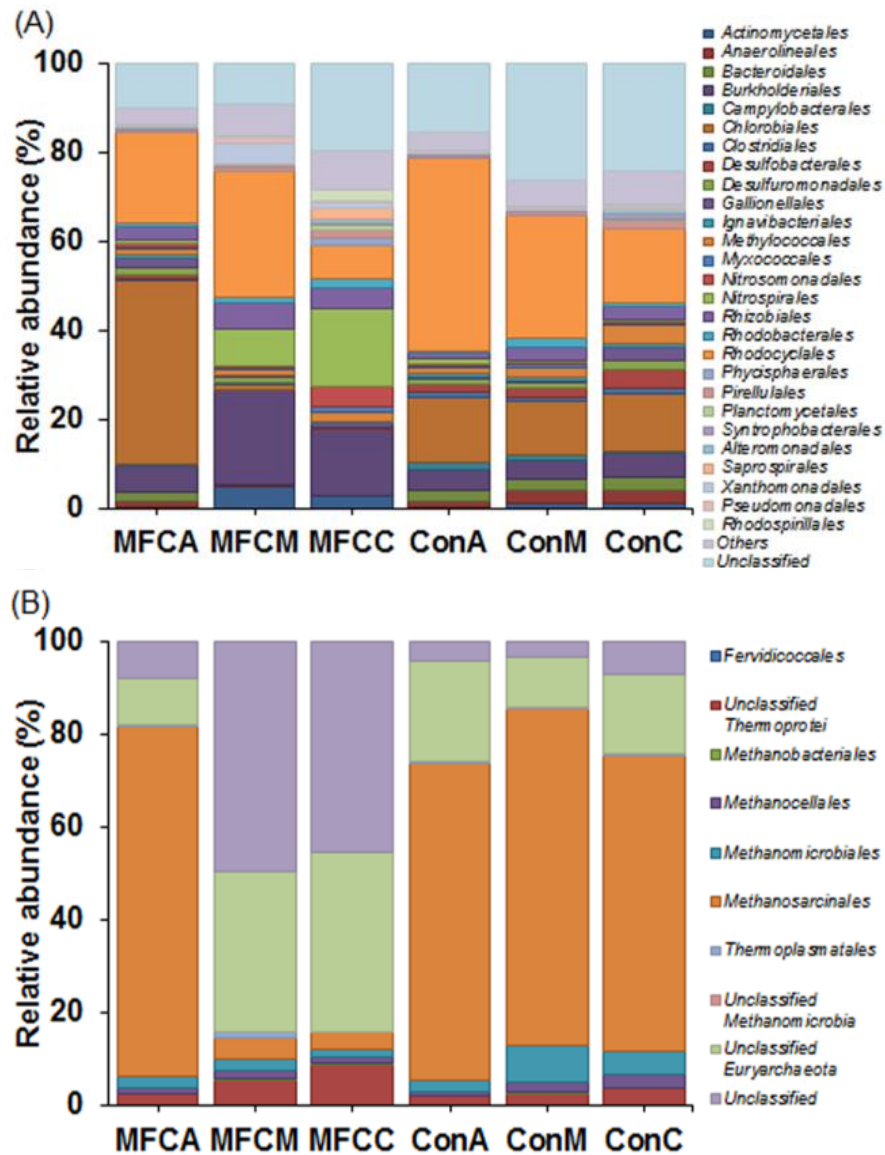


Figure 2-7 Phylogenetic distribution of 16S rRNA genes based on the order of bacteria (A) and archaea (B) detected in the MFC and Control. Bacterial orders with a read abundance < 1% in all of the six samples were pooled in others. MFCA: MFC anode; MFCM: MFC CEM; MFCC: MFC cathode; ConA: Control pseudo-anode; ConM: Control CEM; ConC: Control pseudo-cathode.

Different from the bacterial community at the anode, the dominant bacteria orders at the cathode of the MFC were *Nitrospirales* (18%), *Burkholderiales* (15%), *Rhodocyclales* (7%), *Nitrosomonadales* (4.5%), and *Rhizobiales* (4%). Obviously, the dominant families

of *Comamonadaceae* and *Rhodocyclaceae* affiliated to *Burkholderiales* and *Rhodocyclales* were able to degrade the residual benzene from the anode (van der Zaan et al. 2012). Phylotypes affiliated to *Nitrosomonadales* and *Nitrospirales* belong to the genera of *Nitrosovibrio* and *Nitrospira*, which presented the dominant ammonia-oxidizing and nitrite-oxidizing bacteria respectively (Lucker et al. 2010, Meincke et al. 1989). They were also identified as dominant nitrifying bacteria in wastewater treatment plants and MFC systems for nitrogen removal (Tu et al. 2014, Yu et al. 2011). The data suggests that ammonium was firstly oxidized to nitrite by *Nitrosovibrio*, then nitrite was further oxidized to nitrate by *Nitrospira*, leading to a high rate of nitrification at the cathode of the MFC.

The complexity of anode biofilms usually makes it hard to elucidate electrochemical mechanisms at the anode, but microbial community analysis will help to understand microbial interactions among electrochemically active microorganisms and their syntrophic partners and competitors in anode biofilms and further aid in improving the MFC performance. Various dominant bacterial phylotypes were identified in the MFC and they are able to catalyze syntrophic benzene degradation. Such syntrophic processes has been described to govern anaerobic benzene degradation in both benzene-degrading enrichment cultures and in situ benzene-degrading columns (Vogt et al. 2011). In this study, syntrophic interactions were probably used to break down benzene into simple molecules, which can be used for current generation.

#### *Archaeal community analysis*

The compositions of archaeal communities were shown in Figure 2-7B. The archaeal communities were dominated by phylotypes belonging to the *Methanosarcinales* (64-76%) and *Methanomicrobiales* (1.5-8%) in the three parts of control and the anode of the MFC (Figure 2-7B). Methanogens can compete substrates with electrochemically active microorganisms and hence reduce electron recovery (Jung and Regan 2011). It was shown that electrochemically active microorganisms can outcompete acetoclastic methanogens for organic substrates in MFCs, eliminating electron consumption by methanogens (Jung and Regan 2011, Lee et al. 2008). Electrochemically active microorganisms are not able to completely outcompete hydrogenotrophic methanogens, usually leading to electron loss. In this study, acetoclastic *Methanosarcinales* were the predominant archaea at the MFC anode

(76%), while hydrogenotrophic *Methanomicrobiales* only presented a relatively low abundance (2%). These data indicated electron loss by methanogenesis was probably not significant in this MFC. Notably, *Methanosarcinales* and *Methanomicrobiales* have been identified as syntrophic methanogens in anaerobic benzene-degrading enrichment cultures (Herrmann et al. 2010, Sakai et al. 2009). The data indicates that benzene was likely degraded by a syntrophic consortium of facultative anaerobes, electrochemically active microorganisms, methanogens after the initial activation reaction by monohydroxylation (Vogt et al. 2011). In this study, a well-balanced microbial community consisting of electrochemically active microorganisms and their various syntrophic partners as well as competitors was maintained at the anode, which can support an efficient and robust biofilm.

Different from the archaeal communities in the control and the anode of the MFC, the CEM and cathode of the MFC was dominated by unclassified *Euyarchaeota* (46%), unclassified archaea (39%) and *Methanosarcinales* (12%). It was possible that archaea from anoxic groundwater were not able to grow at the aerobic cathode of the MFC due to the completely different physicochemical conditions.

Due to the complexity of anode biofilms, it is usually very difficult to elucidate concrete electrochemical mechanisms at the anode, e.g. identifying the microorganisms actually transferring electrons to the anode. However, various dominant bacterial phylotypes were identified in the MFC, suggesting that the electrons were transferred to the anode after the initial activation reaction by a network of microorganisms, using different metabolites of benzene degradation as substrates, rather than by a single organism. These processes might be syntrophic; such syntrophic processes have been described to govern anaerobic benzene degradation in both benzene-degrading enrichment cultures and *in situ* benzene-degrading columns (Herrmann et al. 2010).

## 2.4 Supporting information

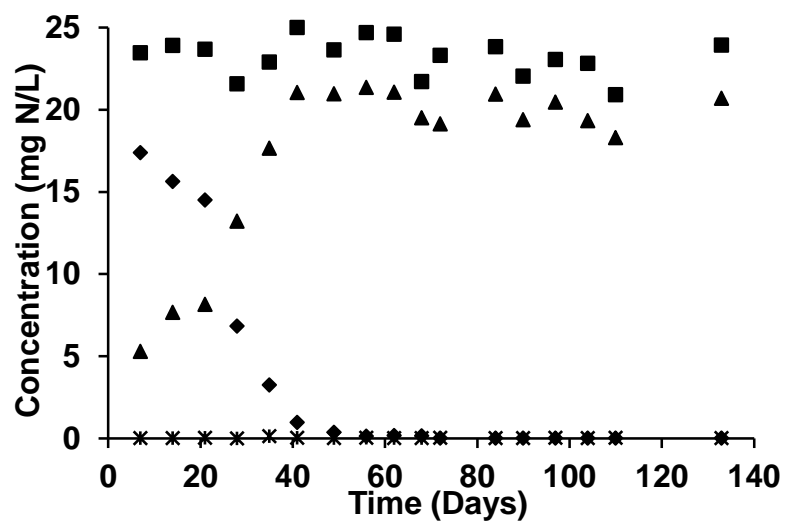


Figure S2-1 Concentration changes of  $\text{NH}_4^+$ ,  $\text{NO}_2^-$ , and  $\text{NO}_3^-$  in the cathodic compartment of the MFC during continuous treatment. Influent  $\text{NH}_4^+$ -N (■), Effluent  $\text{NH}_4^+$ -N (◆), Effluent  $\text{NO}_2^-$ -N (\*), Effluent  $\text{NO}_3^-$ -N (▲).

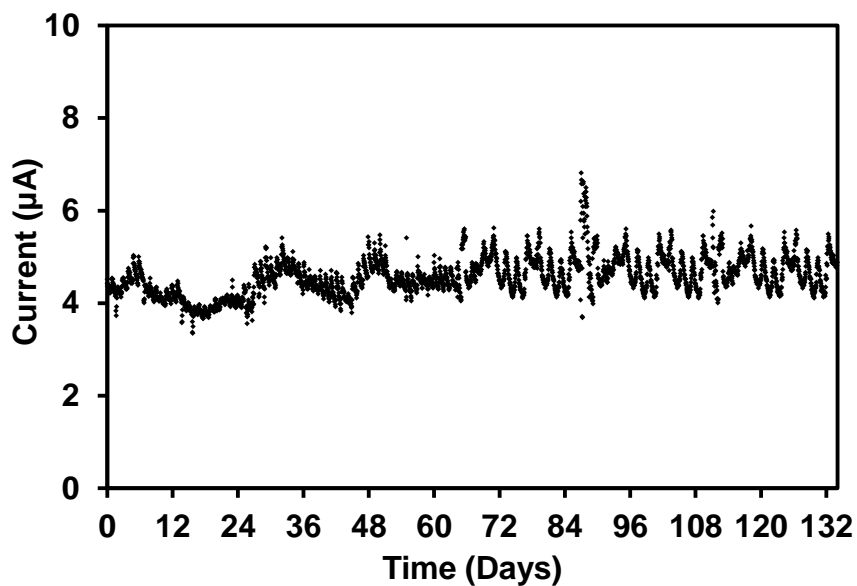


Figure S2-2 Noise Current observed in the control during continuous treatment of contaminated groundwater.

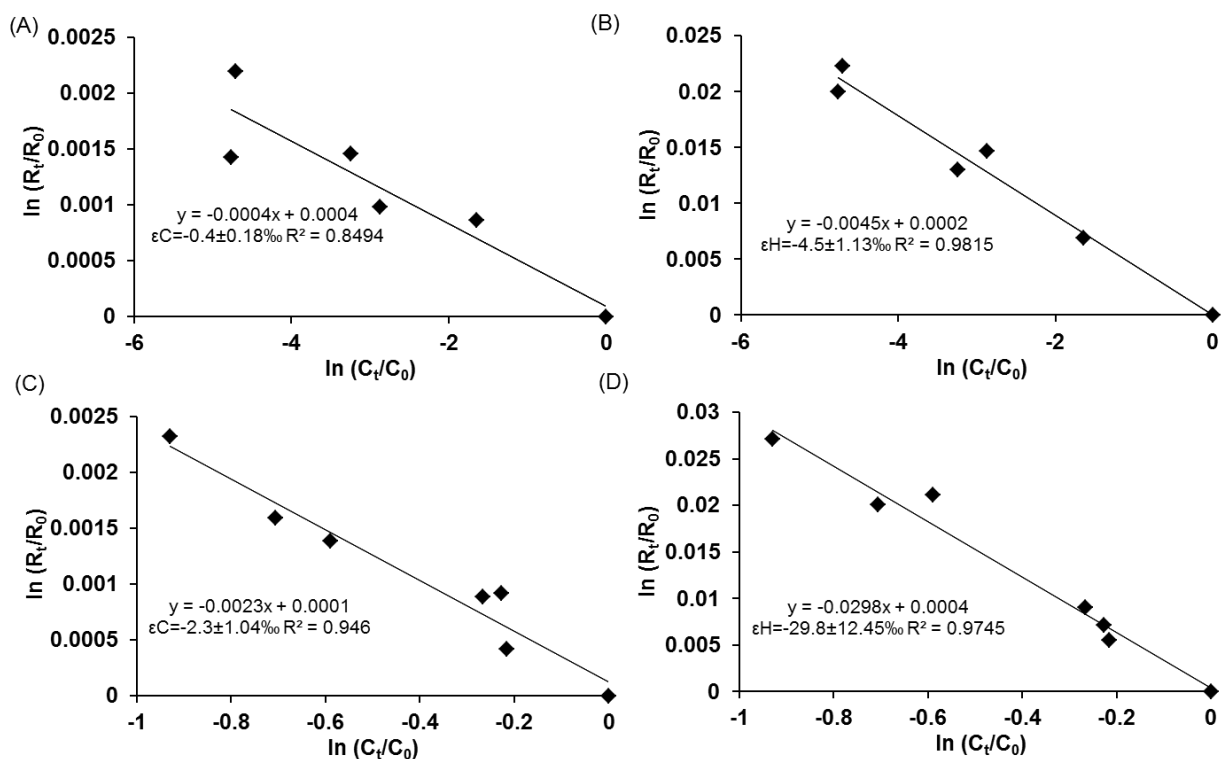


Figure S2-3 Rayleigh plot for carbon and hydrogen stable isotope fractionation of the anodic benzene in the MFC and the control reactor. The lines correspond to a linear regression: carbon (A) and hydrogen (B) isotope fractionation in the MFC; carbon (C) and hydrogen (D) isotope fractionation in the Control.  $C_0$ : the benzene concentration at the influent;  $C_t$ : the benzene concentration at the anodic effluent;  $R_0$ : the isotope ratio determined at the influent;  $R_t$ : the isotope ratio at the anodic effluent. Enrichment factors ( $\epsilon$ ) are given with the uncertainty ( $\pm$  confidence interval 95%).

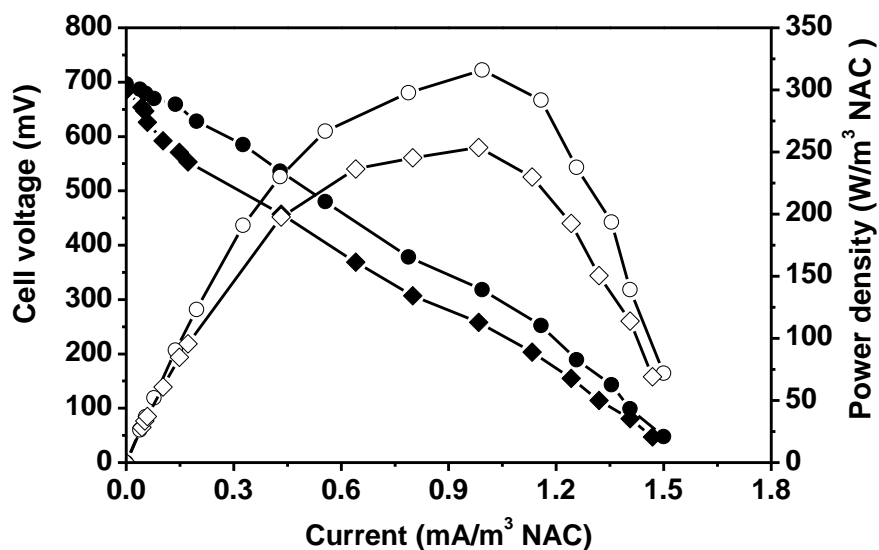


Figure S2-4 Forwards (circle symbol) and backwards (diamond symbol) polarization and power density curves of the MFC at a flow rate of 0.3 mL/min. Solid symbols represent cell voltage; open symbols represent power density. Polarization and power curves usually do not overlap when resistors are switched in forward (from high to low) and backward (from low to high) orders. In our study, a slight hysteresis was observed between the forward and backward curves. The backward polarization curve is below the forward one with a difference of ~50 mV.

## **CHAPTER 3 Enhancement and monitoring of pollutant removal in a constructed wetland by microbial electrochemical technology**

Wei, M., Rakoczy, J., Vogt, C., Harnisch, F., Schumann, R., & Richnow, H. H. (2015). Enhancement and monitoring of pollutant removal in a constructed wetland by microbial electrochemical technology. *Bioresource Technology*, 196: 490-499.

### **Abstract**

A bench-scale constructed wetland combined with microbial electrochemical technology (MET-CW) was run for 400 days with groundwater contaminated with benzene, and ammonium ( $\text{NH}_4^+$ ). Four vertically stacked anode modules were embedded into a sand bed and connected with a stainless steel cathode placed in an open water pond. In the zone where the anode modules were placed, significantly more benzene was removed in the MET-CW compared to the control CW without MET in the first 150 operation days. Benzene was identified as primary electron donor at the anode. Benzene removal and current densities were linearly correlated, implying the potential of the system for electrochemically monitoring benzene biodegradation. Compound-specific isotope analysis (CSIA) indicated that benzene was initially activated by monohydroxylation forming intermediates which were subsequently oxidized accompanied by extracellular electron transfer, leading to current production.  $\text{NH}_4^+$  removal was not stimulated by MET.

**Key words** benzene, ammonium, MET, bioremediation, microbial electrochemical technology, constructed wetland

### 3.1 Introduction

Microbial electrochemical technologies (METs) are a rapidly developing technology platform at the nexus of microbiology and electrochemistry (Schröder et al. 2015). The archetypes of METs are MFCs, which can convert chemical energy of organic or inorganic compounds into electrical power. Recently, METs were described to remove various pollutants from contaminated waters such as organics (Zhang and He 2012a) as well as nitrogen and phosphorus containing compounds (Kelly and He 2014). Especially, the removal of nitrogen compounds (e.g.  $\text{NH}_4^+$ ,  $\text{NO}_2^-$ ,  $\text{NO}_3^-$ ) in METs attracts increasing interest, providing a competitive alternative to traditional wastewater treatment processes (Kelly and He 2014). Recently, it was reported that microbial anodes in METs can effectively enhance the anaerobic biodegradation of petroleum hydrocarbons (e.g. benzene, toluene), providing potential applications for the bioremediation of anaerobic sediment or groundwater contaminated with petroleum hydrocarbons (Wang et al. 2012, Wu et al. 2013, Zhang et al. 2010). In addition to converting the chemical energy of pollutants in electricity, METs were used as biosensors for on-line monitoring of wastewater treatment or anaerobic digestion processes, such as MFC-based sensors for measuring the biological oxygen demand (Di Lorenzo et al. 2009, Liu et al. 2011). Thus, microbial electrochemical technologies possess the attractive potential to allow simultaneously removing pollutants, generating electricity, and monitoring the overall processes.

Constructed wetlands (CWs) have been developed to treat polluted water for decades due to their low cost, easy operation and maintenance (Garcia et al. 2010, Imfeld et al. 2009). In CWs, spatial gradients of DO concentrations and redox conditions support the formation of ecological niches occupied by several eco-physiologically different microorganisms, which can perform several different respiration and/or fermentation processes and generally show broad pollution removal capacities (Faulwetter et al. 2009, Imfeld et al. 2009). Spatially separated oxic zones in the rhizosphere and anoxic zones in the deeper layers of a CW generate a potential difference which can be utilized to operate a MFC, thereby providing an option for the enhancement of *in situ* pollutant removal while simultaneously generating electricity. Systems efficiently combining MFCs and VSSF or HSSF CWs have been previously reported (Fang et al. 2013, Villasenor et al. 2013, Yadav et al. 2012, Zhao et al. 2013). Villasenor et al. (2013) reported electricity generation during

the treatment of synthetic wastewater with glucose as substrate in a lab-scale HSSF-CW by installing a horizontal, rectangular graphite cathode in the upper zone and an identical anode in a deeper layer, respectively. However, the practical application is technically challenging and more studies on the combined HSSF-CW and MET treating naturally polluted waters are essentially needed.

Several different pilot-scale HSSF-CWs have been constructed in order to remediate petroleum hydrocarbons and  $\text{NH}_4^+$  contaminated groundwater at Leuna site (Chen et al. 2012, Seeger et al. 2011, van Afferden et al. 2011). Recently, Wei et al. (2015a) described a small-scale MFC reactor with an aerated cathode by which benzene and  $\text{NH}_4^+$ -N contaminated groundwater from this site was successfully treated under controlled laboratory conditions; benzene biodegradation at the anode was coupled with electricity generation while ammonium was oxidized at the cathode. Although METs and CWs technologies have been separately applied for the effective remediation of contaminated groundwater at the Leuna site, it is worthwhile to develop a combined MET and CW system considering the possibility for exploiting benefits of both METs and CWs.

In this chapter, an integrated MET-CW was established by embedding four anode modules into the sand bed and connecting it to a cathode placed in the open pond inside a bench-scale HSSF-CW; the system was used to treat original Leuna groundwater mainly contaminated with benzene and  $\text{NH}_4^+$ . The objective of the study was to evaluate whether MET can be used to (i) improve the biodegradation of the main contaminants and (ii) to monitor such degradation processes in the HSSF-CW. Furthermore, the performances of anode modules located at the different depths were compared in order to determine favorable depths for anodic reactions.

## **3.2 Materials and methods**

### **3.2.1 Reactor construction and set-up**

The MET reactor was made of acrylic material and comprised four individual anode modules (each  $10.5 \times 4.2 \times 3.3$  cm, 53 cm height in total) as shown in Figure 3-1A. Each module contained 27 holes (diameter 1 cm) covered by nylon gauze allowing water flow-through. The anode consisted of six parallel graphite plates ( $9 \times 3.5 \times 0.4$  cm), connected each

other by a graphite rod with a diameter of 0.5 cm, leading to a total specific surface area of 0.0438 m<sup>2</sup> per module. The four anode modules were connected with a stainless steel cathode (304 SS, 13.5×3.5×1 cm) across the constant external resistances of 200 Ω for operation and varying resistances for polarization curves, respectively.

### 3.2.2 Setup and operation of the MET-CW system

A general scheme of the MET-CW system and detailed information on the experimental design are provided in Figure 3-1B. The horizontal subsurface flow wetland consisted of a stainless steel tank (201×60×5 cm) equipped with a 1 cm thick glass panel on the front side, filled to an average depth of 52 cm with quartz sand (grain size = 0.68 ~ 0.80 mm) and planted with common rush (*Juncus effuses*, L.). The glass panel was covered by a removable light-tight board to avoid light effects. At 150 cm distance from the inflow, a 50 cm long open water pond was created, remaining in direct contact with the atmosphere. The sand bed was separated from the open water pond using a stainless steel plate, which contains many holes (diameter 1 cm) covered with nylon gauze, allowing water flow-through. At the inflow, four inlet pipes were located 4, 12, 20, and 36 cm above the bottom to facilitate a uniform distribution of groundwater through the whole wetland body. Due to the presence of a pore at the outflow part, the water level was kept at 48 cm depth from the bottom. Anoxic groundwater was taken from a contaminated site close to the Leuna refinery (Saxonia, Anhalt, Germany) and kept in a 50 L stainless steel tank under constant dinitrogen pressure (0.5 bar); this water was continuously pumped into the MET-CW at a constant flow rate (0.3 ml min<sup>-1</sup>) by a peristaltic pump (Ismatec REGLO Analog MS-2/6, Wertheim, Germany), yielding an inflow of 1.73 liters per day and resulting in a hydraulic retention time (HRT) of approximately 15 days. The composition of contaminated groundwater is shown in Table 2-1. The system was equipped with a cooling system maintaining the temperature of the tank and the wetland constantly at 14 ± 2°C. Four anode modules were embedded into the sand bed of the CW located between the sampling ports at the flow distance of 94 cm and 139 cm. The module sides containing the holes were placed in the direction of the water flow, allowing water to pass through. The cathode was installed at the surface of the open water body with around 80 cm distance from the anode modules. A control CW containing no MET was similarly constructed and operated; the

mechanisms of benzene biodegradation and hydrogeological parameters in this system have been reported by Rakoczy et al. (2011).

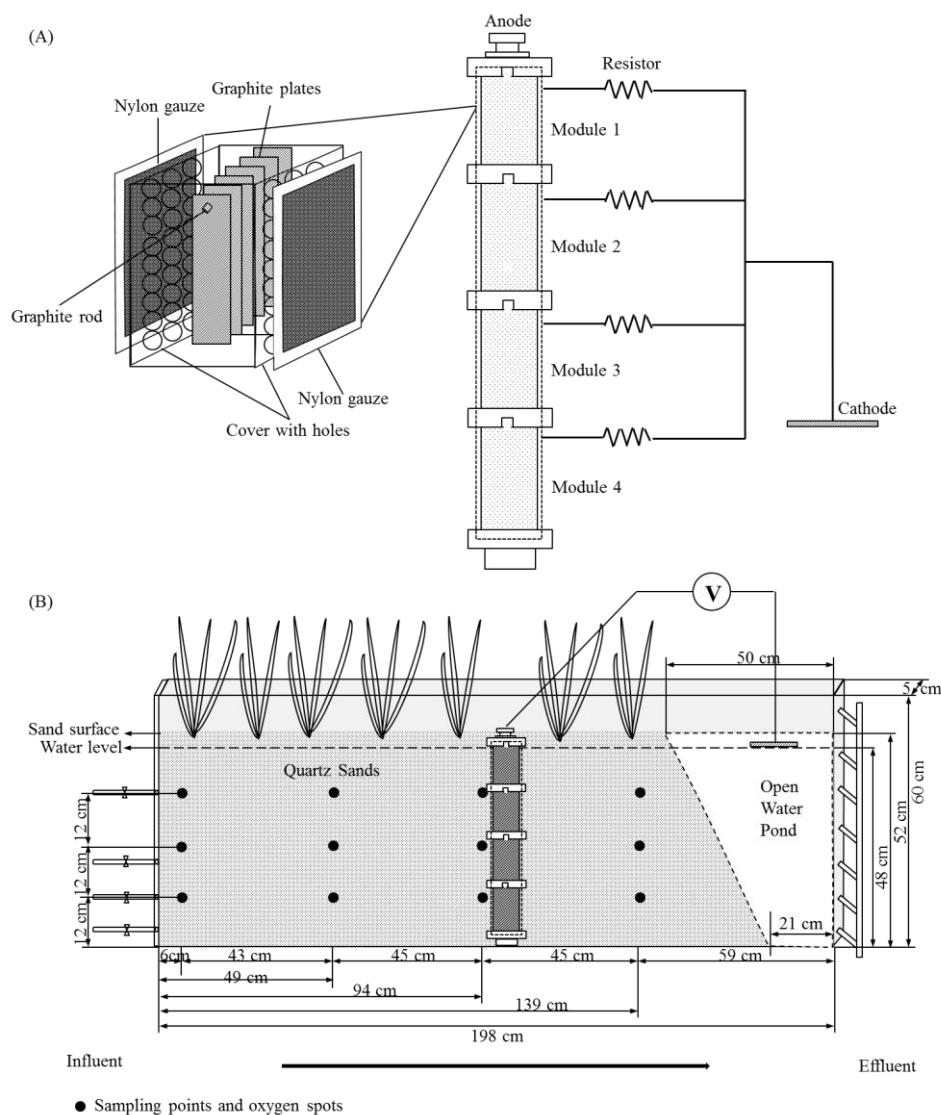


Figure 3-1 Schematic diagram of the MET-CW used in this study.

### 3.2.3 Electrochemical measurements and calculations

The voltage (V) across the resistor (R) was recorded at 20 min intervals using a Paperless Recorder (JUMO LOGOSCREEN 500 cf, Fulda, Germany). The current (I) was calculated by Ohm's law ( $I = V/R$ ). The current and power densities were normalized by the total surface area per anode module (A). The coulombic efficiency (CE) was calculated

as the ratio of total electrons recovered as charge to maximum possible electrons released by all substrate removal. Polarization and power density curves were obtained by varying the resistance in a range from 10000 to 100  $\Omega$  using a multimeter (Metrix MTX 3282, Paris, France). Therefore, the reactor was first disconnected for 5 h to record a stable open circuit voltage (OCV). Data for each resistance adjustment were recorded for at least 30 min interval after the voltage change was less than 2 mV in 1 min. The measurement was carried out in triplicates; a constant resistance of 200  $\Omega$  was reconnected overnight between every replicate measurement. The internal resistance was calculated based on the slope of the linear region of the polarization curve.

### 3.2.4 Sampling procedure

Twelve sampling ports were installed for collecting water samples across the bed (Figure 3-1). Four vertical groups across the sand bed located at 6, 49, 94 and 139 cm distance from the inflow, each consisting of three sampling ports at 24, 36 and 48 cm depth from the top, were systematically investigated. Water samples from the inflow, outflow and the 12 sampling ports were collected using a gas-tight syringe through a valve as previously described (Rakoczy et al. 2011). In order to analyze different biogeochemical parameters, each pore water sample consisted of six subsamples which were stored in completely filled sterile 20 ml vials. Two subsamples for benzene measurements were immediately fixed using sodium hydroxide to inhibit microbial activity. One subsample was adjusted to a pH of 2 with HCl (36%) in order to measure ferrous and total ionic iron. The other water samples were stored at 4 °C until analysis. The outflow volumes were measured in comparison to the inflow volumes in order to determine water loss, allowing the calculation of pollutant load removal.

### 3.2.5 Chemical analysis and calculations

Water samples were analyzed for the concentrations of benzene, ammonium ( $\text{NH}_4^+$ ), nitrite ( $\text{NO}_2^-$ ), nitrate ( $\text{NO}_3^-$ ), sulfate ( $\text{SO}_4^{2-}$ ), phosphate ( $\text{PO}_4^{3-}$ ), chloride ( $\text{Cl}^-$ ), ferrous iron ( $\text{Fe}^{2+}$ ), and total ionic iron. Briefly, benzene were analyzed using a gas chromatograph equipped with a flame ionization detector (Varian CP-3800 GC, Palo Alto, CA) as described elsewhere (Fischer et al. 2008b, Rosell et al. 2010). The concentrations of  $\text{NH}_4^+$ ,  $\text{NO}_2^-$  and  $\text{NO}_3^-$  were analyzed colorimetrically as described before (Bollmann et al.

2011). The pH was monitored by a pH meter168 (Knick, Berlin, Germany). The DO concentration was determined *in situ* by an optical trace sensor system (PreSens sensor spot PSt6 and FIBOX-3 minisensor oxygen meter, 170 Regensburg, Germany). The oxygen sensor spots were attached to the inner side of the glass panel, distributed corresponding to the sampling ports across the sand bed. The redox potential (Eh) was measured with a pH/mV/Temp meter (Jenco Electronics 6230N, San Diego, USA).

Putative water losses through plant transpiration and evaporation from the surface (evapotranspiration) were taken into account in order to make more reliable comparisons and eliminate the effect of evapotranspiration on pollutant concentrations (Hijosa-Valsero et al. 2010). It was assumed that the water loss along the flow path followed a linear change. Therefore, the mass of pollutants was calculated as follows:

$$M_{ij} = C_{ij} \times \left[ Q_{inf} - \frac{(Q_{inf} - Q_{eff})}{L} \times L_i \right] \quad (1)$$

where  $M_{ij}$  is the pollutant mass at distance  $i$  cm and depth  $j$  cm ( $\text{mg d}^{-1}$ );  $C_{ij}$  is the pollutant concentration at distance  $i$  cm and depth  $j$  cm ( $\text{mg L}^{-1}$ );  $Q_{inf}$  is the influent flow rate ( $\text{L d}^{-1}$ );  $Q_{eff}$  is the effluent flow rate ( $\text{L d}^{-1}$ );  $L_i$  is the distance from inflow to the sampling point  $i$  (cm); and  $L$  is the entire length of the CW (cm).

Pollutant removal efficiency was calculated based on the differences of pollutant mass between the influent and the sampling points using the following equation:

$$\text{Removal efficiency (\%)} = \left( 1 - \frac{M_{ij}}{M_{inf}} \right) \times 100 \quad (2)$$

where  $M_{inf}$  is the influent mass load ( $\text{mg d}^{-1}$ ) and  $M_{ij}$  is the mass load of the sampling point  $i$  ( $\text{mg d}^{-1}$ ).

### 3.2.6 Compound-specific stable isotope analysis

Samples from the inflow and sampling ports were collected at operation day 95 and extracted with pentane as previously described (Wei et al. 2015a). The carbon and hydrogen stable isotope compositions were determined using a gas chromatograph-combustion-isotope ratio mass spectrometer system (GC-IRMS). Measurements and calculations were performed as described by Rakoczy et al. (2013). The benzene degradation pathways were analyzed by comparing measured isotope composition shifts with published isotope enrichment factors ( $\epsilon$ ) in a two-dimensional isotope plot (Fischer et al. 2008b).

### 3.2.7 Statistical analysis

Statistical analyses were performed using the SPSS 22.0 package (Chicago, IL, USA). The normality and homogeneity were assessed with a Shapiro-Wilk  $W$  test and a Levene test, respectively. If the data were normally distributed, one-way ANOVA were used to analyze differences in pollutant removal efficiencies between the MET-CW and control CW. The Tukey's post-hoc test was used to further evaluate the difference between the different depths within the same flow paths when significant differences were found. Non-parametric Mann-Whitney  $U$ -tests were performed instead of ANOVA tests, as a normal distribution could not be assumed. Differences were considered to be statistically significant if  $p < 0.05$ . The linear relationship between pollutant loading removal (mass loading difference between 94 and 139 cm) and current densities were analyzed by a regression analysis.

## 3.3 Results and discussion

### 3.3.1 Removal efficiencies of benzene and $\text{NH}_4^+$ -N

The major pollutants in the influent groundwater were benzene and  $\text{NH}_4^+$  (Table 2-1), of which corresponding concentrations were up to 12 and 50  $\text{mg L}^{-1}$ , respectively. The removal efficiencies of these compounds within the MET-CW and control CW during the whole experimental period are shown in Figure 3-2. The depth-dependent spatial variations of removal efficiencies along the flow path were also determined in order to clarify the role

of MET upon pollutant degradation and to detect the most suitable locations of the anode modules; this is exemplarily shown in Figure 3-3 for the MET-CW at operation day 95 and the control CW at day 97, respectively. Pollutant removal efficiencies reached steady state in both the MET-CW and control CW after around 150 days, while current generation of the MET-CW start to become lower until completely disappear. Thus, the first 150 days of operation were termed phase I, and the subsequent experimental time was termed phase II.

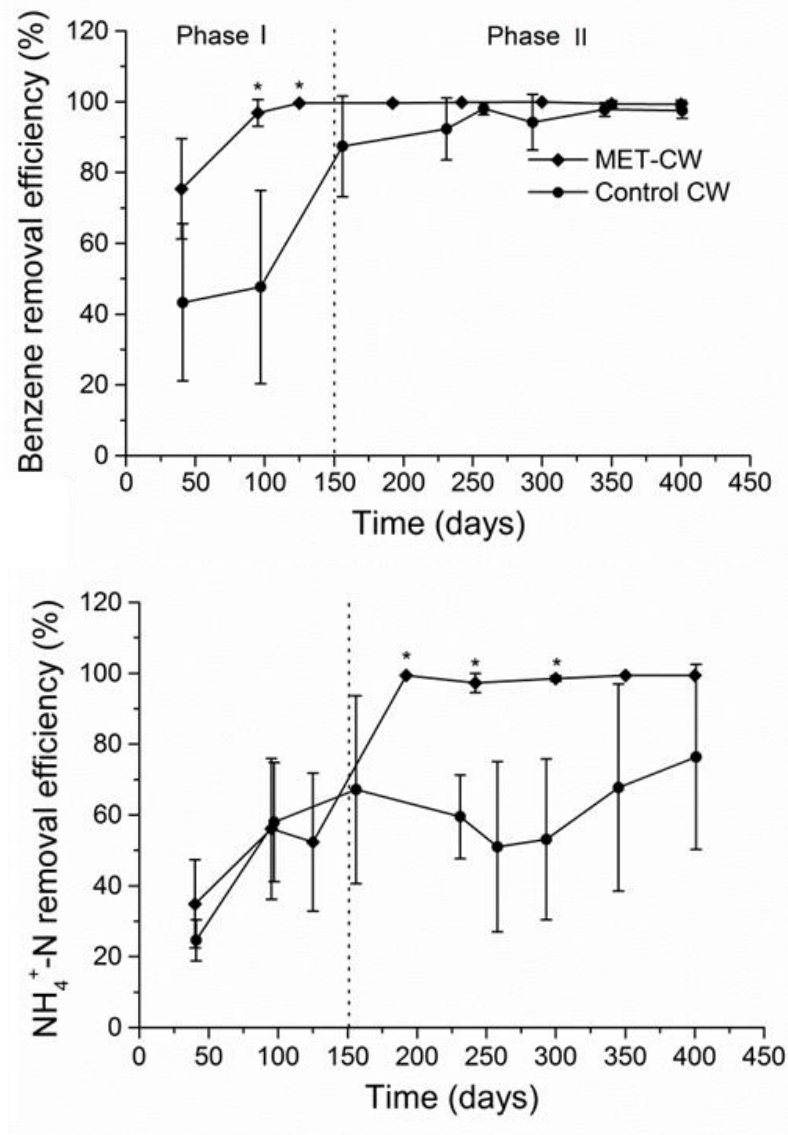


Figure 3-2 Removal efficiencies of benzene and  $\text{NH}_4^+$  in the MET-CW and the control CW within 400 days, calculated based on the averaged mass loads for 24 cm, 36 cm and 48 cm depth at the sampling point after 139 cm flow path (see Fig. 1B). \* represents significant

differences ( $p < 0.05$ ) between the MET-CW and the control CW. Original concentration data in the control CW at days 231, 293 and 345 were already published by Rakoczy et al. (2011).

In phase I, the overall removal efficiencies of benzene and  $\text{NH}_4^+$  gradually increased in both the MET-CW and control CW, indicating the attachment and growth of degraders as it usually occurs in wetland systems (Saeed and Sun 2012). In the first 40 operation days, the removal efficiencies of benzene and  $\text{NH}_4^+\text{-N}$  were similar ( $p > 0.05$ ) in both systems (Figure 3-2). From day 40 to 150, significant differences ( $p < 0.05$ ) were observed between the MET-CW and control CW for benzene removal. In particular, at day 95 and 125, benzene was nearly completely removed in the MET-CW, whereas such high removal efficiencies were obtained in the control CW only after 150 days (Figure 3-2). In phase II (i.e. after 150 days), benzene was almost completely removed in the both MET-CW and control CW. Notably, high removal rates of benzene has also been reported in pilot-scale CWs at the field site Leuna (Chen et al. 2012, Jechalke et al. 2010, Seeger et al. 2011).

Figure 3-3 shows the removal efficiencies of benzene and  $\text{NH}_4^+\text{-N}$  at different sampling points and depths in the MET-CW at day 95 and the control CW at day 97, respectively. Overall, highest removal efficiencies of benzene were observed in the upper layer (24 cm), probably due to a better availability of oxygen reflected by the higher DO concentrations in this layer (Table 3-1). Compared to the control CW, slightly more benzene was removed in the upper layer at 94 cm and 139 cm distance in the MET-CW (Figure 3-3). A hot zone of degradation was detectable in the MET-CW between 94 cm and 139 cm distance; here, the removal efficiencies of benzene in the MET-CW were significantly higher in all three investigated depths (24 cm, 36 cm, 48 cm) compared to the control CW ( $p < 0.05$ ) (Figure 3-3). Notably, the anode modules of MET were placed in this zone (Figure 3-1), indicating that this effect was caused by MET operation. Differences of benzene removal efficiencies between the MET-CW and control CW were much less pronounced at 6 cm, 49 cm and 94 cm distance from the inflow (Figure 3-3). The physico-chemical parameters (pH, DO, Eh,  $\text{Fe}^{2+}$  and  $\text{SO}_4^{2-}$ ) were rather similar in the MET-CW and control CW at all depths along the whole flow path (Table 3-1), indicating that the physico-chemical conditions were generally not changed by the insertion of the anode. In the zone where the MET anodes

where placed (between the sampling points 94 cm and 139 cm), significantly more benzene was removed in the deeper layers (36 and 48 cm depth) where the anode modules 3 and 4 were placed and where the actual DO concentrations were relatively low ( $<0.5 \text{ mg L}^{-1}$ ). Due to the overall higher removal rates in the upper layers of 24 cm depth (Figure 3-2 and 3-3), a large fraction of benzene (88%) was already degraded at 94 cm distance, and only a relatively low percentage of them reached the upper anode modules, thereby leading to less benzene removal at 24 cm depth.

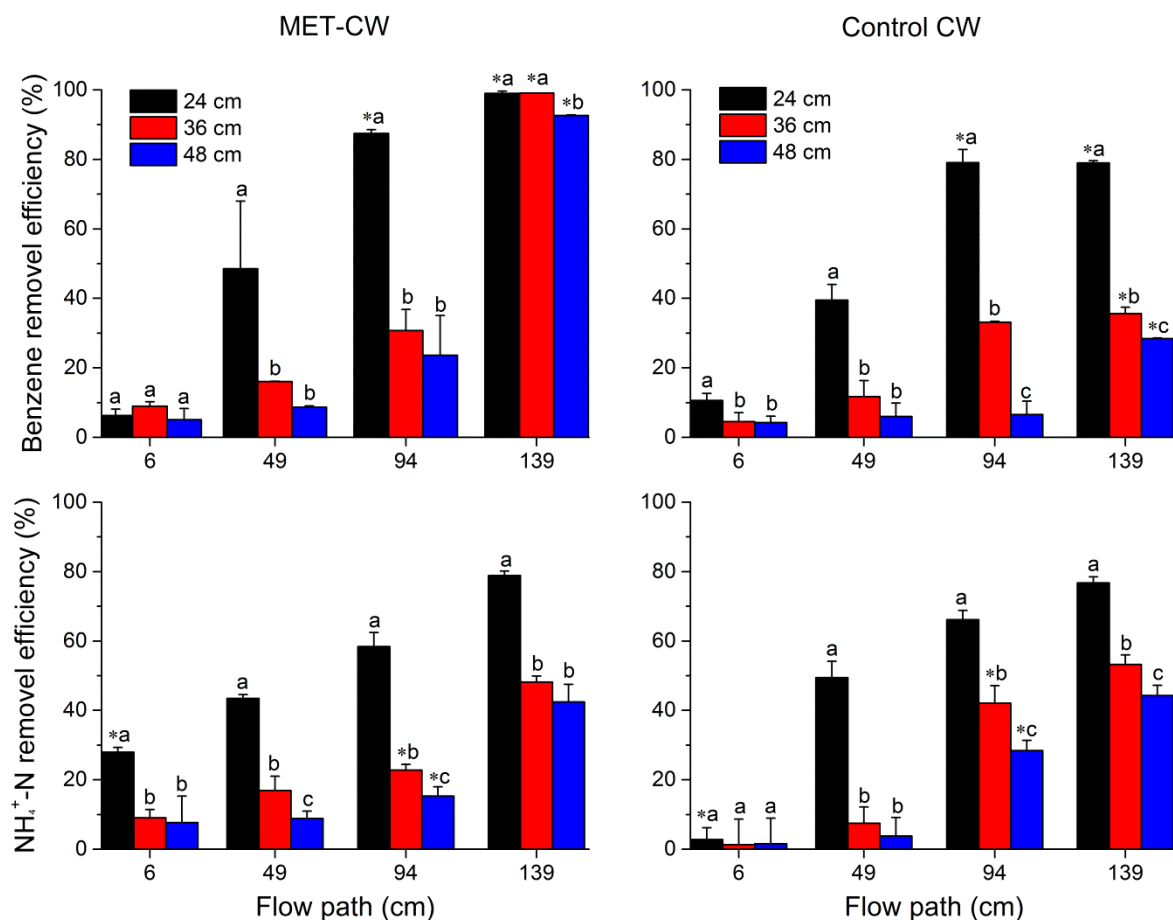


Figure 3-3 Pollutant removal efficiencies along the flow path in the MET-CW at the 95<sup>th</sup> day and the control CW at the 97<sup>th</sup> day. Electricity was effectively generated in the MET-CW (Figure 3-4). \*represents significant differences ( $p < 0.05$ ) between the MET-CW and the control CW at the same sampling sites. <sup>abc</sup>The different letters indicate significant differences ( $p < 0.05$ ) between the different depths at the same flow paths.

Table 3-1 Physico-chemical parameters along the flow path and the depth in the MET-CW and the control CW. Values are the average measured during the whole operation of 400 days.

Flow path	Depths	pH		DO (mg L <sup>-1</sup> )		Eh (mV)		Fe II (mg L <sup>-1</sup> )		SO <sub>4</sub> <sup>2-</sup> (mg L <sup>-1</sup> )	
		MET-CW	Control CW	MET-CW	Control CW	MET-CW	Control CW	MET-CW	Control CW	MET-CW	Control CW
6 cm	24 cm	7.23±0.08 <sup>a</sup>	7.02±0.21 <sup>a</sup>	0.84±0.35 <sup>a</sup>	0.54±0.19 <sup>a</sup>	258±28 <sup>a</sup>	243±87 <sup>a</sup>	1.26±0.92 <sup>a</sup>	3.10±2.88 <sup>ac</sup>	7.52±4.6 <sup>a</sup>	8.24±5.52 <sup>a</sup>
	36 cm	7.26±0.06 <sup>a</sup>	7.05±0.25 <sup>a</sup>	0.16±0.02 <sup>b</sup>	0.26±0.21 <sup>ab</sup>	229±10 <sup>ab</sup>	214±57 <sup>a</sup>	1.85±1.06 <sup>a</sup>	4.13±2.79 <sup>ac</sup>	7.6±4.32 <sup>a</sup>	9.25±4.87 <sup>a</sup>
	48 cm	7.28±0.05 <sup>a</sup>	7.19±0.10 <sup>a</sup>	0.06±0.02 <sup>c</sup>	0.05±0.02 <sup>c</sup>	185±27 <sup>b</sup>	189±64 <sup>ab</sup>	1.80±1.04 <sup>a</sup>	6.33±0.48 <sup>bc</sup>	8.6±5.34 <sup>a</sup>	9.29±5.12 <sup>a</sup>
49 cm	24 cm	7.18±0.14 <sup>a</sup>	6.98±0.14 <sup>b</sup>	0.75±0.39 <sup>a</sup>	0.64±0.02 <sup>a</sup>	270±24 <sup>a</sup>	298±4 <sup>b</sup>	0.62±0.95 <sup>a</sup>	1.84±3.55 <sup>ac</sup>	9.99±4.79 <sup>a</sup>	7.70±5.69 <sup>a</sup>
	36 cm	7.20±0.10 <sup>a</sup>	6.99±0.18 <sup>b</sup>	0.15±0.03 <sup>b</sup>	0.23±0.09 <sup>b</sup>	248±12 <sup>a</sup>	283±25 <sup>b</sup>	1.63±1.27 <sup>a</sup>	3.69±2.71 <sup>ac</sup>	9.43±4.69 <sup>a</sup>	7.83±5.03 <sup>a</sup>
	48 cm	7.22±0.06 <sup>a</sup>	7.08±0.11 <sup>b</sup>	0.05±0.03 <sup>c</sup>	0.04±0.05 <sup>c</sup>	214±17 <sup>bc</sup>	201±35 <sup>c</sup>	2.29±1.41 <sup>a</sup>	5.67±1.09 <sup>bc</sup>	10.16±5.51 <sup>a</sup>	8.83±5.03 <sup>a</sup>
94 cm	24 cm	7.07±0.14 <sup>a</sup>	6.94±0.14 <sup>ac</sup>	0.83±0.29 <sup>a</sup>	0.87±0.19 <sup>a</sup>	288±14 <sup>a</sup>	294±19 <sup>a</sup>	0.20±0.17 <sup>a</sup>	1.32±2.24 <sup>a</sup>	9.31±5.21 <sup>a</sup>	9.03±6.09 <sup>a</sup>
	36 cm	7.11±0.08 <sup>a</sup>	6.95±0.15 <sup>bc</sup>	0.12±0.04 <sup>b</sup>	0.19±0.18 <sup>b</sup>	264±14 <sup>b</sup>	276±25 <sup>ab</sup>	1.44±1.61 <sup>a</sup>	2.42±3.21 <sup>a</sup>	7.27±4.44 <sup>a</sup>	6.46±6.25 <sup>a</sup>
	48 cm	6.89±0.44 <sup>a</sup>	6.99±0.15 <sup>ab</sup>	0.06±0.03 <sup>b</sup>	0.04±0.06 <sup>b</sup>	226±11 <sup>c</sup>	244±36 <sup>bc</sup>	2.38±2.94 <sup>a</sup>	2.99±3.35 <sup>a</sup>	9.07±5.21 <sup>a</sup>	8.70±6.76 <sup>a</sup>
139 cm	24 cm	7.07±0.19 <sup>a</sup>	6.98±0.01 <sup>ac</sup>	0.65±0.30 <sup>a</sup>	0.72±0.28 <sup>a</sup>	294±14 <sup>a</sup>	291±12 <sup>ab</sup>	0.56±0.82 <sup>a</sup>	0.68±0.99 <sup>a</sup>	9.26±4.91 <sup>a</sup>	6.38±3.37 <sup>a</sup>
	36 cm	7.00±0.14 <sup>a</sup>	6.89±0.14 <sup>ac</sup>	0.14±0.03 <sup>b</sup>	0.18±0.13 <sup>b</sup>	277±13 <sup>a</sup>	301±18 <sup>b</sup>	0.77±1.07 <sup>a</sup>	2.37±3.32 <sup>a</sup>	7.75±5.35 <sup>a</sup>	8.39±5.16 <sup>a</sup>
	48 cm	7.06±0.12 <sup>a</sup>	6.93±0.17 <sup>bc</sup>	0.06±0.04 <sup>c</sup>	0.04±0.08 <sup>bc</sup>	236±10 <sup>b</sup>	260±58 <sup>b</sup>	1.06±1.05 <sup>a</sup>	2.70±2.92 <sup>a</sup>	9.69±6.66 <sup>a</sup>	8.19±4.69 <sup>a</sup>

Note: Different superscript letters (<sup>a</sup>, <sup>b</sup> and <sup>c</sup>) indicate significant differences (p<0.05) between the MET-CW and the control CW and between the different sampling depths. If two CWs or two sampling depths share the same letter, the values are not significantly different; if they do not have any letter in common, the values are significantly different (p<0.05).

In contrast to the results for benzene,  $\text{NH}_4^+$  removal efficiencies were similar between the MET-CW and control CW in phase I ( $p > 0.05$ ). However, the mean  $\text{NH}_4^+$  removal efficiency in phase II was significantly higher in the MET-CW (almost 100%) than that observed in the control CW (62%) ( $p < 0.05$ ) (Figure 3-2).  $\text{NO}_3^-$  and  $\text{NO}_2^-$  accumulated only in the upper layers (24 cm) of the MET-CW and control CW (Supporting information Figure S3-2), demonstrating that nitrification was a major removal process. In contrast,  $\text{NO}_3^-$  and  $\text{NO}_2^-$  were not detected in the lower layers of 36 and 48 cm depth, although  $\text{NH}_4^+$  concentrations decreased. This zonation was formed probably due to the levels of DO as average DO values of 0.75 and 0.70  $\text{mg L}^{-1}$  were detected in the upper layers of MET-CW and control CW, respectively, whereas lower average values varying between 0.04 and 0.21  $\text{mg L}^{-1}$  were measured in the lower layers of both CWs (Table 3-1). DO concentrations of less than 0.5  $\text{mg L}^{-1}$  are known to promote denitrification or anaerobic ammonium oxidation and thereby consuming  $\text{NO}_3^-$  and/or  $\text{NO}_2^-$  produced from nitrification (Saeed and Sun 2012). The transformation processes of inorganic nitrogen in the MET-CW will be more deeply described in the chapter 5.

It is known that the availability of substrates and their oxidation activities at the anode are of great importance for electricity generation in METs. In this study, benzene was the main organic substrates in the contaminated groundwater and hence expected to be potential electron donors for the anodic reaction. Our data indicate that the removal of benzene in the first 150 operation days was slightly stimulated by the presence of anode modules in the MET-CW. After 150 days, benzene concentrations in the MET-CW already strongly decreased in the front part of the bed due to the enhanced biodegradation by mature microbial communities, thereby cutting off the anode modules from its fuels, e.g. benzene.

Compared with the control CW, higher  $\text{NH}_4^+$  removal rates in the MET-CW were detected only after 150 days operation. The presence of organic compounds and their metabolic intermediates were described to inhibit the nitrification process in general (Saeed and Sun 2012), as organo-heterotrophic degraders potentially outcompete nitrifiers for the utilization of oxygen and inorganic nitrogen (Ma et al. 2013b), thereby resulting in low nitrification rates under oxygen-limited conditions. The presence of benzene probably inhibited the removal of  $\text{NH}_4^+$ , as also previously observed in field studies at the Leuna site (Jechalke et al. 2011, Seeger et al. 2011). However, the rapid consumption of benzene after 150 days probably leads to a better availability of oxygen for nitrifiers, thereby promoting the  $\text{NH}_4^+$  removal in the MET-CW.

### 3.3.2 Electricity recovery in the MET-CW

#### *The electric energy generation*

The current densities generated from the four anode modules of the MET-CW were recorded during the whole operation as shown in Figure 3-4A. The highest current output was observed in phase I: here, average current densities of  $0.86 \pm 0.74$  and  $1.02 \pm 0.79$  mA m<sup>-2</sup> were obtained in modules 3 and 4, with peak values of 3.39 and 5.46 mA m<sup>-2</sup>, respectively. In contrast, modules 1 and 2 produced very low current during the whole operation, which can be ascribed to the presence of oxygen. In phase II, the current densities of modules 3 and 4 decreased significantly; after 280 days, the current generation ceased completely. Low or no current generation in phase II can be explained by the fact that the more efficient benzene degradation occurred in the front of the bed after the system had been fully developed (Figure 3-2), resulting in less available anodic substrates for the anode modules. The obtained maximum current densities in modules 3 and 4 are too low to make the MET practically competitive for electricity recovery. However, the relationship between the availability of organic substrates and current generation implies the possible application of this MET as a sensor for on-line monitoring pollutant degradation processes *in situ*, as discussed in more detail in section 3.3.3. Huge fluctuations of the current density were probably due to slight variations of the experimental conditions, such as influent pollutant concentrations, pH, or redox potentials (Table 3-1). Fluctuating conditions have been also reported for the integrated HSSF-CW and MFC system studied by Villasenor et al. (2013).

#### *Polarization and power density curves*

The electrochemical performance of the MET-CW was evaluated by determining polarization and power density curves (Figure 3-4B), which were obtained at day 100 in phase I. Modules 3 and 4 showed maximal power densities of 0.86 mW m<sup>-2</sup> at a current density of 3.62 mA m<sup>-2</sup>, and 1.74 mW m<sup>-2</sup> at a current density of 5.75 mA m<sup>-2</sup>, respectively. In contrast, the power densities of modules 1 and 2 were extremely low with maximum values of 0.01 and 0.03 mW m<sup>-2</sup> respectively (corresponding to the observed extremely low current densities, Figure 3-4A), which was attributed to the noise current and thus considered to be negligible. These results suggest that the anodes located in the deeper layer (modules 3 and 4) supported solely the electricity generation. The very low current generations of modules 1 and 2 are possibly due to

higher DO concentrations (Table 3-1) disturbing the anodic reaction of the MET. Oxygen in the upper layers - stemming from atmospheric diffusion - will outcompete the anode as electron acceptor. This result was also consistent with the removed masses of benzene as described in section 3.3.1.

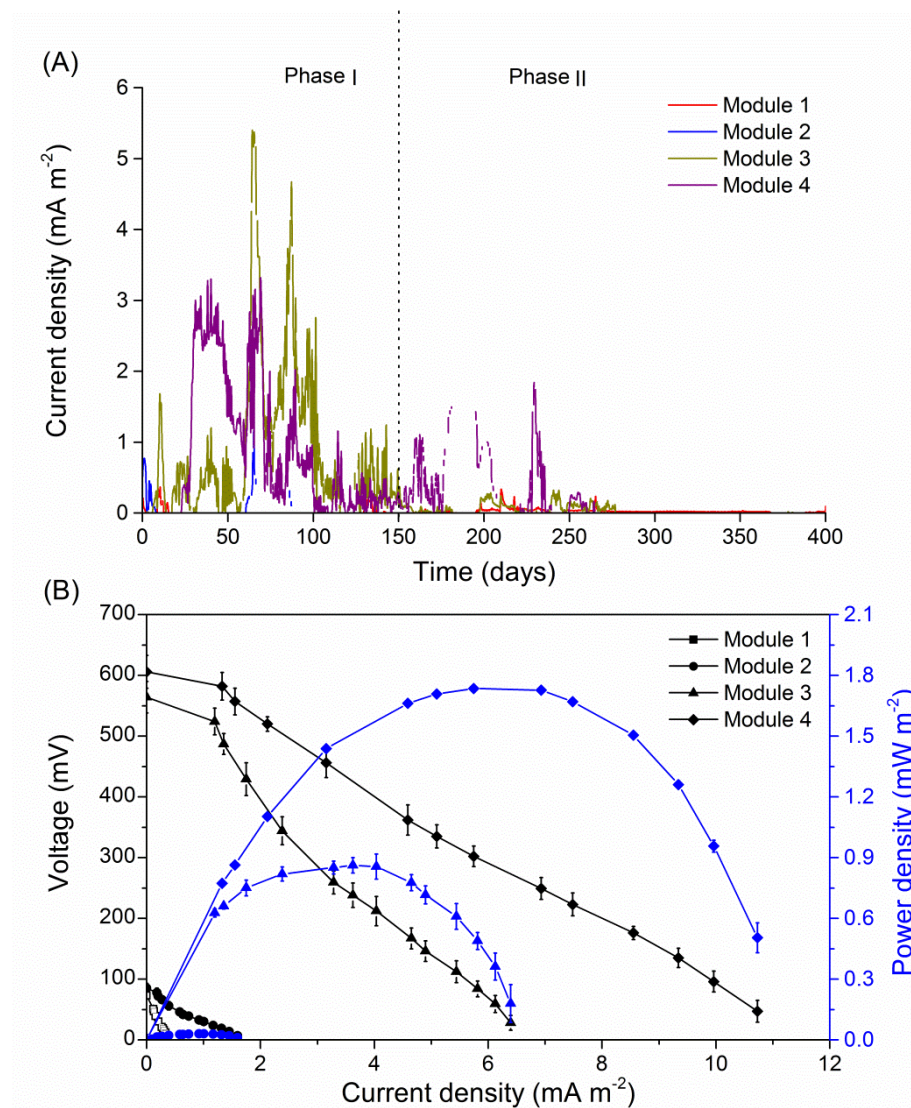


Figure 3-4 Electricity generation performance of the anode modules in the MET-CW. (A) current generation during the whole operation period; (B) polarization and power density curves. Average values and standard deviation were calculated from measurements of three replicates.

In recently described planted MET-CW systems with vertical or horizontal subsurface flow (Fang et al. 2013, Villasenor et al. 2013, Zhao et al. 2013), the cathodes were installed in

the more aerobic upper layer. In the present study, the cathode was located in the open water pond, avoiding the recirculation of pollutants from the anodic compartment to the cathodic compartment; in addition, an open water pond is more effective for storing oxygen, thereby eliminating the negative effect of the residual organic matter on the maintenance of aerobic conditions at the cathode under high organic loading rates as observed by Villasenor et al. (2013).

The maximum power density of  $1.74 \text{ mW m}^{-2}$  obtained in this work is relatively low compared to previously published studies (Villasenor et al. 2013, Yadav et al. 2012, Zhao et al. 2013), in which values in the range between 10 and  $50 \text{ mW m}^{-2}$  were observed (Table 3-2). The relatively low power densities obtained in this study might be due to lower amounts of available substrates, differences in the electrochemical properties of substrates or other operation and construction parameters (e.g., the magnitude of the internal resistance). However, they are comparable with values obtained in the MFC systems treating waters contaminated with petroleum hydrocarbons, e.g. benzene (Rakoczy et al. 2013, Wang et al. 2012, Wu et al. 2013), where power densities from  $0.85$  to  $2.1 \text{ mW m}^{-2}$  were reported. Recently, a maximum power density of  $316 \text{ mW m}^{-3}$  NAC (net anodic compartment) and a coulombic efficiency of 14% was obtained in a lab-scale MFC treating the same groundwater contaminated with benzene and  $\text{NH}_4^+$ -N as used in the present study, in which graphite granules were used as electrode materials (Wei et al. 2015a). In our study, coulombic efficiencies were calculated based on benzene removal since benzene was identified as primary anodic substrate (see section 3. 3. 3). The average coulombic efficiencies of  $3.69 \pm 0.81\%$  and  $4.89 \pm 0.60\%$  were obtained for the modules 3 and 4 in phase I, which are comparable with values reported for other CW-MFC systems (Table 3-2).

Based on the slopes of the polarization curves, internal resistances of  $1588 \pm 83$  and  $1253 \pm 41 \Omega$  were obtained for modules 3 and 4, respectively. It is generally known that the power density reaches its peak value when the external resistance is equal to its internal resistance (Harnisch and Schroder 2010). According to the power density curves, the maximum power densities were obtained at the external resistance of 1500 and 1200  $\Omega$  for module 3 and 4, consistent with the values calculated from the slopes of the polarization curves. The high internal resistances were probably caused by the relative long distance (~80 cm) between the anode modules and the cathode in the MET-CW, leading to a decrease of the electricity generation

performance. However, those values are still in an acceptable range; similar values were reported in our previous study using a ‘classical’ MFC system (Wei et al. 2015a).

Table 3-2 Investigated pollutants, used loading rates, and gained electrochemical parameter in this and other constructed wetland systems combined with microbial electrochemical technology.

Configuration	Wastewater	Pollutants	Loading rate ( $\text{g m}^{-2} \text{d}^{-1}$ )	Maximum power density ( $\text{mW m}^{-2}$ )	Coulombic efficiencies (%)	Reference
VSSF CW	Synthetic	Methylene	Bacth mode	15.73	0.05 - 0.06	Yadav et al. (2012)
VSSF CW	Synthetic	Azo dye	0.73 - 2.63	8.98	0.58 - 1.71	Fang et al. (2013)
VSSF CW	Synthetic	COD	2.82 - 2.99	12.42	0.39 - 1.29	Liu et al. (2013)
HSSF CW	Synthetic	COD	13.9-61.1	43	0.27 - 0.45	Villasenor et al.
VSSF CW	Swine	COD	46.49 - 65.72	9.4	0.1 - 0.6	Zhao et al. (2013)
VSSF CW	Synthetic	COD	1.06 - 5.96	55.05	8.39 - 10.48	Liu et al. (2014)
HSSF CW	Contaminated groundwater	Benzene $\text{NH}_4^+\text{-N}$	0.16 - 0.23 0.62 - 0.84	1.74	3.69 - 4.89	This study

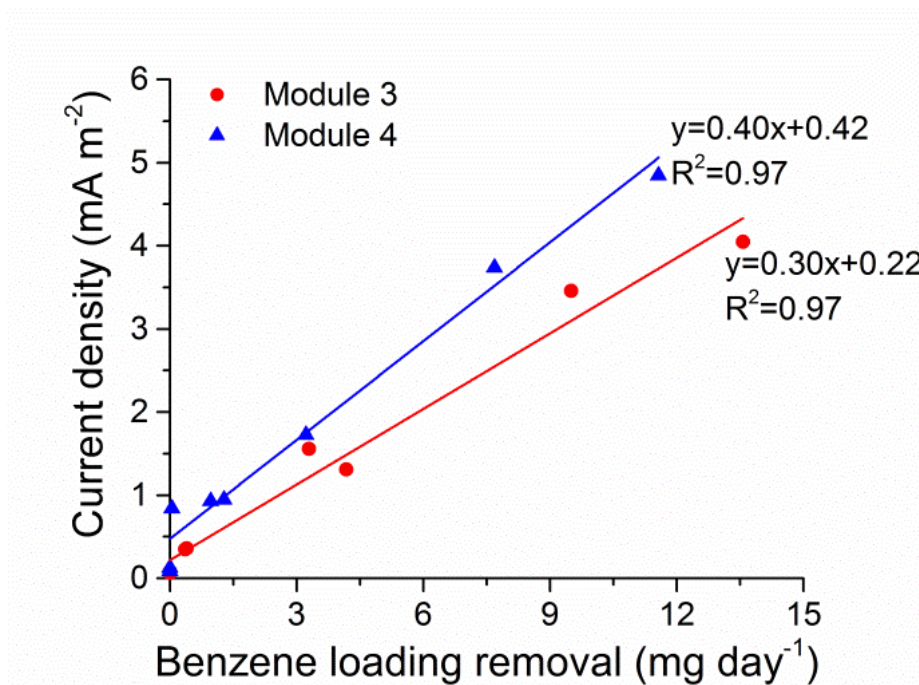


Figure 3-5 Linear relationship between benzene loading removal by the anode modules and current generation in the MET-CW. The pollutant loading removal was calculated as the difference in pollutant loads between the sampling points at 94 cm and 139 cm.

### 3.3.3 Correlations between pollutant removal and electricity generation

In order to further clarify the relationship of benzene removal and electricity generation in the MET-CW, a regression analysis between pollutant loading removal by the anode modules and generated current density was performed. When integrating the two pollutants by multiple-regression analysis, benzene degradation was identified to be the primary correlation factor ( $p < 0.05$ ), explaining 99% and 100% of the variation in current generation for the modules 3 and 4, respectively. As shown in Figure 3-5, benzene loading removal rates and current densities were strongly correlated ( $R = 0.99$ ,  $p < 0.05$ ). The steeper slope for module 4 indicated that this module generated current more efficiently; correspondingly, the higher current generation was also obtained in module 4 (Figure 3-4). In contrast,  $\text{NH}_4^+$  removal was not significantly associated with current densities in the modules 3 and 4 ( $p > 0.05$ ), implying no direct link between  $\text{NH}_4^+$  removal and current generation in the MET-CW. Thus, current was generated mainly by oxidation of benzene at the anode.

The strong linear correlation between current generation and benzene removal indicates the possibility for monitoring benzene degradation using a MET based biosensor. In order to justify and evaluate the potential for the practical application, the operational parameters, such as reproducibility, stability and detection limit, need to be clarified in future studies. Nevertheless, our results indicate a promising technique for monitoring the removal of organic pollutants in constructed wetlands on-line and *in situ*.

### 3.3.4 Electron donors for the anode modules

Benzene was identified as the primary anodic electron donor in this MET-CW. From thermodynamic views, the lower redox potential of the benzene oxidation ( $\text{HCO}_3^-/\text{C}_6\text{H}_6$ ,  $E^0 = -0.28$  V) are favorable for benzene degradation at the anode compared to that of possible reactions involved in  $\text{NH}_4^+$  removal. Comparison of possible Half-cell reactions and thermodynamic cell potential (Eh) for benzene and  $\text{NH}_4^+$  is presented in Table 3-3. Interestingly, the rapid consumption of benzene stimulated by the anode modules eliminates potential negative effects on  $\text{NH}_4^+$  oxidation, and thereby promoting  $\text{NH}_4^+$  removal in the MET-CW in the first 150 days.

Table 3-3 Comparison of possible half-cell reactions and thermodynamic cell potential (Eh) for benzene and  $\text{NH}_4^+$  in this study.

Pollutants	Possible reactions	Eh (V)	$\Delta G^0$ (kJ mol <sup>-1</sup> )
Benzene	Anode: $\text{C}_6\text{H}_6 + 18 \text{H}_2\text{O} \rightarrow 6 \text{HCO}_3^- + 30 \text{e}^- + 36 \text{H}^+$	$E^0(\text{HCO}_3^-/\text{C}_6\text{H}_6) = -0.28$	-3173
	Cathode: $\text{O}_2 + 4 \text{H}^+ + 4 \text{e}^- \rightarrow 2 \text{H}_2\text{O}$	$E^0(\text{O}_2/\text{H}_2\text{O}) = 0.82$	
	Overall: $\text{C}_6\text{H}_6 + 7.5 \text{O}_2 + 3 \text{H}_2\text{O} \rightarrow 6 \text{HCO}_3^- + 6 \text{H}^+$	$E_{\text{cell}} = 1.10$	
$\text{NH}_4^+$	$\text{NH}_4^+ + \text{O}_2 + \text{H}^+ + 2 \text{e}^- \rightarrow \text{NH}_2\text{OH} + \text{H}_2\text{O}$	$E^0(\text{NH}_4^+/\text{NH}_2\text{OH}) = 1.02$	-118
	$\text{NH}_2\text{OH} + \frac{1}{2} \text{O}_2 \rightarrow \text{HNO}_2 + 2 \text{H}^+ + 2 \text{e}^-$	$E^0(\text{NO}_2^-/\text{NH}_2\text{OH}) = 0.06$	-134
	$\text{NO}_2^- + \frac{1}{2} \text{O}_2 \rightarrow \text{NO}_3^-$	$E^0(\text{NO}_3^-/\text{NO}_2^-) = 0.43$	-74
	$\text{NO}_3^- + 6 \text{H}^+ + 5 \text{e}^- \rightarrow \frac{1}{2} \text{N}_2 + 3 \text{H}_2\text{O}$	$E^0(\text{NO}_3^-/\frac{1}{2}\text{N}_2) = 0.74$	-361

Although  $\text{NH}_4^+$  removal from wastewater using electrochemical technologies has been previously reported, there is no unanimous agreement whether  $\text{NH}_4^+$  can be used as a direct substrate for electricity generation in METs. He et al. (2009) showed that electricity production is associated with  $\text{NH}_4^+$  oxidation in a rotating-cathode MFC, where current generation resulted from heterotrophic exoelectrogenesis sustained by nitrifier-produced organic substrates rather than direct ammonium oxidation. Furthermore, You et al. (2009) reported that additional protons produced by  $\text{NH}_4^+$  oxidation can accelerate the cathodic reaction (e.g. oxygen reduction), thereby contributing to electricity generation by reducing the ohmic resistance and maintaining the pH balance. However, intermediates (hydroxylamine and  $\text{NO}_2^-$ ) of ammonium oxidation can release electrons in the view of thermodynamic properties and may possibly serve as anodic substrate to generate current (Chen et al. 2014); the reduction of the end product ( $\text{NO}_3^-$ ) at the cathode can also result in electrochemical denitrification. In this study,  $\text{NH}_4^+$  oxidation was not directly linked with electricity generation in the MET-CW in the presence of benzene as co-contaminants. Nitrification reactions are characterized by more positive redox potentials and generate less available energy compared to benzene oxidation reaction, suggesting that  $\text{NH}_4^+$  is a less favorable anode substrate. Correspondingly, Wei et al. (2015a) reported that  $\text{NH}_4^+$  oxidation did not contribute to electricity generation in a MFC with aerated cathode. The higher removal of  $\text{NH}_4^+$  in phase II can be attributed to the elimination of the inhibitory effects caused by benzene due to their rapid consumption.

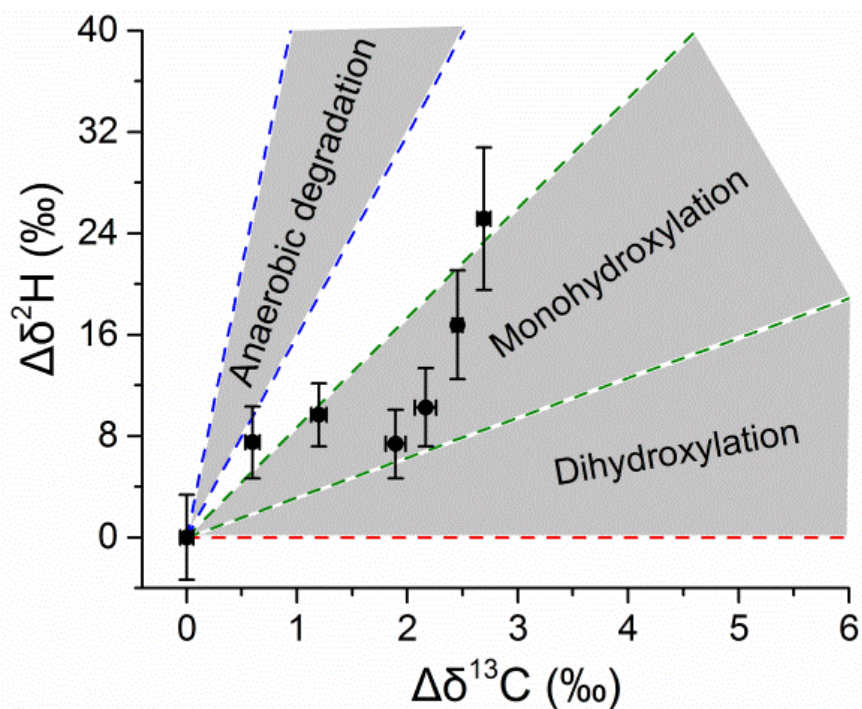


Figure 3-6 Two-dimensional isotope plot of  $\Delta\delta^{13}\text{C}$  versus  $\Delta\delta^2\text{H}$  values of benzene measured from pore water samples of the MET-CW at the 95<sup>th</sup> day. Data were from the depths of 36 cm and 48 cm. Values of  $\Delta\delta$  were calculated by subtracting the measured isotopic value from the initial isotopic value determined at the influent.

### 3.3.5 Implications for the mechanism of benzene activation

Compound-specific isotope analysis (CSIA) was performed in order to identify the initial activation mechanisms for benzene degradation in the MET-CW. Application of CSIA to characterize benzene activation mechanisms has been successfully demonstrated in laboratory and field studies (Fischer et al. 2008b, Rakoczy et al. 2013, Rakoczy et al. 2011). A significant shift in the carbon and hydrogen isotope signature was observed with  $\Delta\delta^{13}\text{C}$  up to +2.7‰ and  $\Delta\delta^2\text{H}$  up to +15‰ (Supporting information Figure S3-3). By comparing the values of two-dimensional CSIA with previously published values for aerobic and anaerobic benzene activation mechanisms, the data from our study mainly matched with those indicative for pathways initiated by benzene monohydroxylation (Figure 3-6). The slope of the linear regression between hydrogen and carbon isotope discrimination ( $\Lambda = \Delta\delta^2\text{H} / \Delta\delta^{13}\text{C}$ ) obtained in the MET-CW was  $\Lambda = 7 \pm 2$  ( $R^2 = 0.71$ ). It has been predicted that the initial activation step of

monohydroxylation reaction leads to  $\Lambda$ -values ranging between 3 and 11 depending on the reaction mechanism of monooxygenase (Fischer et al. 2008b), which can be distinguished significantly from pathways initiated by (i) benzene dihydroxylation, a reaction which is usually not linked to a significant hydrogen isotope effect, and (ii) anaerobic benzene degradation, which is usually characterized by the larger  $\Lambda$  values ( $\Lambda > 13$ ). Benzene monohydroxylation as initial activation mechanism of benzene degradation was already reported by Rakoczy et al. (2011) for the control-CW, and also identified in a MFC treating benzene and sulfide-contaminated groundwater (Rakoczy et al. 2013). However, we cannot exclude that benzene was actually anaerobically activated by a mechanism producing similar carbon and hydrogen isotope fractionation as observed for monohydroxylation, or that the isotope signatures were produced by a mixing of aerobic and anaerobic activation mechanisms due to the coexistence of oxic and anoxic zones in the CW. Due to the detection of at least small amounts of DO at each sampling location during the whole experimental time (Table 3-1), strictly anoxic processes may not have played a significant role for benzene degradation. In any case, the degradation of benzene and/or its intermediates accelerated electricity generation by transferring the released electrons to the anode in the MET-CW.

### 3.4 Supporting information

(A)



(B)

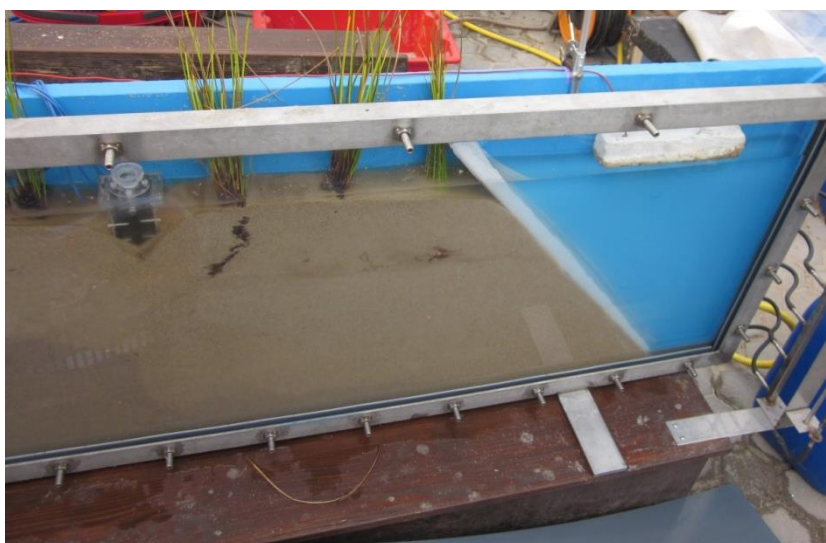


Figure S3-1 Pictures of MET-CW system. (A): the anodic modules, (B): MET-CW.

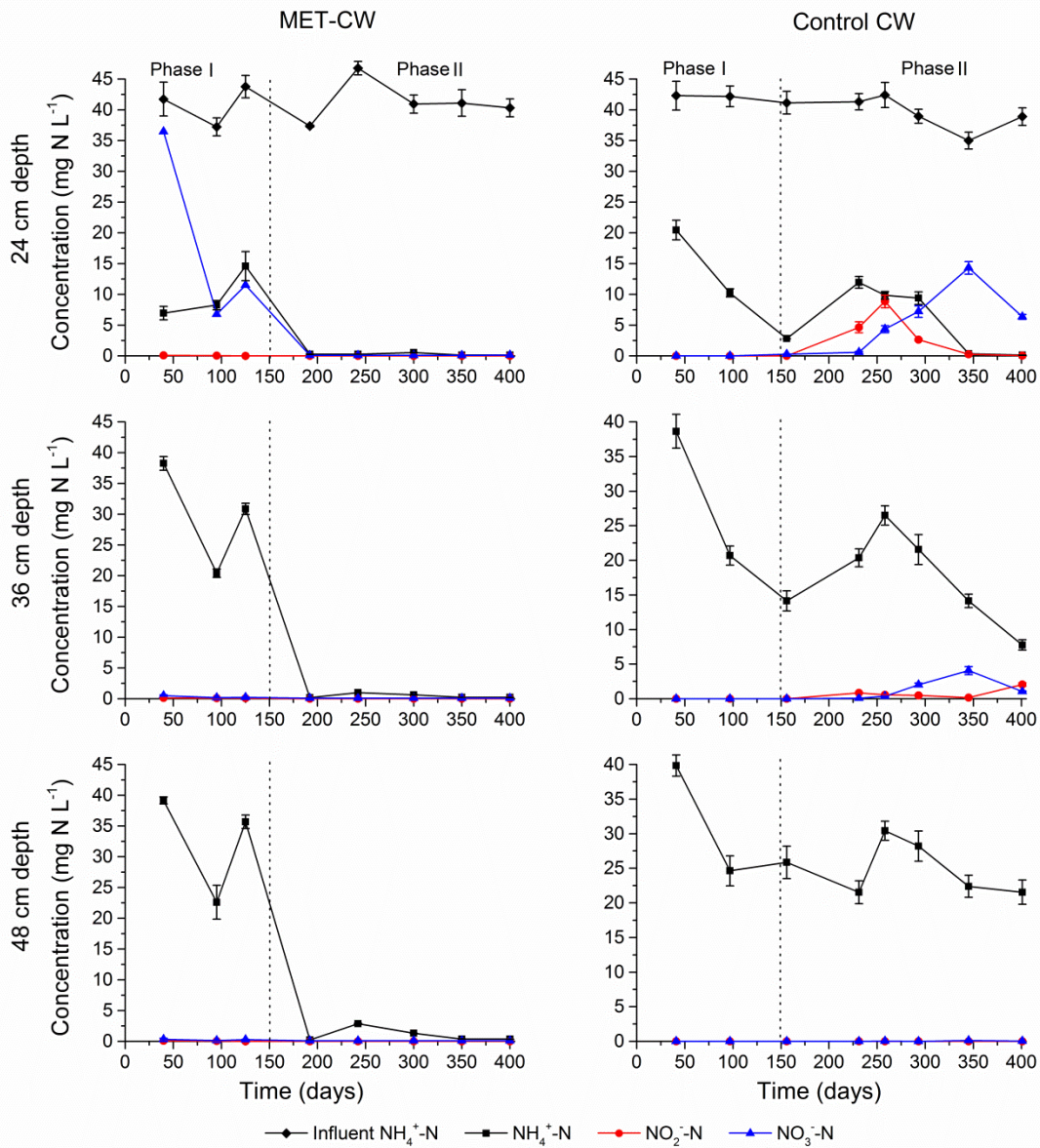


Figure S3-2 Time-dependent concentration changes of inorganic nitrogen compounds ( $\text{NH}_4^+$ ,  $\text{NO}_2^-$ , and  $\text{NO}_3^-$ ) at the sampling points at 139 cm distance to the influent (different depths: 24 cm, 36 cm, 48 cm).

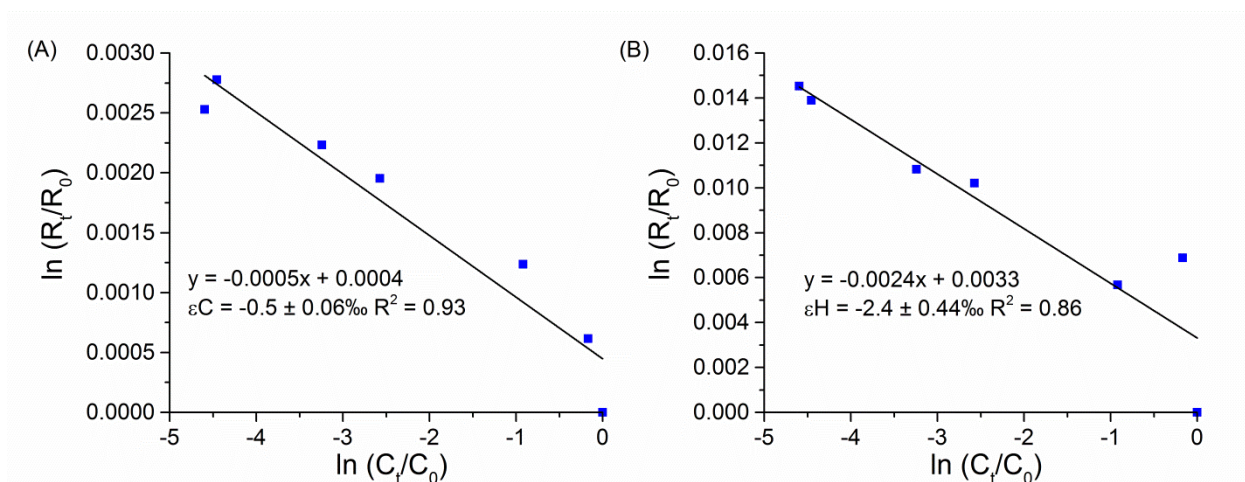


Figure S3-3 Rayleigh plot for carbon (A) and hydrogen (B) stable isotope fractionation of benzene in the MET-CW. The slope in each graph represents the currently lowest isotope fractionation pattern obtained in reference experiments characterizing the benzene monohydroxylation pathway towards the dihydroxylation pathway;  $\varepsilon = -1.7$  and  $-11$  for carbon and hydrogen, respectively (Fischer et al. 2008b, Mancini et al. 2008).

## **CHAPTER 4 Isotopic and proteomic evidence for microbial nitrogen transformation processes in the MET-CW**

Manman Wei<sup>a</sup>, Carsten Vogt<sup>a, \*</sup>, Vanessa Lünsmann<sup>b</sup>, Naomi Susan Wells<sup>c</sup>, Jana Seifert<sup>d</sup>, Nico Jehmlich<sup>b</sup>, Kay Knöller<sup>c</sup>, Hans H. Richnow<sup>a</sup>

<sup>a</sup> Department of Isotope biogeochemistry, Helmholtz Centre for Environmental Research-UFZ, Permoserstraße 15, 04318, Leipzig, Germany

<sup>b</sup> Department of Proteomics, Helmholtz Centre for Environmental Research-UFZ, Permoserstraße 15, 04318 Leipzig, Germany

<sup>c</sup> Department of Catchment Hydrology, Helmholtz Centre for Environmental Research-UFZ, Theodor-Lieser-Straße 4, 06120 Halle, Germany

<sup>d</sup> Institute of Animal Nutrition, Hohenheim University, 70593 Stuttgart, Germany

\*Corresponding author: Carsten Vogt; Tel.: +49-341-235-1357; fax: +49-341-235-1443; E-mail: carsten.vogt@ufz.de

This manuscript is in preparation for publication in a scientific journal.

## Abstract

Microbial nitrogen transformation processes were investigated in a MFC-CW using isotope fractionation,  $^{15}\text{N}$ -isotope tracing, and protein-based stable isotope probing (protein-SIP) with *in situ*  $^{15}\text{N}$ - $\text{NH}_4^+$  feeding.  $\delta^{15}\text{N}$ - $\text{NH}_4^+$  showed a significantly negative relationship with  $\text{NH}_4^+$ -N loads, yielding an isotope fractionation factor that varied between -1.5 to -5.9‰. The  $^{15}\text{N}$  enrichment factors of  $\text{NH}_4^+$  ranged from -1.5 to -5.9‰, which were generally smaller than those reported for ammonia oxidation in pure culture but are comparable to those for nitrification in groundwater and the pilot-scale CWs treating contaminated groundwater. These results implied the occurrence of microbial ammonia oxidation. Metaproteomic analysis revealed that *Nitrosomonadales*, *Burkholderiales*, *Rhizobiales* and *Clostridiales* were dominant genera, which were potential nitrifying or denitrifying bacteria. The proteins related to anammox bacteria showed only a low abundance, implying that anammox was of low importance in nitrogen transformation in the MET-CW. Protein-SIP analysis indicated the occurrence of partial nitrification, heterotrophic denitrification and nitrifier denitrification, and the identification of  $^{15}\text{N}$  incorporated ammonia monooxygenase, hydroxylamine oxidase, and nitrite reductase affiliated to *Nitrosomonas* as well as nitrous oxide reductase belonging to denitrifying bacteria provided direct evidence for the activities of these pathways responsible for  $\text{NH}_4^+$  removal in the MET-CW. Interestingly,  $^{15}\text{N}$  incorporated nitrite reductase were exclusively affiliated to *Nitrosomonas*, illustrating that the existence of nitrite reduction via nitrifier-denitrification by *Nitrosomonas*.  $^{15}\text{N}$ -isotope tracing experiment results showed that denitrification contributed to 84-96% of total  $\text{N}_2$  production with the rates of 0.62-13.37  $\text{nmol N}_2 \text{ g}^{-1} \text{ h}^{-1}$ , whereas anammox showed the rates of 0.11-0.91  $\text{nmol N}_2 \text{ g}^{-1} \text{ h}^{-1}$ , contributing to 4-5% of  $\text{N}_2$  production only at subsequently increased to 15.07% at the 139 cm distance in the front of where anode modules were located. In summary, the isotope data, together with protein-SIP and metaproteomic analysis demonstrated that partial nitrification accompanied by either heterotrophic denitrification or nitrifier-denitrification was mainly responsible for  $\text{NH}_4^+$ -N removal in the MET-CW, whereas anammox played a minor role but anammox contribution was markedly enhanced by the presence of anode modules in the MET-CW. This work is the first report to directly identify functional proteins and active species involved in microbial nitrogen transformation using protein-SIP analysis, and

provides a promising approach to trace functional proteins and active species involved in microbial nitrogen transformation pathways in the complex ecosystems.

**Key words** microbial nitrogen transformation,  $^{15}\text{N}$  isotope tracing technique, protein-SIP, and microbial electrochemical technology-constructed wetland

## 4.1 Introduction

Constructed wetlands (CWs) represent an effective and cost-saving alternative for the treatment of a variety of wastewater, e.g. domestic or municipal sewage, industrial and agricultural wastewater, or contaminated groundwater (Imfeld et al. 2009). Different types of CWs including free-water-surface (FWS), horizontal subsurface flow (HSSF) and vertical subsurface flow (VSSF) CWs have been developed to remove N compounds from wastewater or groundwater (Wu et al. 2014). In general, VSSF-CWs can efficiently convert  $\text{NH}_4^+$  to  $\text{NO}_3^-$  due to its greater oxygen transfer capacity in comparison to FWS and HSSF-CWs but very limited denitrification usually results in the accumulation of  $\text{NO}_3^-$  in the outflow; whereas, the HSSF-CWs provide anoxic/anaerobic conditions suitable for denitrification but the ability to nitrify  $\text{NH}_4^+$  is very limited due to the absence of oxygen, therefore, high efficient  $\text{NH}_4^+$ -N removal is not easily achievable in the HSSF-CWs (Vymazal 2007). The use of microbial electrochemical technology (MET), e.g. microbial fuel cells (MFCs), to treat N-rich wastewater has been reported and attracted growing attentions due to the potential benefits of electricity recovery associated with nitrogen removal (Mook et al. 2012). More recently, the integration of MFCs into CWs was shown to be a promising alternative to enhance wastewater treatment and achieve energy recovery based on the complementary point of two individual processes (Fang et al. 2013, Villasenor et al. 2013, Yadav et al. 2012, Zhao et al. 2013). The separated anoxic and oxic zones, where oxidation and reduction reactions take place, can function as anode and cathode of MFCs, thereby supporting the combination of MFCs with CWs. The integration of MFCs into HSSF-CWs was also proved to be feasible at lab scale. Villasenor et al. (2013) installed a horizontal, rectangular graphite anode located in the gravel bed and an identical graphite cathode in the upper rhizosphere of a HSSF-CW treating wastewater. The system efficiently removed COD while effectively generating electricity. In chapter 4, we

integrated a MET into a HSSF-CW and observed the enhanced removal of benzene and  $\text{NH}_4^+\text{-N}$  from contaminated groundwater. Thus, combining MET and HSSF-CWs seems to also be a promising technique to treat wastewater containing higher concentrations of  $\text{NH}_4^+$ . These previous studies primarily focused on optimizing the operational parameters of the integrated systems for efficient nitrogen removal. However, knowledge about nitrogen transformation and removal pathways in the integrated MET-CW systems is still not well understood.

Nitrogen removal mechanisms in the HSSF-CWs have been studied in several previous reports and it is generally accepted that microbial conversion is the main process responsible for nitrogen removal (Lee et al. 2009). Hence, the knowledge about microbial nitrogen transformation processes and the responsible organisms is a key issue for improving nitrogen removal efficiencies in CWs and optimizing the technical design. In addition to conventional nitrification and denitrification processes, partial nitrification and anammox were also reported to likely occur in the HSSF-CWs (Coban et al. 2015a, Zhang et al. 2011). Although these potential nitrogen removal processes have been reported in HSSF-CWs, the contribution of each process and microbial populations catalyzing these processes are yet not well understood.

Microbial nitrogen transformation processes have been investigated using a variety of analytical methods, including physicochemical measurements, classical cultivation techniques, molecular methods and stable isotope tools.  $^{15}\text{N}$  isotope-based approaches, especially  $^{15}\text{N}$  isotope fractionation signatures and  $^{15}\text{N}$  isotope tracing techniques, have been used to evaluate nitrogen transformation processes and their individual contributions in marine sediments, soils and also wetland systems (Coban et al. 2015b, Erler et al. 2008, Reinhardt et al. 2006, Song et al. 2013a).  $^{15}\text{N}$  isotope fractionation can potentially reflect the source of N; due to different magnitudes of isotope fractionation of the respective pathway, it is possible to distinguish different nitrogen transformation processes (e.g. nitrification, denitrification and biological  $\text{N}_2$ -fixation) (Brunner et al. 2013, Coban et al. 2015b, Reinhardt et al. 2006, Robinson et al. 2012).  $^{15}\text{N}$  isotope tracer incubation has become a valuable tool for measuring rates of potential denitrification and anammox, also allowing the identification of the relative contribution of denitrification and anammox (Coban et al. 2015a, Zhu et al. 2011). Protein-based stable isotope probing (protein-SIP) is

a powerful method with a higher sensitivity in comparison with DNA- or RNA-SIP, which can not only provide taxonomic information similar to DNA or RNA analysis but also reflect the metabolic properties and actual activities of cells (von Bergen et al. 2013). However, the application of protein-SIP to trace microbial nitrogen transformation processes and reveal active species has not yet been reported.

The objective of this study was to reveal nitrogen transformation processes in order to understand their importance for nitrogen removal in the MET-CW. The nitrogen transformation processes in the MET-CW were qualitatively and quantitatively analyzed by stable isotope analysis of inorganic N species (N isotope fractionation signatures) and  $^{15}\text{N}$  isotope tracing techniques. Active microbial species involved in nitrogen transformation processes were detected using *in situ* protein-SIP and metaproteomic analysis. In addition, the effect of anode insertion on nitrogen transformation processes in the HSSF-CW was discussed.

## 4.2 Materials and Methods

### 4.2.1 N isotopic analysis of $\text{NH}_4^+$

Water samples from the inflow and four flow distances of 6, 49, 94 and 139 cm in the deep layer (36 and 48 cm) were collected at operation days of 95, 192, 300 and 400 according to methods described elsewhere (Rakoczy et al. 2011). 50 mL of samples were stored at  $-20^\circ\text{C}$  until  $\text{NH}_4^+$  isotope analysis.

The  $\text{NH}_4^+$  isotope composition was analyzed using hypobromite ( $\text{BrO}^-$ ) oxidation and azide reaction method described by Zhang et al. (2007). The product  $\text{N}_2\text{O}$  was measured on an isotope ratio mass spectrometer (IRMS) Delta V plus (Thermo Electron GmbH, Bremen, Germany) with a Gasbench II (Thermo Electron GmbH, Bremen, Germany). Each sample batch was run with two international reference standards of USGS25 ( $\delta^{15}\text{N}$ ,  $-30.4\text{‰}$ ), and USGS26 ( $\delta^{15}\text{N}$ ,  $+53.7\text{‰}$ ) plus an internal standard ( $\delta^{15}\text{N}$ ,  $0\text{‰}$ ) for calibration. The analytical precision was  $\pm 0.4\text{‰}$ . The  $^{15}\text{N}/^{14}\text{N}$  isotope ratios are expressed as delta ( $\delta$ )-notation in per mil ( $\text{‰}$ ) relative to the standards of atmospheric  $\text{N}_2$  (AIR). The kinetic isotope fractionation is calculated according to (Mariotti et al. 1981) using the Rayleigh equation:

$$\ln\left(\frac{\delta^{15}N+1}{\delta^{15}N_0+1}\right) = \varepsilon \times \ln(f)$$

where  $\varepsilon$  is the enrichment factor and  $f$  is the fraction of the initial  $\text{NH}_4^+\text{-N}$  remaining at the point of measurement. In our case,  $f$  was modified by  $\text{NH}_4^+\text{-N}$  loads when considering water loss as previously described (Wei et al. 2015b); the inflow is defined as zero point.

#### 4.2.2 *In situ* $^{15}\text{N}$ labelling experiment

After continuously running for 400 days, a  $^{15}\text{N}$  labeling experiment was *in situ* carried out by pumping artificial groundwater containing  $^{15}\text{N-NH}_4\text{Cl}$  instead of contaminated groundwater from the Leuna site into the MET-CW system. The artificial groundwater medium was prepared according to the chemical components of original Leuna groundwater as follows:  $0.15 \text{ g L}^{-1} \text{ }^{15}\text{N-NH}_4\text{Cl}$ ,  $0.01 \text{ g L}^{-1} \text{ KH}_2\text{PO}_4$ ,  $0.006 \text{ g L}^{-1} \text{ K}_2\text{HPO}_4$ ,  $0.84 \text{ g L}^{-1} \text{ NaHCO}_3$ ,  $0.03 \text{ g L}^{-1} \text{ FeSO}_4 \cdot 7\text{H}_2\text{O}$ ,  $0.3 \text{ g L}^{-1} \text{ MgCl}_2 \cdot 6\text{H}_2\text{O}$ ,  $0.1 \text{ g L}^{-1} \text{ CaCl}_2$  and  $1 \text{ mL L}^{-1}$  trace elements solution as described in Verhagen and Laanbroek (1991). The medium was autoclaved, flushed with  $\text{N}_2$ , and then stored in a 50 L stainless steel tank under constant dinitrogen pressure (0.5 bar) at  $14 \pm 2^\circ\text{C}$ . The MET-CW was continuously fed with artificial groundwater containing  $^{15}\text{N}$ -labelled  $\text{NH}_4^+\text{-N}$  for 28 days similar to the operation in the first 400 days of the experiment. At day 28, sand samples in the MET-CW were taken from the deep layer (36-48 cm) at the four flow distances of 6, 49, 94 and 139 cm, respectively, and were subsequently analyzed by protein-SIP. In this depth, the actual oxygen concentrations were below  $0.05 \text{ mg L}^{-1}$ ; here,  $\text{NH}_4^+\text{-N}$  was efficiently removed but no  $\text{NO}_2^-\text{-N}$  and  $\text{NO}_3^-\text{-N}$  accumulations were observed in supporting information Figure S3-2.

#### 4.2.3 Protein-SIP and metaproteomic analysis

Proteins extraction was performed using a modified protocol as described previously (Wang et al. 2011). Briefly, 5 g of sands were homogenized and extracted by shaking for 1 h at room temperature with 10 mL extraction buffer (1.25% SDS, 0.1 M Tris-HCl, pH 6.8, 20 mM dithiothreitol), followed by sonication on ice for  $2 \times 1 \text{ min}$  at 70% power (25 W) and 70% duty cycle (UP50H, Hielscher Ultrasonics GmbH, Teltow, Germany). The supernatant was filtered through a nylon mesh (0.45 mm) and shaken for 30

min with 5 mL buffered phenol (pH 8). The two phases were separated by centrifugation for 30 min at 12000 rpm at 4 °C. Subsequently, the proteins in the lower phenol phase were precipitated with 5 fold volume of 0.1 M ammonium acetate dissolved in methanol at -20 °C overnight. The protein pellet was washed once with cold methanol and twice with cold acetone; the air-dried pellet was stored at -20 °C until further analysis. Proteins were separated by sodium dodecyl sulfate-polyacrylamide (SDS) gel electrophoresis, and subsequently tryptic digestion was performed according to Jehmlich et al. (2010), followed by purification using ZipTip<sub>C18</sub> columns (Merck Millipore, Billerica, MA, USA).

Peptides were reconstituted in 0.1% formic acid and analyzed on an Orbitrap Fusion MS (Thermo Fisher Scientific, Waltham, MA, USA). Briefly, the mobile phase A of 0.1% formic acid and mobile phase B containing 80% acetonitrile and 0.08% formic acid were prepared. Peptides were loaded for 5 min on a precolumn ( $\mu$ -precursor column, cartridge column, 5  $\mu$ m particle size, 300  $\mu$ m inner diameter, 2 cm length, C18, Thermo Scientific) at 4% mobile phase B and eluted from the analytical column (Accucore<sup>TM</sup> C18 LC Column, 50 cm length, 2.6  $\mu$ m particle size, Thermo Scientific) over a 120 min gradient of 4-55% mobile phase B.

Raw data obtained were processed for database searches using Thermo Proteome Discoverer (v1.4.0.288; Thermo Fisher Scientific, Waltham, MA, USA). Searches were performed using the Sequest HT algorithm with the following parameters: tryptic cleavage with maximal two missed cleavages, a peptide tolerance threshold of  $\pm 10$  ppm and an MS/MS tolerance threshold of  $\pm 0.1$  Da, and carbamidomethylation at cysteines as static and oxidation of methionines as variable modifications. In the metagenome databases, contigs were considered identified with at least two unique peptides with high confidence (false discovery rate < 0.01).

For the identification of <sup>15</sup>N-labeled peptides, the respective <sup>14</sup>N peptides were measured as well to compare chromatographic retention time and MS/MS fragmentation patterns, as described previously (Jehmlich et al. 2008a). The <sup>15</sup>N incorporation into peptides was analyzed using OpenMS and the MetaProSIP node according to Starke et al. (2016). For <sup>15</sup>N incorporated peptides, the relative isotope abundance (RIA) and the labeling ratio (lr) were calculated as described by Taubert et al. (2011). The RIA represents the percentage of the incorporated <sup>15</sup>N in relation to the total nitrogen atoms in a peptide.

The  $I_r$  represents the proportion of a peptide's heavy isotope-labeled isotopologues to all isotopologues of that peptide, ranging between 0 (no labelled peptide) and 1 (fully labelled peptide). The  $I_r$  of a protein was calculated averaging the  $I_r$  of at least three peptides.

#### 4.2.4 Potential ammonia oxidation rates

Potential nitrification rates (PNR) were measured using the chlorate inhibition method (Kurola et al. 2005) with minor modifications. Briefly, 5 g of fresh sands was incubated in 50 mL centrifuge tubes containing 20 mL of 1 mM phosphate buffer solution (NaCl, 8.0 g L<sup>-1</sup>; KCl, 0.2 g L<sup>-1</sup>; NaH<sub>2</sub>PO<sub>4</sub>, 0.2 g L<sup>-1</sup>; Na<sub>2</sub>HPO<sub>4</sub>, 0.2 g L<sup>-1</sup>; pH 7.4) and 1mM (NH<sub>4</sub>)<sub>2</sub>SO<sub>4</sub>. Potassium chlorate with a final concentration of 10 mM was added to inhibit nitrite oxidation. The suspension was incubated in the dark at 25 °C and shaken at 180 rpm for 24 h. NO<sub>2</sub><sup>-</sup> was extracted using 5 mL of 2 M KCl and centrifuged. The supernatant was determined spectrophotometrically at 540 nm using N-(1-naphthyl) ethylenediamine dihydrochloride. The calibration was determined with KNO<sub>2</sub> over a concentration range of 10-100 μM. The PNR were calculated from the linear increase in NO<sub>2</sub><sup>-</sup> concentrations during the incubation. The actual nitrification rates might be slightly higher because loss of NO<sub>2</sub><sup>-</sup> cannot be fully excluded owing to the possibility of denitrification even in strictly oxidic incubations.

#### 4.2.5 Measuring anammox and denitrification rates using <sup>15</sup>N isotope tracing method

<sup>15</sup>N isotope incubation experiments were performed to measure potential rates of anammox and denitrification and to quantify their contributions based on that described by Risgaard-Petersen et al. (2004). Triplicate sand samples were collected for <sup>15</sup>N-tracing experiments. After return to laboratory, 2 g of homogenized fresh sands were intermediately transferred to the helium-flushed, 10 mL gas-tight glass vials, followed by filling vials with N<sub>2</sub>-purged sterile MilliQ water without headspace. The slurries were then pre-incubated for 24 h to eliminate residual O<sub>2</sub> and NO<sub>x</sub><sup>-</sup> in the incubation media. Three treatments were subsequently performed by adding (1) 100 μM <sup>15</sup>NH<sub>4</sub><sup>+</sup> (<sup>15</sup>N > 98%), (2) 100 μM <sup>15</sup>NO<sub>2</sub><sup>-</sup> (<sup>15</sup>N > 98%), and (3) 100 μM <sup>15</sup>NH<sub>4</sub><sup>+</sup> (<sup>15</sup>N > 98%) and 100 μM <sup>14</sup>NO<sub>2</sub><sup>-</sup> using a Hamilton syringe (Sigma-aldrich). All isotope solutions were flushed with helium before addition. Every treatment was conducted in three replicates and incubated in the

dark at 25 °C. At seven intervals of 0, 3, 6, 8, 10, 12, and 18 h, incubations were stopped adding 200 µL of a 7 M ZnCl<sub>2</sub> solution. Vials were stored upside down until gas analysis.

The isotope ratios of <sup>28</sup>N<sub>2</sub>, <sup>29</sup>N<sub>2</sub> and <sup>30</sup>N<sub>2</sub> were measured using a gas chromatograph-isotope ratio mass spectrometer (GC-C-IRMS) equipped with a ShinCarbon ST column (100/120 mesh, 1.33 m × 1 mm ID, Restek) connected downstream via an automatic injector (Valco Instruments Co. Inc.) to a Molsieve 5A column (10 m × 0.53 mm ID, 0.50 µm film, Agilent). 100 µL of headspace gas samples were manually injected into a gas chromatograph (Agilent 7890A, USA) in split mode interface to an Finnigan MAT 252 IRMS (Thermo Electron GmbH, Germany) using helium as carrier gas. The following program was used for N<sub>2</sub> analyses: 40 °C oven temperature, 200 °C I/F and ion source temperature, total flow 14 mL min<sup>-1</sup> and column flow 8 mL min<sup>-1</sup>. The concentration of N<sub>2</sub> was calculated based on a calibration function gained from standard gas calibration (N<sub>2</sub> 2530 ppm, loop size: 0.01, 0.5, and 2 mL, 5 repeats for each loop size). The amount of N<sub>2</sub> produced by anammox and denitrification was calculated from the mole fraction of <sup>29</sup>N<sub>2</sub> and <sup>30</sup>N<sub>2</sub> according to the equations described by Thamdrup and Dalsgaard (2002). The rates were calculated from the slopes of the linear regression based on the N<sub>2</sub> concentration produced through denitrification and anammox as a function of time during the whole incubation. The significant difference of the slopes from zero (p<0.05) was determined using one-way analysis of variance (ANOVA F-test).

#### **4.2.6 Statistical analysis**

One-way analysis of variance (ANOVA) was performed to compare the difference among different flow distances and the significant difference was defined at p<0.05. The statistical analyses were performed using the SPSS 22.0 package (SPSS Inc., Chicago, IL, USA).

### **4.3 Results and discussion**

#### **4.3.1 Microbial ammonia oxidation confirmed by N-NH<sub>4</sub><sup>+</sup> isotope fractionation (δ<sup>15</sup>N-NH<sub>4</sub><sup>+</sup>)**

The specific shifts in the isotopic composition of N compounds (e.g. NH<sub>4</sub><sup>+</sup> and NO<sub>3</sub><sup>-</sup>) can reflect their sources and nitrogen transformation, and thereby can provide insightful

information on nitrogen transformation mechanisms during wastewater treatment. The  $\delta^{15}\text{N-NH}_4^+$  values and  $\text{NH}_4^+\text{-N}$  loads along the flow path at the deep layers of the MET-CW are shown in Figure 4-1, showing that decreasing  $\text{NH}_4^+$  loads correlated with increasing  $\delta^{15}\text{N-NH}_4^+$  values. For example, at the 95<sup>th</sup> day,  $\text{NH}_4^+\text{-N}$  loads decreased from 64.3 mg N day<sup>-1</sup> at the inflow to 37.4 mg N day<sup>-1</sup> at the flow distance of 139 cm, whereas  $\delta^{15}\text{N-NH}_4^+$  values increased from 18.5‰ to 23.9‰. Similarly, the progressive increase of  $\delta^{15}\text{N-NH}_4^+$  with decrease of  $\text{NH}_4^+\text{-N}$  loads along the flow path was observed at day 192, 300 and 400. The significant enrichment of <sup>15</sup>N in  $\text{NH}_4^+$  indicated the occurrence of microbial  $\text{NH}_4^+$  oxidation, which has been reported for a significant shift in isotope signature of  $\delta^{15}\text{N-NH}_4^+$  in pure nitrifying cultures and can be readily distinguished from other processes (e.g. plant uptake and mineralization) without or only with minor  $\delta^{15}\text{N-NH}_4^+$  change (Casciotti 2009, Casciotti et al. 2003).

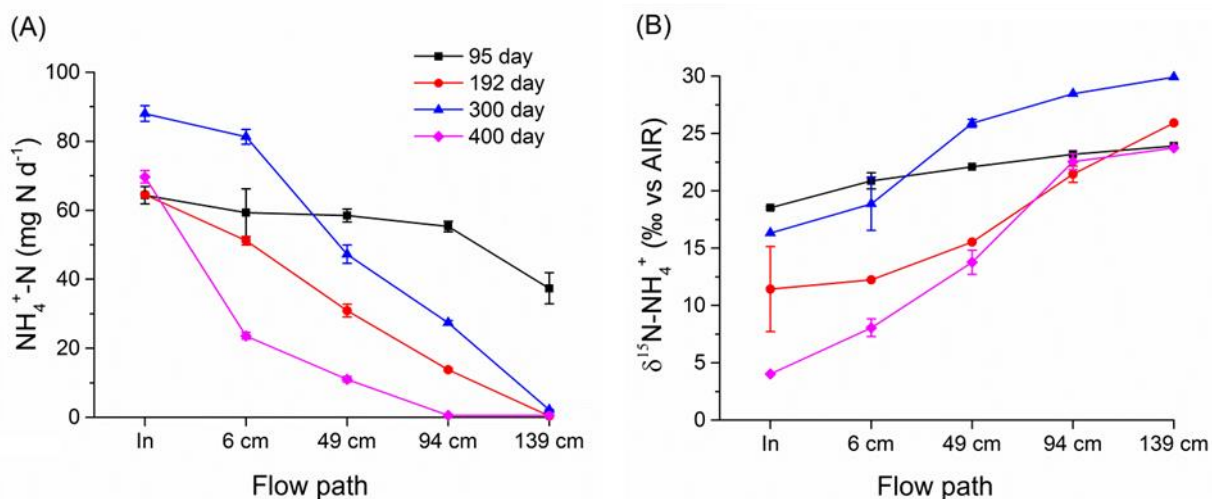


Figure 4-1 Change of  $\text{NH}_4^+\text{-N}$  loads (A) and  $\delta^{15}\text{N-NH}_4^+$  values (B) at the deep layer along the flow path in the MET-CW.

The calculated <sup>15</sup>N enrichment factors of  $\text{NH}_4^+$  were generally small, ranging from -1.5 to -5.9‰ (Supporting information Figure S4-1), which were smaller in absolute values than what has previously been reported for bacterial nitrification with absolute values of 14.2 to 38.2‰ (Casciotti 2009, Casciotti et al. 2003). In fact, the isotope effect for AOB was generally estimated based on  $\delta^{15}\text{N-NO}_2^-$ , which could be overestimated because the accumulation of intermediates (e.g., hydroxylamine) would lead to a second <sup>15</sup>N

fractionation step to increase  $\delta^{15}\text{N-NO}_2^-$  difference between the initial  $\text{NH}_4^+$  and the produced  $\text{NO}_2^-$  (Casciotti et al. 2011). Additionally, these reported  $\epsilon$  values were determined in batch culture experiments, which are unlikely to precisely evaluate microbial ammonia oxidation in CW systems and natural environments considering the complex physio-chemical conditions and co-occurrence of multiple N conversion processes (Vymazal 2007). In this study, although the enrichment factors were lower in comparison with the strong isotope fractionation effects based on  $\delta^{15}\text{N-NO}_2^-$  in pure cultures (2009, Casciotti et al. 2003), the large increase of  $\delta^{15}\text{N-NH}_4^+$  values ( $>10\text{‰}$ ) with the decrease of  $\text{NH}_4^+$  loads implied the presence of microbial ammonia oxidation. The calculated  $^{15}\epsilon$ , however, are closer to the range of these factors ( $-3.5$  to  $-16\text{‰}$ ) for nitrification reported in groundwater (Böhlke et al. 2006, Jacob et al. 2016), also in agreement with average yearly enrichment factors of  $-5.8\text{‰}$  and  $-7.9\text{‰}$  reported in a study of pilot-scale CWs treating contaminated groundwater (Coban et al. 2015b). The N isotope enrichment factors associated with ammonia oxidation in our MET-CW were smaller than those found in the pure cultures, which could be probably attributed to substrate limitation, low nitrification rates or microbial species with low process-specific isotope fractionation. This is also consistent with the previous reports that isotope factors in wetlands were usually lower than determined in laboratory experiments (Coban et al. 2015b, Erler and Eyre 2010, Sovik and Morkved 2008). Nevertheless, the substantial isotope effect that occurred in the MET-CW is an evidence for microbial ammonia oxidation process.

The N isotope effects by archaeal ammonia oxidation (AOA) and anammox, ranging from 13 to 41‰ and 23.5 to 29.1‰ respectively (Brunner et al. 2013, Santoro et al. 2011), also falls in the range of that reported for AOB. Thus, it is not possible to distinguish ammonia oxidation activity performed by AOA, AOB or anammox only based on N isotope effect. Estimates of ammonia oxidation based on the determination of a N isotope effect are complex because the influences of substrate concentration and rate constants associated with the different processes involved in ammonia oxidation (e.g. transport/diffusion, hydroxylamine oxidation) could lead to different isotope effects for ammonia oxidation among nitrifying microorganisms and even among different extracellular conditions with the same microorganisms as well as in different natural or experimental environment (Casciotti et al. 2011). Additionally, co-occurring processes may

lead to overlapping or counteracting influence on isotope fractionation factor for ammonia oxidation, thus it is critical to use multiple isotope analysis (e.g.  $\delta^{15}\text{N}$  and  $\delta^{18}\text{O}$  in  $\text{NH}_4^+$ ,  $\text{NO}_2^-$ ,  $\text{NO}_3^-$  or  $\text{N}_2\text{O}$ ) and combine the physico-chemical measurements as well as molecular biological approaches for proper evaluation of nitrogen transformation processes. In our case,  $\text{NO}_2^-/\text{NO}_3^-$  in the inflow was negligible and also not detectable at the other flow distances (Wei et al. 2015b), thus it was not possible to measure  $\delta^{15}\text{N}$  and  $\delta^{18}\text{O}$  in  $\text{NO}_2^-$  or  $\text{NO}_3^-$  for better understanding of ammonia oxidation and the subsequent processes (e.g. denitrification). In the previous report on several types of pilot-scale CWs,  $\delta^{15}\text{N}\text{-NO}_3^-$  showed no change along the flow path and isotope fractionation of denitrification was masked by nitrification (Coban et al. 2015b), indicating that it is difficult to estimate denitrification using the isotope fractionation approach in the CW system treating  $\text{NH}_4^+$  rich contaminated water. In order to evaluate nitrogen transformation processes in more detail, the reactive rates (i.e. nitrification, denitrification and anammox), functional proteins and active species involved in nitrogen transformation processes in the MET-CW will be further characterized and discussed below.

#### **4.3.2 Identification of functional proteins and active species involved in microbial nitrogen transformation**

$^{15}\text{N}$  labelling experiments were *in situ* conducted by continuously feeding artificial groundwater containing  $^{15}\text{N}\text{-NH}_4\text{Cl}$  instead of contaminated groundwater. Protein-SIP was used to detect functional proteins and active species involved in microbial nitrogen transformation in the MET-CW. The shift in mass spectra derived from  $^{15}\text{N}$  incorporation into proteins was analyzed, and relative isotope abundance (RIA) and labelling ratio (lr) were calculated by comparison with the spectra of the corresponding unlabeled peptides. Figure 4-2 shows an example for mass spectra shift of a peptide with the sequence VTHANYDVPGR (m/z 410.2071), which is corresponding to ammonia monooxygenase from *Nitrosomonas*.  $^{15}\text{N}$  incorporation into the peptides was remarkably reflected by the shift of the isotopic peaks to higher m/z values and the shape change of the isotopic distribution.

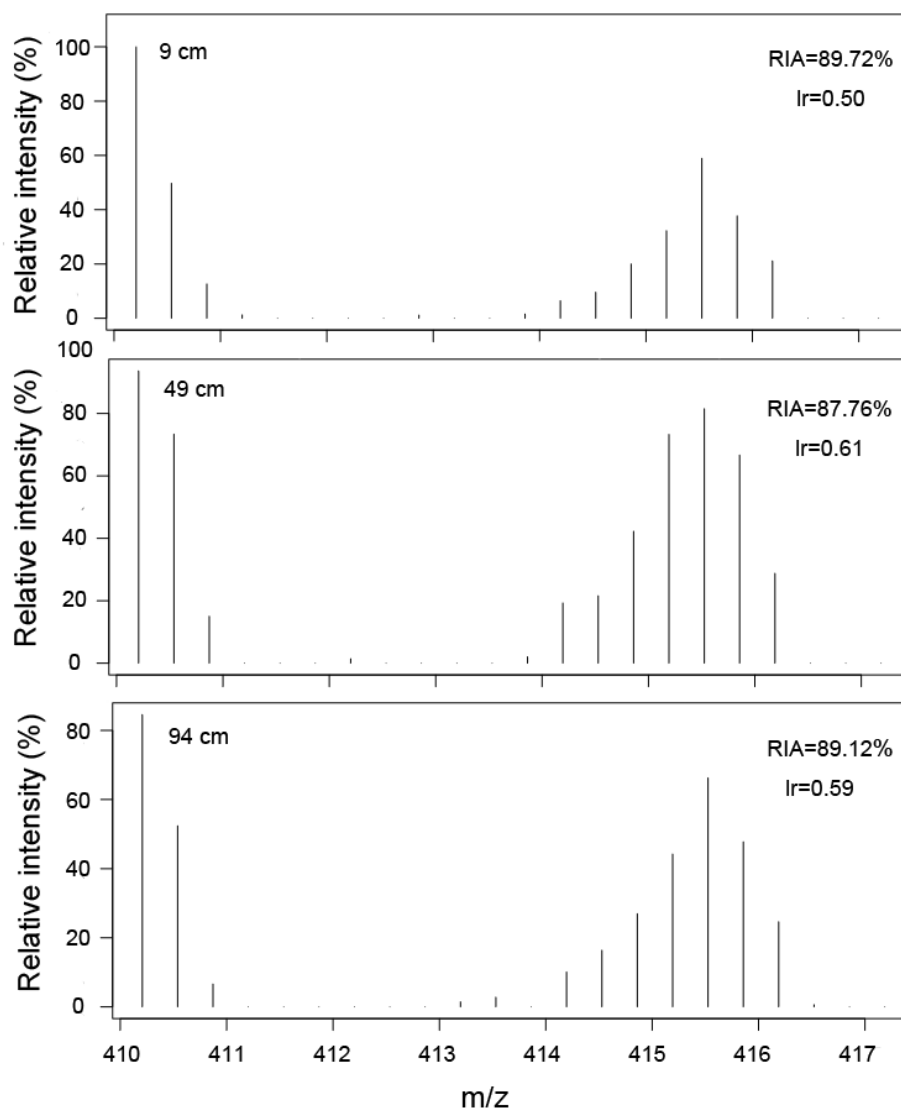


Figure 4-2 Mass spectra of the peptide VTHANYDVPGR ( $m/z$  410.2071) from ammonia monooxygenase subunit B, which showed a high degree of  $^{15}\text{N}$  incorporation. The peptide was affiliated to *Nitrosomonas* sp..

As shown in Figure 4-3,  $^{15}\text{N}$  incorporated peptides were identified at the 6, 49 and 94 cm distance, but not at the distance of 139 cm. This result is in accordance with that undetectable potential nitrification rate and low rates of anammox and denitrification at the 139 cm distance as described in section 4. 3. 4. The labelled proteins involved in nitrogen transformation showed the high RIAs, ranging from 80% to 90%. The Ir values varied from 0.1 to 0.6, reflecting the different extent in protein biosynthesis and turnover.

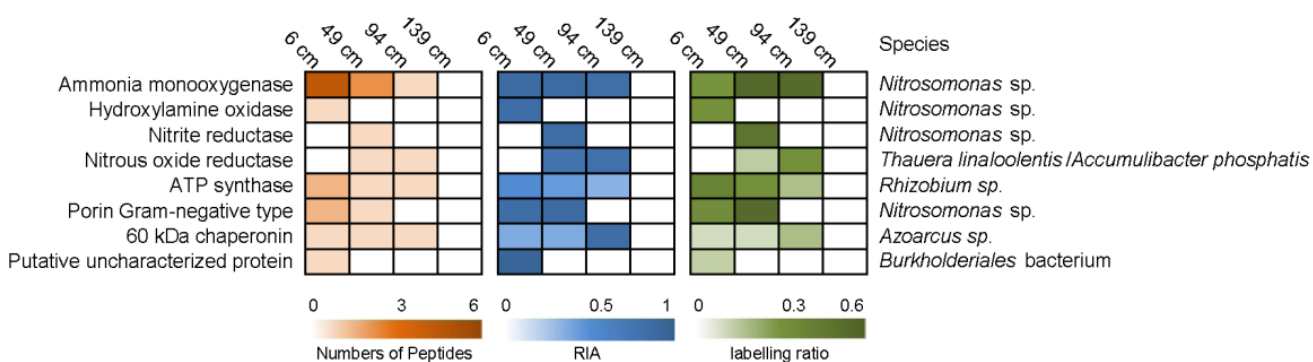


Figure 4-3 The numbers of  $^{15}\text{N}$ -labelled peptides, relative isotope abundance (RIA), labelling ratio (lr) and their respective phylogenetic assignment obtained from *in situ* protein-SIP analysis.

Eight proteins from a total of 30 peptides were  $^{15}\text{N}$  incorporated, four of which were directly involved in nitrogen transformation, i.e. ammonia monooxygenase, hydroxylamine oxidase, nitrite reductase and nitrous oxide reductase (Figure 4-3). Ammonia monooxygenase and hydroxylamine oxidase are two key enzymes of nitrification, catalyzing the oxidation of  $\text{NH}_3$  to  $\text{NH}_2\text{OH}$  and the oxidation of  $\text{NH}_2\text{OH}$  to  $\text{NO}_2^-$ , respectively (Arp et al. 2002). The identified ammonia monooxygenase and hydroxylamine oxidase with  $^{15}\text{N}$  incorporation were assigned to *Nitrosomonas*, indicating that *Nitrosomonas* was the dominant species involved in nitrification. Nitrite reductase, one of the key enzymes catalyzing the reduction of  $\text{NO}_2^-$  to  $\text{NO}$  in the dissimilatory denitrification, was also identified for  $^{15}\text{N}$  incorporation. Interestingly,  $^{15}\text{N}$  incorporated nitrite reductase was exclusively affiliated to *Nitrosomonas*, illustrating that the existence of the nitrite reduction via nitrifier-denitrification by *Nitrosomonas* in our MET-CW. *Nitrosomonas* was found to reduce nitrite to nitric oxide with nitrous oxide or dinitrogen as terminal products under  $\text{O}_2$  limiting conditions; this process was named nitrifier-denitrification and generally occurs under the condition with low  $\text{O}_2$  availability and low organic carbon content (Kool et al. 2011). In our case, the low  $\text{O}_2$  ( $<0.05$  mg/L) and relatively low organic carbon content with a C/N ratio of about 2 provided favorable conditions for nitrifier-denitrification. Another key enzyme in denitrification, nitrous oxide reductase, was also identified with  $^{15}\text{N}$  incorporation, which was assigned to either *Thauera linaloolentis* or

Candidatus *Accumulibacter phosphatis*, demonstrating the activity of heterotrophic denitrification in the MET-CW. Nitrate reductase was inactive in the MET-CW and not identified in both labelled and all identified proteins from metaproteome. In addition, no accumulation of  $\text{NO}_3^-$  was detected in this study, suggesting that  $\text{NO}_3^-$  was not produced from  $\text{NO}_2^-$  oxidation via nitrification processes. Together with that nitrate reductase was undetectable, full nitrification to  $\text{NO}_3^-$  was restricted in our MET-CW, which is accordance with the result presented in section 4. 3. 4 that no production of  $\text{NO}_3^-$  was measured in the incubation for nitrification rates measurement. Protein-SIP analysis suggests that influent  $\text{NH}_4^+$  was firstly oxidized by AOB to nitrite, which was subsequently reduced by heterotrophic denitrification or nitrifier-denitrification.

The other four proteins with  $^{15}\text{N}$  incorporation were not directly involved in nitrogen transformation pathways (Figure 4-3), which were affiliated to *Rhizobium*, *Azoarcus* and *Burkholderiales* bacterium, respectively, phylotypes belonging to these orders have been described as being capable to denitrify. Electron donors for denitrification could have been organic compounds released by the plants of the CW, or benzene, the main contaminant of the system, which were shown to be removed in the investigated CW (Wei et al., 2015a).

### 4.3.3 Functional and phylogenetic distributions of identified proteins

The metaproteomic analysis was used to reveal the phylogenetic and functional diversity of microbial communities in the MET-CW. Phylogenetic distributions derived from identified proteins are given in Figure 4-4. Identified proteins were mainly assigned to *Nitrosomonadales*, *Burkholderiales*, *Rhizobiales* and *Clostridiales*, with the shift for relative abundances along the flow path. The proteins affiliated to *Nitrosomonadales* were highly abundant at the 6 cm distance, but decreased from 13.4 to 1.1% at the 139 cm distance, which is in agreement with variation trend of potential nitrification rates along the flow path (section 4. 3. 4). The majority of proteins from *Nitrosomonadales* were affiliated to *Nitrosomonas* (>90%), suggesting that *Nitrosomonas* are the predominant ammonia-oxidizing bacteria in the MET-CW. *Nitrospira* was another AOB genus identified in the metaproteomes, but accounted for only 0.56-0.6%, implying a minor role in nitrification process. The predominance of *Nitrosomonas* has been extensively reported in various

wastewater treatment systems eg. biofilm reactors, biofilters and different types of CW (Adrados et al. 2014, Song et al. 2013b). In contrast, proteins related to nitrite oxidizing bacteria (NOB) were affiliated to *Nitrospirales* and were found with a low abundance (1.2%) only at the 6 cm flow distance but not at the other flow distances, suggesting that the complete oxidation of ammonia to nitrate was minor or absent in nitrogen transformation in this study. This is in accordance with the above-mentioned result that no evidence for NOB-related proteins with  $^{15}\text{N}$  incorporation was found by protein-SIP analysis.

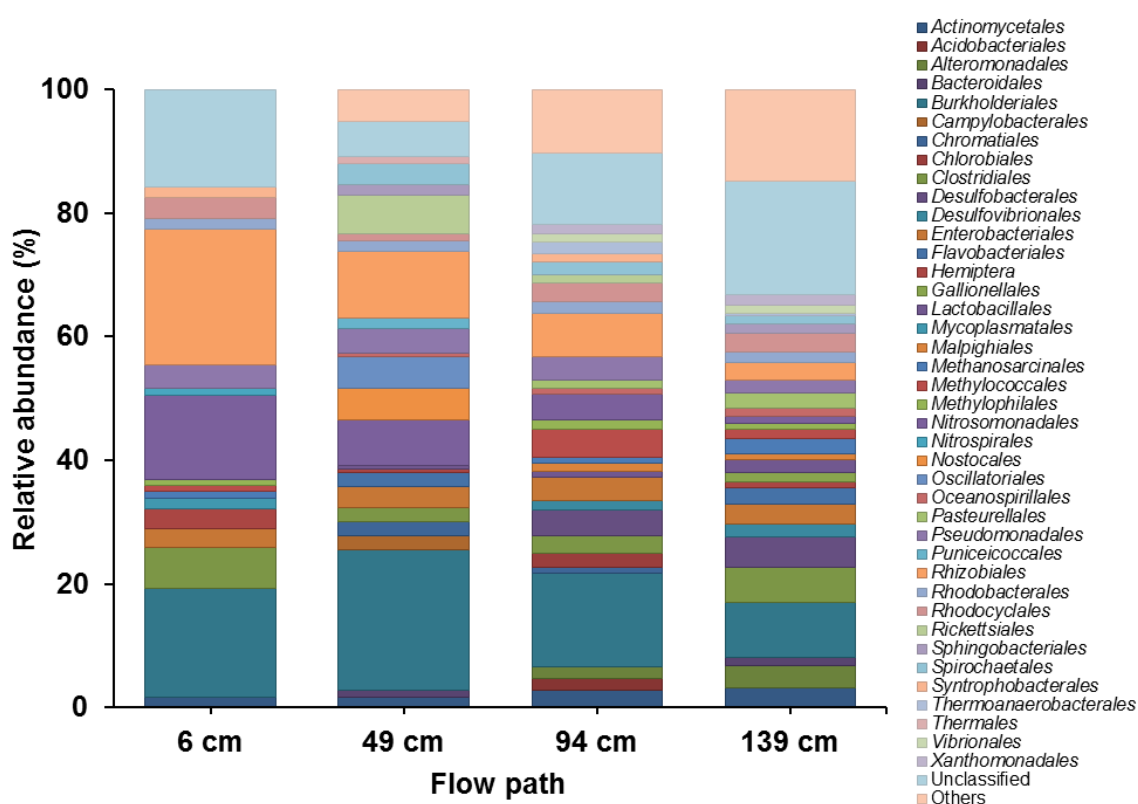


Figure 4-4 Phylogenetic distribution of microbial orders based on the numbers of all identified proteins by the metaproteomic analysis. Microbial Orders with a relative abundance <1% in all samples were pooled into others.

In addition to proteins for AOB, the majority of the remaining proteins identified in the metaproteomes were related to these potential denitrifying bacteria (Figure 4-4). Remarkably, proteins belonging to *Burkholderiales* and *Rhizobiales* showed the dominant abundance, accounting for up to 17.5% and 22.0% at the 6 cm flow distance, respectively.

Proteins from *Clostridiales* were also found in the metaproteomic data, with a relatively high percentage of 6.8% at the 6 cm flow distance. *Burkholderiales*, *Rhizobiales* and *Clostridiales* were also reported to participate in anaerobic degradation of benzene and other aromatic compounds with nitrite or nitrate as the terminal electron acceptors under denitrifying conditions (Aburto-Medina and Ball 2015, Vogt et al. 2011). Our previous study also confirmed that *Burkholderiales* and *Clostridiales* were the dominant populations during treatment of benzene and ammonium contaminated groundwater in a microbial fuel cell (Wei et al. 2015a). A recent *in situ* microcosms study by Herbst et al. (2013) revealed that *Burkholderiales* and *Rhizobiales* were the most active microorganisms in groundwater contaminated by aromatic hydrocarbons. In addition to these proteins belonging to the above-mentioned three orders, proteins related to *Actinomycetales*, *Enterobacteriales*, *Pseudomonadales*, *Rhodobacterales*, and *Rhodocyclales* were also identified despite having a low abundance (<3.5%), which are also known for their potential denitrification capability. The majority of the identified proteins related to denitrifying bacteria were not <sup>15</sup>N incorporated in protein-SIP analysis, but it cannot be excluded that these species were actually involved in nitrogen transformation because the low identification coverage for protein-SIP analysis usually is caused by a lack of protein sequence data (Jehmlich et al. 2016).

Notably, only one protein related to anammox was detected at the 139 cm flow distance, belonging to genus *Brocadia*. This could be attributed to enough cell density at the 139 cm distance, here higher contribution of anammox was also observed. Although no <sup>15</sup>N incorporation into proteins related to anammox was detected by protein-SIP, metaproteomic analysis implied the occurrence of anammox process in the MET-CW, but this process probably only had low contribution to nitrogen removal. The occurrence of anammox activity was also confirmed by measurement of potential anammox rates (section 4.3.4). In a similar constructed wetland, anammox bacteria with low abundance were detected by quantifying hydrazine synthase (*hzsA*) genes, but anammox rate could not be measured, which also implied that this process appeared to be of low importance in nitrogen transformation (Coban et al. 2015a). Nevertheless, in our study, the identification of proteins related to nitrifying, anammox and denitrifying bacteria further confirmed potential activity of these nitrogen transformation pathways in the MET-CW.

#### 4.3.4 Potential nitrification, anammox and denitrification rates

The potential nitrification rates (PNR) were determined at the different flow distances. As shown in table 4-1, the average PNR values of 23.61, 28.84 and 23.82 nmol N g<sup>-1</sup> h<sup>-1</sup> were detected at the flow distances of 6, 49 and 94 cm, showing no significant difference ( $p>0.05$ ). Thus, stable nitrification activities occurred at these three flow distances, corresponding to the continuously decreasing NH<sub>4</sub><sup>+</sup>-N loads observed along the flow path (Figure 4-1). However, no PNR was detected at the flow distance of 139 cm; here, a relatively high NH<sub>4</sub><sup>+</sup>-N load (37.36 mg N d<sup>-1</sup>) was found only at the day 95 whereas minor or no NH<sub>4</sub><sup>+</sup>-N loads were observed at the day 192, 300 and 400, respectively, as shown in Figure 4-1. These results indicate that a mature nitrifying community had developed under the long-term supply of NH<sub>4</sub><sup>+</sup>-N in the MET-CW, which carried out the first step of the nitrification process, converting NH<sub>4</sub><sup>+</sup> into NO<sub>2</sub><sup>-</sup> and thus consequently driving the subsequent nitrogen transformation and removal processes. The accumulation of NO<sub>2</sub><sup>-</sup> rather than NO<sub>3</sub><sup>-</sup> during the incubations for PNR measurements further indicated that the oxidation of NO<sub>2</sub><sup>-</sup> to NO<sub>3</sub><sup>-</sup> did not take place in the MET-CW.

Table 4-1 Calculated rates of potential nitrification, anammox and denitrification (nmol N<sub>2</sub> g<sup>-1</sup> h<sup>-1</sup>) at the deep layers along the flow path.

Flow distance	Nitrification	Anammox	Denitrification	Total	% Anammox	% Denitrification
6 cm	23.61±1.67	0.91±0.07	17.37±1.13	18.28±2.71	4.98	95.02
49 cm	28.84±3.79	0.56±0.11	13.27±1.72	13.83±2.25	4.05	95.95
94 cm	23.82±2.78	0.17±0.03	3.78±0.42	3.95±0.43	4.31	95.70
139 cm	ND	0.11±0.01	0.62±0.07	0.73±0.11	15.07	84.93

Potential anammox and denitrification rates were calculated based on <sup>29</sup>N<sub>2</sub> and <sup>30</sup>N<sub>2</sub> production in the <sup>15</sup>NO<sub>2</sub><sup>-</sup> incubation as shown in table 4-1. The decrease of anammox rates was observed along the flow path, varying from 0.91 to 0.11 nmol N<sub>2</sub> g<sup>-1</sup> h<sup>-1</sup> (Table 4-1). A similar variation trend was also found for denitrification rates, which decreased from 13.37 to 0.62 nmol N<sub>2</sub> g<sup>-1</sup> h<sup>-1</sup> along the flow path. This could be explained by decreasing substrate (NH<sub>4</sub><sup>+</sup> and NO<sub>2</sub><sup>-</sup> produced by nitrification) availability for anammox and denitrification along the flow path due to the gradually consumption of NH<sub>4</sub><sup>+</sup>. Denitrification rates were much higher than anammox rates at the four flow distances, contributing 84.93 to 95.95%

of total  $N_2$  production. This result was consistent with previous reports that denitrification is the major pathway involved in nitrogen removal in CWs (Coban et al. 2015a, Saeed and Sun 2012). The relative contribution of anammox to total  $N_2$  production were similar at the flow distances of 6, 49 and 94 cm, ranging between 4.05% and 4.98% (Table 4-1), and subsequently increased to 15.07% at the distance of 139 cm in the front of where anode modules located. The strong increase in the relative significance of anammox from 94 cm to 139 cm distance indicated that anammox activity was probably enhanced by the presence of the anode in the MET-CW.

The relative contributions of anammox were reported up to 24% and 33% in the surface flow constructed wetland (SFCW) and the vertical flow constructed wetland (VFCW), respectively (Erler et al. 2008, Zhu et al. 2011). Moreover, the anammox process was identified as the major nitrogen removal pathway, contributing for 55.6-60.0% of  $N_2$  production in an integrated VFCW system (Hu et al. 2016). In contrast, the absence of active anammox was reported in the HSSF-CW although anammox bacteria were detected by analyzing hydrazine synthase (hzsA) genes (Coban et al. 2015a). In this study, the percentages of anammox contribution were lower than that reported in the SFCWs and VFCWs but remarkably higher than that reported in the HSSF-CW. Generally, HSSF-CWs are predominantly anoxic and thus not favorable for nitrification, resulting in the production of limited substrate  $NO_2^-$  for anammox when treating wastewater only with  $NH_4^+$  and without  $NO_3^-$ . In contrast, VFCWs provide conditions generally favoring nitrification; also SFCWs have a thin aerobic layer to enhance nitrification, therefore producing  $NO_2^-$  and further stimulating anammox activity. The C/N ratio is also a critical factor determining the existence and activity of anammox; a C/N ratio lower than 2 is suitable for the growth of anammox bacteria (Kumar and Lin 2010). In our study, the C/N ratio in the influent groundwater was about 2, which was favorable for denitrification, supporting denitrification as dominant nitrite removal process in the MET-CW. Additionally, the higher potential nitrification rates than the denitrification rates indicated that anammox might be responsible for consuming the remaining  $NO_2^-$  produced by partial nitrification process. In summary, our results confirmed the existence and their activities of partial nitrification, anammox and denitrification (heterotrophic denitrification and nitrifier denitrification) process in the MET-CW.

### 4.3.5 Implications for nitrogen transformation and removal

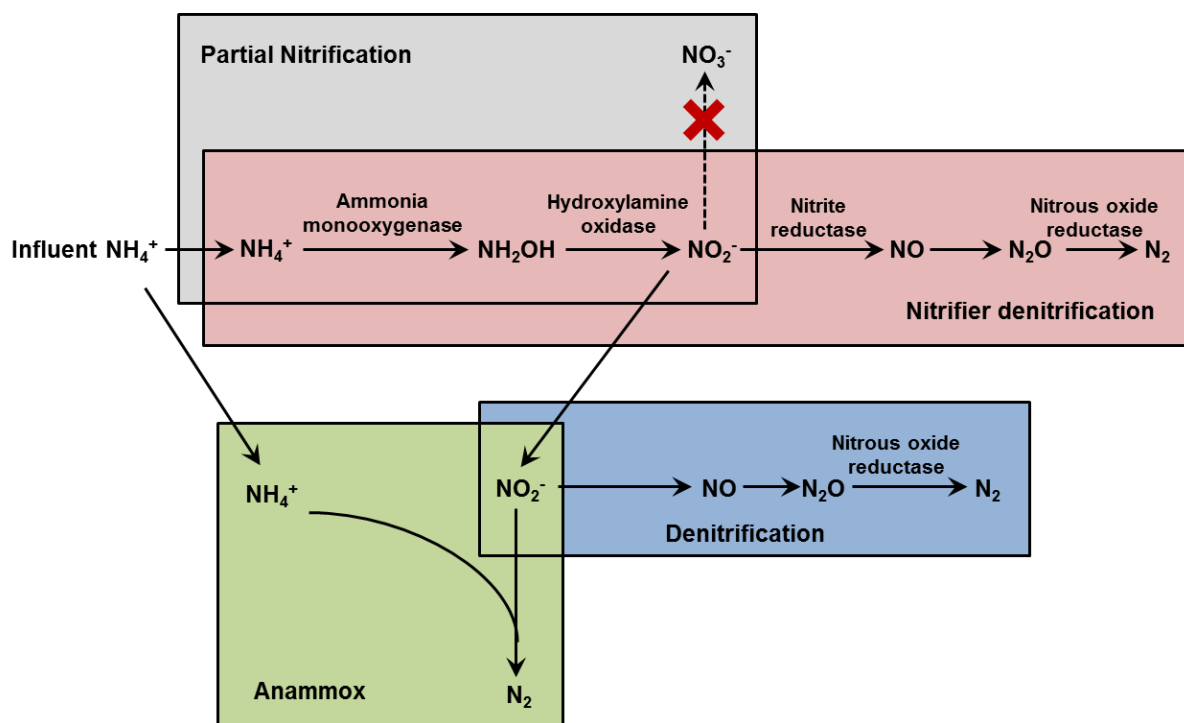


Figure 4-5 Schematic illustrations of microbial nitrogen transformation processes and  $^{15}\text{N}$  incorporated proteins identified in the MET-CW. The coexistence of partial nitrification, anammox, heterotrophic denitrification and nitrifier denitrification were revealed to involve in  $\text{NH}_4^+$ -N removal in the MET-CW.

Based on our results, a schematic diagram of microbial nitrogen transformation pathways are presented in Figure 4-5. Influent  $\text{NH}_4^+$  was firstly oxidized to  $\text{NO}_2^-$  by partial nitrification, which was directly confirmed by identification of  $^{15}\text{N}$  labelled ammonia monooxygenase and hydroxylamine oxidase;  $\text{NO}_2^-$  was further used by denitrifying bacteria, and thus are either successively reduced to  $\text{NO}$ ,  $\text{N}_2\text{O}$  and  $\text{N}_2$  by denitrification or react with  $\text{NH}_4^+$  to produce  $\text{N}_2$  by anammox. In addition, nitrite reductase involved in denitrification was affiliated to *Nitrosomonas*, strongly indicating the occurrence of nitrifier-denitrification. These results demonstrate that partial nitrification, anammox, heterotrophic denitrification and nitrifier-denitrification were involved in  $\text{NH}_4^+$ -N removal in the MET-CW, and that partial nitrification and denitrification were dominant nitrogen transformation processes. This process saves energy and resources as the nitrite oxidation

step and the following nitrate reduction is avoided. Compared to conventional nitrification and denitrification in a sequence reactor, the partial nitrification and denitrification process can theoretically save 25% of O<sub>2</sub> consumption for nitrification and up to 40% of organic carbon for denitrification, reducing CO<sub>2</sub> emission by 20% (Peng and Zhu 2006). In addition, rates of denitrification via NO<sub>2</sub><sup>-</sup> can be 1.5 to 2 times higher than via NO<sub>3</sub><sup>-</sup>. Moreover, partial nitrification and denitrification combined with the anammox process provides an energy-saving and cost-effective alternative for nitrogen removal from wastewater with the significant advantages, such as low oxygen demand, no requirement for external carbon sources and negligible sludge production (Paredes et al. 2007). More recently, the activities of simultaneous partial nitrification, anammox and denitrification process was also reported for the removal of N and organic matters in vertical flow constructed wetlands (Hu et al. 2016, Wen et al. 2017).

In the MET-CW, the co-existence of functional microorganisms for nitrification, anammox and denitrification was directly confirmed by protein-SIP and metaproteomic analysis. In general, chemoautotrophic nitrification occurs under aerobic conditions, whereas anammox and denitrification occur preferentially under anoxic conditions. In the HSSF-CW, the presence of plants usually establishes microsites with the deep oxygen gradient around the rhizosphere, favoring the growth for aerobic nitrifying bacteria as well as anaerobic anammox and denitrifying bacteria (Saeed and Sun 2012). In this study, nitrification rates were slightly higher than denitrification rates, indicating that the excess nitrite produced from nitrification process can be used as electron acceptors for anammox. However, anammox rates were much lower than denitrification rates, resulting in a minor role to NH<sub>4</sub><sup>+</sup>-N removal in the MET-CW, which may be attributed to less competition of anammox bacteria due to the lower the standard free energy for anammox reaction and lower growth yield compared to denitrifying bacteria (Kumar and Lin 2010). In our study, nitrate reduction from NO<sub>3</sub><sup>-</sup> to NO<sub>2</sub><sup>-</sup> was not detected and no NO<sub>2</sub><sup>-</sup> accumulation was detected, suggesting that NO<sub>2</sub><sup>-</sup> was probably consumed immediately after production by nitrification processes. Although anammox played a minor role in NH<sub>4</sub><sup>+</sup>-N removal under the current operational conditions, the coexistence of nitrifiers, anammox bacteria and denitrifiers provides a potentially possibility to enhance anammox activity via controlling operating conditions ( e.g. C/N ratios and hydraulic retention time) in the MET-CW.

The activity of nitrifier denitrification was confirmed in the MET-CW based the identification of  $^{15}\text{N}$  incorporated nitrite reductase affiliated to *Nitrosomonas*. The previous studies have reported that AOB was able to anaerobically reduce  $\text{NO}_2^-$  to  $\text{NO}$ ,  $\text{N}_2\text{O}$  and  $\text{N}_2$  under the oxygen limiting condition; this process was named nitrifier denitrification (Wrage et al. 2001), which is able to couple ammonia oxidation and nitrite reduction, thus can be utilized for more efficient nitrogen removal in wastewater treatment systems (Stein 2011). It was reported that nitrifier denitrification is favored by low DO and high  $\text{NO}_2^-$  level (Stein 2011). Given that DO concentration was low at the deep layer ( $<0.05 \text{ mg L}^{-1}$ ) in the MET-CW and full nitrification to  $\text{NO}_3^-$  was ruled out, these conditions would favor nitrifier denitrification in the MET-CW. Recently, nitrifier denitrification has been reported as the dominant source of  $\text{N}_2\text{O}$  in soils and also in two lab-scale sequencing batch reactors (Su et al. 2017, Zhu et al. 2013). Erler et al. (2008) found evidence that nitrifier-denitrification was potentially responsible for the production of  $\text{N}_2\text{O}$  in a surface flow wetland. A novel  $^{15}\text{N}$  and  $^{18}\text{O}$  isotope tracing approach was presented and used to discriminate the contribution of nitrifier denitrification from that of heterotrophic denitrification (Kool et al. 2010). In our study, although the occurrence of nitrifier denitrification and heterotrophic denitrification were confirmed, of which the contribution to nitrite reduction was not possible due to undetectable  $\text{NO}_2^-$  and  $\text{NO}_3^-$  concentration in the MET-CW.

#### 4.4 Supporting information

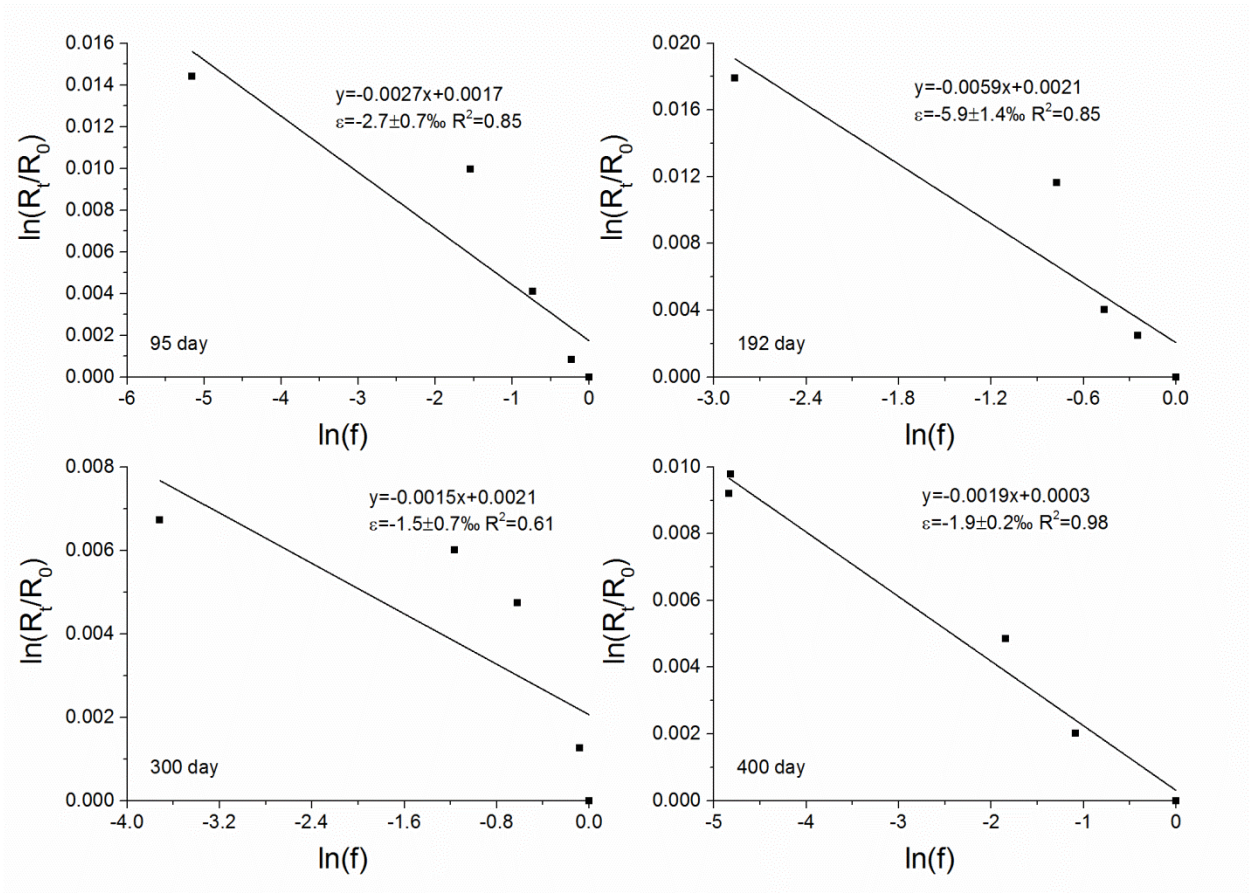


Figure S4-1. Rayleigh plots for N isotopic fractionation of  $\text{NH}_4^+$ . Kinetic isotopic effects were calculated according to the Rayleigh equation of a substrate.  $f$  is the fraction of the initial  $\text{NH}_4^+$ -N loads remaining in the MET-CW.

## CHAPTER 5 Conclusions and outlook

### 5.1 Treatment of benzene and ammonium contaminated groundwater using a MFC

One of the objectives of this work is to investigate whether MFC can be used to treat benzene and ammonium contaminated groundwater while simultaneously recovering energy. Results demonstrated that it is principal feasible to treat benzene and ammonium contaminated groundwater by a MFC equipped with an aerated cathode. Benzene was initially activated by enzymatic monohydroxylation at the oxygen-limited anode; the further anaerobic oxidation of the intermediate metabolites released electrons, which were transferred to the anode and eventually captured by oxygen at the cathode, driving oxygen reduction and accelerating electricity production. Benzene is considered thermodynamically favorable as the electron donor at the anode of MFCs, due to the low redox potential of the benzene oxidation ( $\text{HCO}_3^-/\text{C}_6\text{H}_6$ ,  $E^{\circ} = -0.28 \text{ V}$ ) (Luo et al. 2010). Theoretically, the complete mineralization of benzene to  $\text{CO}_2$  releases 30 electrons. However, the biodegradation of benzene in the MFC produced fewer than the 30 electrons expected from the complete oxidation, which is mainly caused by the incomplete oxidation of benzene or alternative substances as electron acceptors (e.g. carbonate leading to methanogenesis or organic or inorganic metabolites upon fermentation processes) (Wu et al. 2013). In this study, the coulombic and energy efficiencies of 14% and 4% were obtained for the anodic benzene degradation, indicating a sustainable loss of electrons in the MFC system. Wu et al. (2013) recently reported benzene degradation in the MFC with potassium ferricyanid as the catholyte, showing a coulombic efficiency of 3.3%. Although power densities and coulombic efficiencies obtained here were not as high as the glucose based MFC, this work demonstrated that it is feasible to use benzene as the electron donor at the anode in the MFC, providing valuable insights for practical applications of MFCs to remediate benzene-contaminated groundwater.

Nitrification took place at the aerated cathode of the MFC and was catalyzed by nitrifiers; the process was not directly linked to electricity generation. As  $\text{NH}_4^+\text{-N}$  can

release maximally eight electrons via oxidation to nitrate, ammonium can theoretically serve as an anodic electron donor (He et al. 2009). However, although  $\text{NH}_4^+$  removal from wastewater using electrochemical technologies has been previously reported, there is no unanimous agreement whether  $\text{NH}_4^+$  can be used as a direct substrate for electricity generation in MFCs. So far, several different strategies have been used to remove ammonium in MFCs: (i) recovering ammonia at the cathode chamber based on ammonia migration across ion exchange membranes driven by electricity generation or diffusion (Kuntke et al. 2012), (ii) using an external nitrifying bioreactor followed by a subsequent denitrification accomplished by microorganisms in the cathode chamber (Viridis et al. 2008), (iii) by simultaneous cathodic nitrification-denitrification process (Viridis et al. 2010). Viridis and colleagues revealed that the nitrifying bacteria colonized the outer layer of the biofilm and the denitrifying organisms occupied the inner layer, confirming the feasibility of simultaneous nitrification and denitrification at the cathode of a MFC (Viridis et al. 2011). The separated aerobic and anoxic cathodes for nitrification and denitrification were also designed to remove nitrogen (Xie et al. 2011, Zhang and He 2012b). Recently, a simultaneous nitrification and denitrification in the MFC was achieved by intermittent aeration at the cathode chamber (Sotres et al. 2016). However, these MFC systems often possess two-stage reactor configurations or require extra energy consumption, and thus limit their practical application. For improving nitrogen removal without extra energy consumption, an integrated wastewater treatment system is proposed by combining the anammox process with a MFC system (Ali and Okabe 2015). Several recent studies reported that the couple of anammox process and denitrification contributed to nitrogen removal in MFCs (Di Domenico et al. 2015, Li et al. 2015), confirming the feasibility of the anammox process in microbial electrochemical systems. In this study, although it is promising that nitrification occurred with high rates at the cathode of the MFC, the accumulated nitrate still needs to be removed by an additional treatment reactor. Considering the partial removal of ammonium, further research is of particular interest in order to promote simultaneous benzene and ammonium removal using MFC with an anoxic cathode, e.g. by addition of nitrite to accelerate anaerobic ammonium oxidation, avoiding the need of aeration, or the set-up of an additional denitrification reactor.

Despite the fact that in recent years the electricity generation from MFCs have been considerably improved and also reached the level of primary power target at least in small lab-scale systems, the scaling-up application under field conditions is still a big challenge. Currently, the high costs of cation exchange membranes, the potential for biofouling and associated high internal resistance restrain the electricity generation and limit the practical application of MFCs (Pant et al. 2010). In fact, the major MFC type that has been used for practical applications is the sediment MFC which can harvest power from sediment by embedding an anode in sediment and connect it via an electrical circuit to a cathode placed in the overlying aerobic seawater, making it feasible to power on-site to sensors and telemetry devices in remote oceanic areas (Huang et al. 2011, Lu et al. 2014). Additionally, rather than electricity generation, the MFC was also reported to be used as a wastewater refinery to produce or recover valuable chemicals such as hydrogen gas (Logan and Rabaey 2012). Recently, two 4 L tubular MFCs were successfully installed in a municipal wastewater treatment facility and operated for more than 400 days on primary effluent, showing efficient removal of organics and nitrogen (Zhang et al. 2013a). Therefore, in the near future the scaling-up application of MFCs could become commercially available along with the developments of cost-effective materials and designs.

## 5.2 The integration of MET and CWs

To improve benzene and ammonium removal, an integrated MET-CW was established by embedding four anode modules into the sand bed and connecting it to a cathode placed in the open pond inside a bench-scale HSSF-CW. Results indicated that benzene and  $\text{NH}_4^+$  removal in the HSSF-CW can be enhanced by combination with microbial electrochemical technology. The enhanced benzene removal was linked to its direct use as electron donor for the anode modules which acted as electron acceptor. Efficient removal of  $\text{NH}_4^+$  was probably due to the enhanced benzene removal so that inhibition by the co-contaminant benzene had no longer effect. The linear relationship between current density and benzene removal implied the potential biosensor application for monitoring benzene oxidation processes *in situ*. This is the first study to apply the integrated microbial electrochemical technology and constructed wetlands for treating benzene and ammonium co-contaminated groundwater.

To achieve higher treatment effects, integrating CWs and other technologies, such as membrane bio-reactors and MFCs, have emerged in recent years (Liu et al. 2015). A merged technique of integrating microbial electrochemical technology with constructed wetlands (e.g. CW-MFCs) has been developed (Wang et al. 2017). The fact that CWs naturally possess redox gradients provides the favorable conditions for MFCs; aerobic zones at the air-water interface or surrounding plant roots, and anoxic areas in the inner/lower layers support the operation of an anaerobic anode and an aerobic cathode in MFCs (Doherty et al. 2015). The integration of MFC with CW allows it for wastewater treatment and simultaneously electricity generation, making CWs more sustainable and environmentally friendly. By incorporating MFCs into CWs, the performance of pollutant removal is substantially improved (Fang et al. 2013, Villasenor et al. 2013), which was also demonstrated in our study (Wei et al. 2015b). However, it is also worth to note that power output and energy recovery efficiencies are still low, and thus more research is required in future to increase the power output. The small electrode surface area and the huge electrode spacing may result in comparatively low power densities (Zhao et al. 2013), and thus new strategies should be considered to increase the surface area of the electrode and to reduce the electrode spacing in order to achieve high power output. Another challenge for the integrated MET-CW is its full-scale application, which is usually restricted by substrate clogging especially when treating high strength wastewater (Doherty et al. 2015). Thus, another topic for future studies is to optimize the configuration and operational parameters of the integrated systems for scaling-up application.

In subsurface flow CWs, nitrogen removal efficiencies are often low due to the limited nitrification as a result of low oxygen transfer or the limited denitrification caused by low amounts of available organics (Saeed and Sun 2012), especially under high nitrogen loading rates. The integration of MFCs with CWs is able to improve nitrogen removal by promoting the nitrification and denitrification processes. The outstanding removal rates of total nitrogen, ammonium nitrogen ranging between 95% and 99% were reported in a pilot-scale CW-MFC (Wu et al. 2015a). Nitrate can be theoretically used as a final electron acceptor at the cathode of MFCs (Virdis et al. 2008, Xie et al. 2011, Zhang and He 2012b). In the CW-MFC, the cathode is typically placed at the wetland surface or in the rhizosphere, where aerobic conditions favor nitrification; meanwhile, the biofilm at the

cathode may provide a anoxic niches suitable for denitrification (Vymazal 2013). Therefore, the integration of MET with CWs is a promising technology to enhance nitrogen removal in CW systems.

### 5.3 Investigation of microbial nitrogen transformation processes

Microbial nitrogen transformation processes in the MET-CW were qualitatively and quantitatively characterized using N isotope fractionation,  $^{15}\text{N}$ -isotope tracing technique and *in situ* protein-SIP. Microbial ammonia oxidation was implied by negative relationships of  $\delta^{15}\text{N-NH}_4^+$  and  $\text{NH}_4^+\text{-N}$  loads. The significant enrichment of  $^{15}\text{N}$  in  $\text{NH}_4^+$  indicated the occurrence of microbial  $\text{NH}_4^+$  oxidation, which has been reported for a significant shift in isotope signature of  $\delta^{15}\text{N-NH}_4^+$  in pure nitrifying cultures and can be readily distinguished from other processes (e.g. plant uptake and mineralization) showing no or only minor  $\delta^{15}\text{N-NH}_4^+$  changes (Casciotti 2009, Casciotti et al. 2003). However, quantifying ammonia oxidation based on the determination of N isotope effects is difficult due to the influences of substrate concentrations and rate constants. Rate constants are associated with the different processes involved in ammonia oxidation (e.g. transport/diffusion, hydroxylamine oxidation), which could lead to different isotope effects for ammonia oxidation among different nitrifying microorganisms and even for the same microorganisms due to different extracellular conditions in different natural or experimental environments (Casciotti et al. 2011). Additionally, co-occurring processes may lead to masking of isotope fractionation for ammonia oxidation, thus it is appropriate to use multiple isotope analysis (e.g.  $\delta^{15}\text{N}$  and  $\delta^{18}\text{O}$  in  $\text{NH}_4^+$ ,  $\text{NO}_2^-$ ,  $\text{NO}_3^-$  or  $\text{N}_2\text{O}$ ) and combine the physico-chemical measurements as well as molecular biological approaches for proper evaluation of nitrogen transformation processes.

Protein-SIP and metaproteomic analysis revealed the potential activities of partial nitrification, anammox, heterotrophic denitrification and nitrifier denitrification in the MET-CW. A much higher contribution of denitrification was observed compared to anammox, indicating that denitrification played the major role in  $\text{NH}_4^+\text{-N}$  removal. Unfortunately, it is not feasible to distinguish nitrifier denitrification from heterotrophic denitrification due to the small  $\text{NO}_2^-$  and  $\text{NO}_3^-$  accumulation. Conventionally, nitrogen removal is achieved by nitrification followed by a denitrification process (Saeed and Sun

2012). In subsurface flow constructed wetlands, novel biological nitrogen removal processes, including partial nitrification and denitrification, simultaneous nitrification and denitrification, and anammox were found to contribute nitrogen transformation and removal (Vymazal 2007). In this work, partial nitrification and denitrification were detected as the dominant nitrogen transformation processes, which can theoretically save 25% of O<sub>2</sub> consumption and 40% of organic carbon requirement, and reduce CO<sub>2</sub> emission by 20% (Peng and Zhu 2006). Additionally, the presence of anammox bacteria provided a promising alternative for nitrogen removal from contaminated groundwater in the MET-CW system.

The nitrogen transformation process is complex and dynamic during wastewater treatment, which has a strong effect on nitrogen removal efficiency (Faulwetter et al. 2009). Therefore, understanding nitrogen transformation processes and their individual contributions more in-depth is valuable for optimization of nitrogen removal process and improvement of nitrogen removal efficiency. Many studies have been performed to elucidate nitrogen transformation processes and nitrogen transformation communities using cultivation or molecular methods, e.g. DGGE, FISH, and real-time PCR (Truu et al. 2009). Metagenomics approaches offer the ability to directly examine the genomic content of microbial communities, complementing taxonomic information with functional capability. However, these techniques can only provide information on the functional potential rather than actually metabolic activities for microbial communities. Stable isotope probing (SIP) techniques offers a powerful new technique allowing for the targeted detection and identification of organisms, metabolic pathways and elemental fluxes active in specific processes within complex microbial communities (Radajewski et al. 2000). This study provides a promising protein-SIP approach to allow to *in situ* assess nitrogen transformation processes and active species in the complex ecosystems.

---

## REFERENCES

- Abu Laban, N., Selesi, D., Jobelius, C. and Meckenstock, R.U. (2009) Anaerobic benzene degradation by Gram-positive sulfate-reducing bacteria. *FEMS Microbiol. Ecol.* 68(3), 300-311.
- Abu Laban, N., Selesi, D., Rattei, T., Tischler, P. and Meckenstock, R.U. (2010) Identification of enzymes involved in anaerobic benzene degradation by a strictly anaerobic iron-reducing enrichment culture. *Environ. Microbiol.* 12(10), 2783-2796.
- Aburto-Medina, A. and Ball, A.S. (2015) Microorganisms involved in anaerobic benzene degradation. *Ann. Microbiol.* 65(3), 1201-1213.
- Adrados, B., Sanchez, O., Arias, C.A., Becares, E., Garrido, L., Mas, J., Brix, H. and Morato, J. (2014) Microbial communities from different types of natural wastewater treatment systems: vertical and horizontal flow constructed wetlands and biofilters. *Water Res.* 55, 304-312.
- Afferden, M., Rahman, K.Z., Mosig, P., De Biase, C., Thullner, M., Oswald, S.E. and Muller, R.A. (2011) Remediation of groundwater contaminated with MTBE and benzene: the potential of vertical-flow soil filter systems. *Water Res.* 45(16), 5063-5074.
- Ali, M. and Okabe, S. (2015) Anammox-based technologies for nitrogen removal: Advances in process start-up and remaining issues. *Chemosphere* 141, 144-153.
- Arp, D.J., Sayavedra-Soto, L.A. and Hommes, N.G. (2002) Molecular biology and biochemistry of ammonia oxidation by *Nitrosomonas europaea*. *Arch. Microbiol.* 178(4), 250-255.
- Badalamenti, J.P., Torres, C.I. and Krajmalnik-Brown, R. (2013) Light-responsive current generation by phototrophically enriched anode biofilms dominated by green sulfur bacteria. *Biotechnol. Bioeng.* 14(4), 1020-1027.
- Balcke, G.U., Wegener, S., Kiesel, B., Benndorf, D., Schlomann, M. and Vogt, C. (2008) Kinetics of chlorobenzene biodegradation under reduced oxygen levels. *Biodegradation* 19(4), 507-518.
- Bartrons, M., Camarero, L. and Catalan, J. (2009) Nitrogen stable isotopes of ammonium and nitrate in high mountain lakes of the Pyrenees. *Biogeosciences Discuss.* 6, 11479-11499.
- Bastida, F., Rosell, M., Franchini, A.G., Seifert, J., Finsterbusch, S., Jehmlich, N., Jechalke, S., von Bergen, M. and Richnow, H.H. (2010) Elucidating MTBE degradation in a mixed consortium using a multidisciplinary approach. *FEMS Microbiol. Ecol.* 73(2), 370-384.

- Ben-Youssef, C., Zepeda, A., Texier, A. and Gomez, J. (2009) A two-step nitrification model of ammonia and nitrite oxidation under benzene inhibitory and toxic effects in nitrifying batch cultures. *Chem. Eng. J.* 152(1), 264-270.
- Bergmann, F.D., Abu Laban, N.M., Meyer, A.H., Elsner, M. and Meckenstock, R.U. (2011) Dual (C, H) isotope fractionation in anaerobic low molecular weight (poly) aromatic hydrocarbon (PAH) degradation: potential for field studies and mechanistic implications. *Environ. Sci. Technol.* 45(16), 6947-6953.
- Böhlke, J.K., Smith, R.L. and Miller, D.N. (2006) Ammonium transport and reaction in contaminated groundwater: Application of isotope tracers and isotope fractionation studies. *Water Sci. Technol.* 42(5), 1-19.
- Bollmann, A., French, E. and Laanbroek, J.L. (2011) Isolation, cultivation, and characterization of ammonia-oxidizing bacteria and archaea adapted to low ammonium concentrations. Abelson, J., Melvin, I.S., Colowick, S.P. and Nathan, A.K. (eds), pp. 55-88, Elsevier, Oxford, USA.
- Braeckevelt, M., Fischer, A. and Kastner, M. (2012) Field applicability of Compound-Specific Isotope Analysis (CSIA) for characterization and quantification of in situ contaminant degradation in aquifers. *Appl. Microbiol. Biot.* 94(6), 1401-1421.
- Brunner, B., Contreras, S., Lehmann, M.F., Matantseva, O., Rollog, M., Kalvelage, T., Klockgether, G., Lavik, G., Jetten, M.S.M., Kartal, B. and Kuypers, M.M.M. (2013) Nitrogen isotope effects induced by anammox bacteria. *P Natl. Acad. Sci. USA* 110, 18994-18999.
- Burland, S.M. and Edwards, E.A. (1999) Anaerobic benzene biodegradation linked to nitrate reduction. *Appl. environ. microb.* 65(2), 529-533.
- Burmaster, D.E. (2013) Groundwater contamination in the United States. *Sci.* 65(12), 713-718.
- Casciotti, K.L. (2009) Inverse kinetic isotope fractionation during bacterial nitrite oxidation. *Geochim. Cosmochim. Acta* 73(7), 2061-2076.
- Casciotti, K.L., Buchwald, C., Santoro, A.E. and Frame, C. (2011) Assessment of nitrogen and oxygen isotopic fractionation during nitrification and its expression in the marine environment. *Methods Enzymol.* 486, 253-280.
- Casciotti, K.L., Sigman, D.M. and Ward, B.B. (2003) Linking diversity and stable isotope fractionation in ammonia-oxidizing bacteria. *Geomicrobiol. J.* 20(4), 335-353.
- Cercado-Quezada, B., Delia, M.L. and Bergel, A. (2010) Testing various food-industry wastes for electricity production in microbial fuel cell. *Bioresour. Technol.* 101(8), 2748-2754.
- Chen, H., Zheng, P., Zhang, J., Xie, Z., Ji, J. and Ghulam, A. (2014) Substrates and pathway of electricity generation in a nitrification-based microbial fuel cell. *Bioresour. Technol.* 161, 208-214.

- Chen, Z., Kuschik, P., Reiche, N., Borsdorf, H., Kastner, M. and Koser, H. (2012) Comparative evaluation of pilot scale horizontal subsurface-flow constructed wetlands and plant root mats for treating groundwater contaminated with benzene and MTBE. *J. Hazard. Mater.* s 209-210 (1), 510-515.
- Chiang, C.Y., Salanitro, J.P., Chai, E.Y., Colthart, J.D. and Klein, C.L. (1989) Aerobic biodegradation of benzene, toluene, and xylene in a sandy aquifer-data analysis and computer modeling. *Ground Water* 27, 823-834.
- Clark, I., Timlin, R., Bourbonnais, A., Jones, K., Lafleur, D. and Wickens, K. (2008) Origin and fate of industrial ammonium in anoxic ground water -  $^{15}\text{N}$  evidence for anaerobic oxidation (anammox). *Groundwater Monit. Remediat.* 28(3), 73-82.
- Coban, O., Kuschik, P., Kappelmeyer, U., Spott, O., Martiensen, M., Jetten, M.S. and Knoeller, K. (2015a) Nitrogen transforming community in a horizontal subsurface-flow constructed wetland. *Water Res.* 74, 203-212.
- Coban, O., Kuschik, P., Wells, N.S., Strauch, G. and Knoeller, K. (2015b) Microbial nitrogen transformation in constructed wetlands treating contaminated groundwater. *Environ. Sci. Pollut. Res.* 22, 128-129.
- Dan, T.H., Quang, L.N., Chiem, N.H. and Brix, H. (2011) Treatment of high-strength wastewater in tropical constructed wetlands planted with *Sesbania sesban*: Horizontal subsurface flow versus vertical downflow. *Ecol. Eng.* 37(5), 711-720.
- Davis, E.M., Murray, H.E., Liehr, J.G. and Powers, E.L. (1981) Basic microbial degradation rates and chemical byproducts of selected organic compounds. *Water Res.* 15(9), 1125-1127.
- Davis, J.W., Klier, N.J. and Carpenter, C.L. (1994) Natural biological attenuation of benzene in ground water beneath a manufacturing facility. *Groundwater* 32(2), 215-226.
- de la Torre, J.R., Walker, C.B., Ingalls, A.E., Konneke, M. and Stahl, D.A. (2008) Cultivation of a thermophilic ammonia oxidizing archaeon synthesizing crenarchaeol. *Environ. Microbiol.* 10(3), 810-818.
- Di Domenico, E.G., Petroni, G., Mancini, D., Geri, A., Di Palma, L. and Ascenzioni, F. (2015) Development of electroactive and anaerobic ammonium-oxidizing (anammox) biofilms from digestate in microbial fuel cells. *Biomed. Res. Int.* 2015, 80-97.
- Di Lorenzo, M., Curtis, T.P., Head, I.M. and Scott, K. (2009) A single-chamber microbial fuel cell as a biosensor for wastewaters. *Water Res.* 43(13), 3145-3154.
- Diaz, E., Jimenez, J.I. and Nogales, J. (2013) Aerobic degradation of aromatic compounds. *Curr. Opin. Chem. Biol.* 24(3), 431-442.

- Doherty, L., Zhao, Y., Zhao, X., Hu, Y., Hao, X., Xu, L. and Liu, R. (2015) A review of a recently emerged technology: constructed wetland--microbial fuel cells. *Water Res.* 85, 38-45.
- Du, Y., Feng, Y.J., Dong, Y., Qu, Y.P., Liu, J., Zhou, X.T. and Ren, N.Q. (2014) Coupling interaction of cathodic reduction and microbial metabolism in aerobic biocathode of microbial fuel cell. *RSC Adv.* 4(65), 34350-34355.
- Environment agency 1998 Proposed environmental quality standards for list II substances in water: ammonia, p. 260, Bristol.
- Erler, D.V. and Eyre, B.D. (2010) Quantifying nitrogen process rates in a constructed wetland using natural abundance stable isotope signatures and stable isotope amendment experiments. *J. Environ. Qual.* 39(6), 2191-2199.
- Erler, D.V., Eyre, B.D. and Davison, L. (2008) The contribution of anammox and denitrification in a surface flow constructed wetland. *Environ. Sci. Technol.* 42, 9144-9150.
- European Council (1998) Council Directive 98/83/EC of 3 November 1998 on the quality of water intended for human consumption, Brussels.
- Fahy, A., McGenity, T.J., Timmis, K.N. and Ball, A.S. (2006) Heterogeneous aerobic benzene-degrading communities in oxygen-depleted groundwaters. *FEMS Microbiol. Ecol.* 58(2), 260-270.
- Fang, Z., Song, H.L., Cang, N. and Li, X.N. (2013) Performance of microbial fuel cell coupled constructed wetland system for decolorization of azo dye and bioelectricity generation. *Bioresour. Technol.* 144, 165-171.
- Farhadian, M., Vachelard, C., Duchez, D. and Larroche, C. (2008) In situ bioremediation of monoaromatic pollutants in groundwater: a review. *Bioresour. Technol.* 99(13), 5296-5308.
- Faulwetter, J.L., Gagnon, V., Sundberg, C., Chazarenc, F., Burr, M.D., Brisson, J., Camper, A.K. and Stein, O.R. (2009) Microbial processes influencing performance of treatment wetlands: A review. *Ecol. Eng.* 35(6), 987-1004.
- Feng, X., Tang, K.H., Blankenship, R.E. and Tang, Y.J. (2010) Metabolic flux analysis of the mixotrophic metabolisms in the green sulfur bacterium *Chlorobaculum tepidum*. *J. Biol. Chem.* 285(50), 39544-39550.
- Feng, Y., He, W., Liu, J., Wang, X., Qu, Y. and Ren, N. (2014) A horizontal plug flow and stackable pilot microbial fuel cell for municipal wastewater treatment. *Bioresour. Technol.* 156, 132-138.
- Fischer, A., Gehre, M., Breinfeld, J., Richnow, H.H. and Vogt, C. (2009) Carbon and hydrogen isotope fractionation of benzene during biodegradation under sulfate-reducing conditions: a laboratory to field site approach. *Rapid Commun. Mass Spectrom.* 23(16), 2439-2447.

- Fischer, A., Herklotz, I., Herrmann, S., Thullner, M., Weelink, S.A., Stams, A.J., Schlomann, M., Richnow, H.H. and Vogt, C. (2008) Combined carbon and hydrogen isotope fractionation investigations for elucidating benzene biodegradation pathways. *Environ. Sci. Technol.* 42(12), 4356-4363.
- Fischer, A., Theuerkorn, K., Stelzer, N., Gehre, M., Thullner, M. and Richnow, H.H. (2007) Applicability of stable isotope fractionation analysis for the characterization of benzene biodegradation in a BTEX-contaminated aquifer. *Environ. Sci. Technol.* 41(10), 3689-3696.
- Garcia, J., Rousseau, D.P.L., MoratÓ, J., Lesage, E.L.S., Matamoros, V. and Bayona, J.M. (2010) Contaminant removal processes in subsurface-flow constructed wetlands: a review. *Crit. Rev. Environ. Sci. Technol.* 40(7), 561-661.
- Ge, S., Wang, S., Yang, X., Qiu, S., Li, B. and Peng, Y. (2015) Detection of nitrifiers and evaluation of partial nitrification for wastewater treatment: A review. *Chemosphere* 140, 85-98.
- Ghaffar, A.K., Fischer, F., Wick, A. and Ternes, T.A. (2017) Anaerobic biodegradation of (emerging) organic contaminants in the aquatic environment. *Water Res.* 116, 268-295.
- Gibson, D.T. (1968) Microbial degradation of aromatic compounds. *Sci.* 161(3846), 1093-1097.
- Gieg, L.M., Fowler, S.J. and Berdugo-Clavijo, C. (2014) Syntrophic biodegradation of hydrocarbon contaminants. *Curr. Opin. Biotechnol.* 27, 21-29.
- Gleick, P.H. (2014) *The world's water volume 8: The biennial report on freshwater resources*, Island Press.
- Ha, P.T., Lee, T.K., Rittmann, B.E., Park, J. and Chang, I.S. (2012) Treatment of alcohol distillery wastewater using a Bacteroidetes-dominant thermophilic microbial fuel cell. *Environ. Sci. Technol.* 46(5), 3022-3030.
- Harnisch, F. and Schroder, U. (2010) From MFC to MXC: chemical and biological cathodes and their potential for microbial bioelectrochemical systems. *Chem. Soc. Rev.* 39(11), 4433-4448.
- Hashim, M.A., Mukhopadhyay, S., Sahu, J.N. and Sengupta, B. (2011) Remediation technologies for heavy metal contaminated groundwater. *J. Environ. Manage.* 92(10), 2355-2388.
- Hatzenpichler, R. (2012) Diversity, physiology, and niche differentiation of ammonia-oxidizing archaea. *Appl. Environ. Microbiol.* 78(21), 7501-7510.
- Hatzenpichler, R., Lebedeva, E.V., Spieck, E., Stoecker, K., Richter, A., Daims, H. and Wagner, M. (2008) A moderately thermophilic ammonia-oxidizing crenarchaeote from a hot spring. *Proc. Natl. Acad. Sci. USA* 105(6), 2134-2139.
- He, T., Li, Z., Sun, Q., Xu, Y. and Ye, Q. (2016) Heterotrophic nitrification and aerobic denitrification by *Pseudomonas tolaasii* Y-11 without nitrite accumulation during nitrogen conversion. *Bioresour. Technol.* 200, 493-499.

- He, Z., Kan, J., Wang, Y., Huang, Y., Mansfeld, F. and Neilson, K.H. (2009) Electricity production coupled to ammonium in a microbial fuel cell. *Environ. Sci. Technol.* 43(9), 3391-3397.
- Heffer, P. and Prud'homme, M. (2016) *Fertilizer outlook 2016–2020*. Heffer, P. and Prud'homme, M. (eds), Paris.
- Herbst, F.A., Bahr, A., Duarte, M., Pieper, D.H., Richnow, H.H., von Bergen, M., Seifert, J. and Bombach, P. (2013) Elucidation of in situ polycyclic aromatic hydrocarbon degradation by functional metaproteomics (protein-SIP). *Proteomics* 13(18-19), 2910-2920.
- Herrmann, S., Kleinsteuber, S., Chatzinotas, A., Kuppardt, S., Lueders, T., Richnow, H.H. and Vogt, C. (2010) Functional characterization of an anaerobic benzene-degrading enrichment culture by DNA stable isotope probing. *Environ. Microbiol.* 12(2), 401-411.
- Hijosa-Valsero, M., Matamoros, V., Sidrach-Cardona, R., Martin-Villacorta, J., Becares, E. and Bayona, J.M. (2010) Comprehensive assessment of the design configuration of constructed wetlands for the removal of pharmaceuticals and personal care products from urban wastewaters. *Water Res.* 44(12), 3669-3678.
- Hu, Y., He, F., Ma, L., Zhang, Y. and Wu, Z. (2016) Microbial nitrogen removal pathways in integrated vertical-flow constructed wetland systems. *Bioresour. Technol.* 207, 339-345.
- Huang, D.-Y., Zhou, S.-G., Chen, Q., Zhao, B., Yuan, Y. and Zhuang, L. (2011) Enhanced anaerobic degradation of organic pollutants in a soil microbial fuel cell. *Chem. Eng. J.* 172(2-3), 647-653.
- Imfeld, G., Braeckevelt, M., Kusch, P. and Richnow, H.H. (2009) Monitoring and assessing processes of organic chemicals removal in constructed wetlands. *Chemosphere* 74, 349-362.
- Jacob, J., Sanders, T. and Dähnke, K. (2016) Nitrification and Nitrite Isotope Fractionation as a Case Study in a major European River. *Biogeosciences Discuss.*, 1-17.
- Jechalke, S., Rosell, M., Vogt, C. and Richnow, H.H. (2011) Inhibition of nitrification by low oxygen concentrations in an aerated treatment pond system with biofilm promoting mats. *Water Environ. Res.* 83(7), 622-626.
- Jechalke, S., Vogt, C., Reiche, N., Franchini, A.G., Borsdorf, H., Neu, T.R. and Richnow, H.H. (2010) Aerated treatment pond technology with biofilm promoting mats for the bioremediation of benzene, MTBE and ammonium contaminated groundwater. *Water Res.* 44(6), 1785-1796.
- Jehmlich, N., Schmidt, F., Hartwich, M., von Bergen, M., Richnow, H.H. and Vogt, C. (2008a) Incorporation of carbon and nitrogen atoms into proteins measured by protein-based stable isotope probing (Protein-SIP). *Rapid Commun. Mass Spectrom.* 22(18), 2889-2897.
- Jehmlich, N., Schmidt, F., Taubert, M., Seifert, J., Bastida, F., von Bergen, M., Richnow, H.H. and Vogt, C. (2010) Protein-based stable isotope probing. *Nat. Protoc.* 5(12), 1957-1966.

- Jehmlich, N., Schmidt, F., von Bergen, M., Richnow, H.H. and Vogt, C. (2008b) Protein-based stable isotope probing (Protein-SIP) reveals active species within anoxic mixed cultures. *ISME J.* 2(11), 1122-1133.
- Jehmlich, N., Vogt, C., Lunsman, V., Richnow, H.H. and von Bergen, M. (2016) Protein-SIP in environmental studies. *Curr. Opin. Biotechnol.* 41, 26-33.
- Jetten, M.S., Wagner, M., Fuerst, J., van Loosdrecht, M., Kuenen, G. and Strous, M. (2001) Microbiology and application of the anaerobic ammonium oxidation ("anammox") process. *Curr. Opin. Biotechnol.* 12(3), 283-288.
- Ji, B., Yang, K., Zhu, L., Jiang, Y., Wang, H., Zhou, J. and Zhang, H. (2015) Aerobic denitrification: A review of important advances of the last 30 years. *Biotechnol. Bioprocess Eng.* 20(4), 643-651.
- Jiang, Y., Martinez-Guerra, E., Gnanaswar Gude, V., Magbanua, B., Truax, D.D. and Martin, J.L. (2016) Wetlands for wastewater treatment. *Water Environ. Res.* 88(10), 1160-1191.
- Jung, S. and Regan, J.M. (2011) Influence of external resistance on electrogenesis, methanogenesis, and anode prokaryotic communities in microbial fuel cells. *Appl. Environ. Microb.* 77(2), 564-571.
- Junier, P., Molina, V., Dorador, C., Hadas, O., Kim, O.S., Junier, T., Witzel, J.P. and Imhoff, J.F. (2010) Phylogenetic and functional marker genes to study ammonia-oxidizing microorganisms (AOM) in the environment. *Appl. Microb. Biot.* 85(3), 425-440.
- Kadlec, R.H. and Wallace, S.D. (2009) *Treatment Wetlands*, second ed, CRC press/Taylor & Francis Group, Boca Raton, USA.
- Kartal, B., Maalcke, W.J., de Almeida, N.M., Cirpus, I., Gloerich, J., Geerts, W., Op den Camp, H.J., Harhangi, H.R., Janssen-Megens, E.M., Francoijs, K.J., Stunnenberg, H.G., Keltjens, J.T., Jetten, M.S. and Strous, M. (2011) Molecular mechanism of anaerobic ammonium oxidation. *Nature* 479(7371), 127-130.
- Kasai, Y., Takahata, Y., Manefield, M. and Watanabe, K. (2006) RNA-based stable isotope probing and isolation of anaerobic benzene-degrading bacteria from gasoline-contaminated groundwater. *Appl. Environ. Microb.* 72(5), 3586-3592.
- Kelly, P.T. and He, Z. (2014) Nutrients removal and recovery in bioelectrochemical systems: a review. *Bioresour. Technol.* 153, 351-360.
- Kim, J.R., Zuo, Y., Regan, J.M. and Logan, B.E. (2008) Analysis of ammonia loss mechanisms in microbial fuel cells treating animal wastewater. *Biotechnol. Bioeng.* 99(5), 1120-1127.

- Kleinstaub, S., Schleinitz, K.M., Breithof, J., Harms, H., Richnow, H.H. and Vogt, C. (2008) Molecular characterization of bacterial communities mineralizing benzene under sulfate-reducing conditions. *FEMS Microbiol. Ecol.* 66(1), 143-157.
- Kool, D.M., Dolfing, J., Wrage, N. and Van Groenigen, J.W. (2011) Nitrifier denitrification as a distinct and significant source of nitrous oxide from soil. *Soil Biol. Biochem.* 43(1), 174-178.
- Kool, D.M., Wrage, N., Zechmeister-Boltenstern, S., Pfeffer, M., Brus, D., Oenema, O. and Van Groenigen, J.W. (2010) Nitrifier denitrification can be a source of N<sub>2</sub>O from soil: a revised approach to the dual-isotope labelling method. *Eur. J. Soil. Sci.* 61(5), 759-772.
- Kumar, M. and Lin, J.G. (2010) Co-existence of anammox and denitrification for simultaneous nitrogen and carbon removal-Strategies and issues. *J. Hazard. Mater.* 178(1-3), 1-9.
- Kunapuli, U., Lueders, T. and U., M.R. (2007) The use of stable isotope probing to identify key iron-reducing microorganisms involved in anaerobic benzene degradation. *ISME J.* 1(7), 643-653.
- Kuntke, P., Smiech, K.M., Bruning, H., Zeeman, G., Saakes, M., Sleutels, T.H., Hamelers, H.V. and Buisman, C.J. (2012) Ammonium recovery and energy production from urine by a microbial fuel cell. *Water Res.* 46(8), 2627-2636.
- Kurola, J., Salkinoja-Salonen, M., Aarnio, T., Hultman, J. and Romantschuk, M. (2005) Activity, diversity and population size of ammonia-oxidising bacteria in oil-contaminated landfarming soil. *FEMS Microbiol. Lett.* 250(1), 33-38.
- Ladino-Orjuela, G., Gomes, E., da Silva, R., Salt, C. and Parsons, J.R. (2016) Metabolic Pathways for Degradation of Aromatic Hydrocarbons by Bacteria. *Rev. Environ. Contam. Toxicol.* 237, 105-121.
- Lauchnor, E.G., Radniecki, T.S. and Semprini, L. (2011) Inhibition and gene expression of *Nitrosomonas europaea* biofilms exposed to phenol and toluene. *Biotechnol. Bioeng.* 108(4), 750-757.
- Lee, C., Fletcher, T.D. and Sun, G. (2009) Nitrogen removal in constructed wetland systems. *Eng. Life Sci.* 9, 11-22.
- Lee, H.S., Prathap, P., Andrew, K.M., Cešar, I.T. and Rittmann, B.E. (2008) Evaluation of energy-conversion efficiencies in microbial fuel cells (MFCs) utilizing fermentable and non-fermentable substrates. *Water Res.* 42, 1501-1510.
- Li, C., Ren, H., Xu, M. and Cao, J. (2015) Study on anaerobic ammonium oxidation process coupled with denitrification microbial fuel cells (MFCs) and its microbial community analysis. *Bioresour. Technol.* 175, 545-552.

- Liou, J.S., Derito, C.M. and Madsen, E.L. (2008) Field-based and laboratory stable isotope probing surveys of the identities of both aerobic and anaerobic benzene-metabolizing microorganisms in freshwater sediment. *Environ. Microbiol.* 10(8), 1964-1977.
- Liu, R., Zhao, Y., Doherty, L., Hu, Y. and Hao, X. (2015) A review of incorporation of constructed wetland with other treatment processes. *Chem. Eng. J.* 279, 220-230.
- Liu, S., Song, H., Li, X. and Yang, F. (2013) Power generation enhancement by utilizing plant photosynthate in microbial fuel cell coupled constructed wetland system. *Int. J. Photoenergy* 2013, 1-10.
- Liu, S., Song, H., Wei, S., Yang, F. and Li, X. (2014) Bio-cathode materials evaluation and configuration optimization for power output of vertical subsurface flow constructed wetland - Microbial fuel cell systems. *Bioresour. Technol.* 166, 575-583.
- Liu, Z., Liu, J., Zhang, S., Xing, X.H. and Su, Z. (2011) Microbial fuel cell based biosensor for in situ monitoring of anaerobic digestion process. *Bioresour. Technol.* 102(22), 10221-10229.
- Logan, B.E. (2008) *Microbial fuel cells*, John Wiley & Sons, New York.
- Logan, B.E., Hamelers, B., Rozendal, R., Schroder, U., Keller, R.G., Freguia, S., Aelterman, P., Verstraete, W. and Rabaey, K. (2006) Microbial fuel cell: methonology and technology. *Environ. Sci. Technol.* 40(17), 5181-5191.
- Logan, B.E. and Rabaey, K. (2012) Conversion of wastes into bioelectricity and chemicals by using microbial electrochemical technologies. *Sci.* 337(6095), 686-690.
- Logan, B.E. and Regan, J.M. (2006) Microbial fuel cell - challenge and application. *Environ. Sci. Technol.* 40, 5172-5180.
- Lotti, T., van der Star, W.R., Kleerebezem, R., Lubello, C. and van Loosdrecht, M.C. (2012) The effect of nitrite inhibition on the anammox process. *Water Res.* 46(8), 2559-2569.
- Lovley, D.R. (1997) Potential for anaerobic bioremediation of BTEX in petroleum - contaminated aquifers. *J. Ind. Microbiol. Biotechnol.* 18(2), 75-81.
- Lu, L., Yazdi, H., Jin, S., Zuo, Y., Fallgren, P.H. and Ren, Z.J. (2014) Enhanced bioremediation of hydrocarbon-contaminated soil using pilot-scale bioelectrochemical systems. *J. Hazard. Mater.* 274, 8-15.
- Lucker, S., Wagner, M., Maixner, F., Pelletier, E., Koch, H., Vacherie, B., Rattei, T., Damste, J.S.S., Spieck, E., Le Paslier, D. and Daims, H. (2010) A *Nitrospira* metagenome illuminates the physiology and evolution of globally important nitrite-oxidizing bacteria. *P. Natl. Acad. Sci. USA* 107(30), 13479-13484.
- Lunsmann, V., Kappelmeyer, U., Benndorf, R., Martinez-Lavanchy, P.M., Taubert, A., Adrian, L., Duarte, M., Pieper, D.H., von Bergen, M., Muller, J.A., Heipieper, H.J. and Jehmlich, N. (2016)

- In situ protein-SIP highlights Burkholderiaceae as key players degrading toluene by para ring hydroxylation in a constructed wetland model. *Environ. Microbiol.* 18(4), 1176-1186.
- Luo, F., Gitiafroz, R., Devine, C.E., Gong, Y., Hug, L.A., Raskin, L. and Edwards, E.A. (2014) Metatranscriptome of an anaerobic benzene-degrading, nitrate-reducing enrichment culture reveals involvement of carboxylation in benzene ring activation. *Appl. Environ. Microb.* 80(14), 4095-4107.
- Luo, H., Zhang, C., Song, H., Liu, G. and Zhang, R. (2010) Electricity production of microbial fuel cell with biodegradation of benzene. *Acta Sci. Nat. Univ. Sunyatseni* 49(1), 113-118.
- Ma, B., Peng, Y., Zhang, S., Wang, J., Gan, Y., Chang, J., Wang, S., Wang, S. and Zhu, G. (2013a) Performance of anammox UASB reactor treating low strength wastewater under moderate and low temperatures. *Bioresour. Technol.* 129, 606-611.
- Ma, J., Wang, Z., Zhu, C., Liu, S., Wang, Q. and Wu, Z. (2013b) Analysis of nitrification efficiency and microbial community in a membrane bioreactor fed with low COD/N-ratio wastewater. *Plos one* 8(5), p. e63059.
- Mancini, S.A., Devine, C.E., Elsner, M., Nandi, M.E., Ulrich, A.C., Edwards, E.A. and Lollar, B.S. (2008) Isotopic evidence suggests different initial reaction mechanisms for anaerobic benzene biodegradation. *Environ. Sci. Technol.* 42(22), 8290-8296.
- Mariotti, A., Germon, J.C., Hubert, P., Kaiser, P., Letolle, R., Tardieux, A. and Tardieux, P. (1981) Experimental determination of nitrogen kinetic isotope fractionation: some principles; illustration for the denitrification and nitrification process. *Plant Soil* 62(3), 413-430.
- Martienssen, M., Fabritius, H., Kukla, S., Balcke, G.U., Hasselwander, E. and Schirmer, M. (2006) Determination of naturally occurring MTBE biodegradation by analysing metabolites and biodegradation by - products. *J. Contam. Hydrol.* 87(1-2), 37-53.
- Meckenstock, R.U., Boll, M., Mouttaki, H., Koelschbach, J.S., Cunha Tarouco, P., Weyrauch, P., Dong, X. and Himmelberg, A.M. (2016) Anaerobic Degradation of Benzene and Polycyclic Aromatic Hydrocarbons. *J. Mol. Microbiol. Biotechnol.* 26(1-3), 92-118.
- Meckenstock, R.U., Morasch, B., Griebler, C. and Richnow, H.H. (2004) Stable isotope fractionation analysis as a tool to monitor biodegradation in contaminated aquifers. *J. Contam. Hydrol.* 75(3-4), 215-255.
- Meija, J., Coplen, T.B., Berglund, M., Brand, W.A., De Bièvre, P., Gröning, M., Holden, N.E., Irrgeher, J., Loss, R.D., Walczyk, T. and Prohaska, T. (2016) Isotopic compositions of the elements 2013 (IUPAC Technical Report). *Pure Appl. Chem.* 88(3), 293-306.
- Meincke, M., Krieg, E. and Bock, E. (1989) *Nitrosovibrio* spp, the dominant ammonia-oxidizing bacteria in building sandstone. *Appl. Environ. Microbiol.* 55(8), 2108-2110.

- Meng, P., Pei, H., Hu, W., Shao, Y. and Li, Z. (2014) How to increase microbial degradation in constructed wetlands: Influencing factors and improvement measures. *Bioresource Technology* 157, 316-326.
- Merchant Research and Consulting Ltd. (2014) *Benzene: 2013 World Market Outlook and Forecast up to 2017*, Dublin, Ireland.
- Mook, W.T., Chakrabarti, M.H., Aroua, M.K., Khan, G.M.A., Ali, B.S., Islam, M.S. and Abu Hassan, M.A. (2012) Removal of total ammonia nitrogen (TAN), nitrate and total organic carbon (TOC) from aquaculture wastewater using electrochemical technology: A review. *Desalination* 285, 1-13.
- Morris, J.M. and Jin, S. (2012) Enhanced biodegradation of hydrocarbon-contaminated sediments using microbial fuel cells. *J. Hazard. Mater.* 213-214, 474-477.
- Mulder, A. (2003) The quest for sustainable nitrogen removal technologies. *Wat. Sci. Tech.* 48(1), 67-75.
- Nisi, B., Raco, B. and Dotsika, E. (2014) *Threats to the Quality of Groundwater Resources*, pp. 115-150, Springer Berlin Heidelberg.
- Ohte, N., Nagata, T., Tayasu, I., Kohzu, A. and Yoshimizu, C. (2007) Nitrogen and oxygen isotope measurements of nitrate to survey the sources and transformation of nitrogen loads in rivers, pp. 31-39, *Bulletin of Terrestrial Environment Research Center, University of Tsukuba, Tsukuba.*
- Olmos, A., Olguin, P., Fajardo, C., Razo, E. and Monroy, O. (2004) Physicochemical characterization of spent caustic from the OXIMER process and sour waters from Mexican oil refineries. *Energy & Fuels* 18(2), 302-304.
- Panagos, P., Van Liedekerke, M., Yigini, Y. and Montanarella, L. (2013) Contaminated sites in Europe: review of the current situation based on data collected through a European network. *J. Environ. Public. Health.* 2013.
- Pant, D., Van Bogaert, G., Diels, L. and Vanbroekhoven, K. (2010) A review of the substrates used in microbial fuel cells (MFCs) for sustainable energy production. *Bioresour. Technol.* 101(6), 1533-1543.
- Paredes, D., Kuschik, P., Mbwette, T.S.A., Stange, F., Müller, R.A. and Köser, H. (2007) New aspects of microbial nitrogen transformations in the context of wastewater treatment – a review. *Eng. Life Sci.* 7(1), 13-25.
- Peng, Y. and Zhu, G. (2006) Biological nitrogen removal with nitrification and denitrification via nitrite pathway. *Appl. Microb. Biot.* 73(1), 15-26.

- Perez-Pantoja, D., Donoso, R., Agullo, L., Cordova, M., Seeger, M., Pieper, D.H. and Gonzalez, B. (2012) Genomic analysis of the potential for aromatic compounds biodegradation in Burkholderiales. *Environ. Microbiol.* 14(5), 1091-1117.
- Radajewski, S., Ineson, P., Parekh, N.R. and Murrell, J.C. (2000) Stable-isotope probing as a tool in microbial ecology. *Nature* 403(6770), 646-649.
- Radniecki, T.S., Dolan, M.E. and Semprini, L. (2008) Physiological and transcriptional responses of *Nitrosomonas europaea* to toluene and benzene inhibition. *Environ. Sci. Technol.* 42(11), 4093-4098.
- Rakoczy, J., Feisthauer, S., Wasmund, K., Bombach, P., Neu, T.R., Vogt, C. and Richnow, H.H. (2013) Benzene and sulfide removal from groundwater treated in a microbial fuel cell. *Biotechnol. Bioeng.* 110(12), 3104-3113.
- Rakoczy, J., Remy, B., Vogt, C. and Richnow, H.H. (2011) A bench-scale constructed wetland as a model to characterize benzene biodegradation processes in freshwater wetlands. *Environ. Sci. Technol.* 45(23), 10036-10044.
- Reinhardt, M., Müller, B., Gächter, R. and Wehrli, B. (2006) Nitrogen removal in a small constructed wetland: an isotope mass balance approach. *Environ. Sci. Technol.* 40, 3313-3319.
- Risgaard-Petersen, N., Meyer, R.L., Schmid, M.C., Jetten, M.S., Enrich-Prast, A., Rysgaard, S. and Revsbech, N.P. (2004) Anaerobic ammonium oxidation in an estuarine sediment. *Aquat. Microb. Ecol.* 36(3), 293-304.
- Robinson, R.S., Kienast, M., Luiza Albuquerque, A., Altabet, M.A., Contreras, S., De Pol Holz, R., Dubois, N., Francois, R., Galbraith, E., Hsu, T.C., Ivanochko, T., Jaccard, S., Kao, S.J., Kiefer, T., Kienast, S., Lehmann, M., Martinez, P., McCarthy, M., Möbius, J., Pedersen, T., Quan, T.M., Ryabenko, E., Schmittner, A., Schneider, R., Schneider-Mor, A., Shigemitsu, M., Sinclair, D., Somes, C., Studer, A., Thunell, R. and Yang, J.Y. (2012) A review of nitrogen isotopic alteration in marine sediments. *Paleoceanography* 27(4).
- Rosell, M., Finsterbusch, S., Jechalke, S., Hubschmann, T., Vogt, C. and Richnow, H.H. (2010) Evaluation of the effects of low oxygen concentration on stable isotope fractionation during aerobic MTBE biodegradation. *Environ. Sci. Technol.* 44(1), 309-315.
- Rozendal, R.A., Hamelers, H.V., Rabaey, K., Keller, J. and Buisman, C.J. (2008) Towards practical implementation of bioelectrochemical wastewater treatment. *Trends Biotechnol.* 26(8), 450-459.
- Saeed, T. and Sun, G. (2012) A review on nitrogen and organics removal mechanisms in subsurface flow constructed wetlands: dependency on environmental parameters, operating conditions and supporting media. *J. Environ. Manage.* 112, 429-448.

- Sakai, N., Kurisu, F., Yagi, O., Nakajima, F. and Yamamoto, K. (2009) Identification of putative benzene-degrading bacteria in methanogenic enrichment cultures. *J. Biosci. Bioeng.* 108(6), 501-507.
- Santoro, A.E., Buchwald, C., McIlvin, M.R. and Casciotti, K.L. (2011) Isotopic signature of N<sub>2</sub>O produced by marine ammonia-oxidizing archaea. *Sci.* 333, 1282-1285.
- Schirmer, M. and Niemes, H. (2010) Sustainable technologies and social costs for eliminating contamination of an aquifer. *Sustainability* 2(7), 2219-2231.
- Schröder, U., Harnisch, F. and Angenent, L.T. (2015) Microbial electrochemistry and technology: terminology and classification. *Energy Environ. Sci.* 8, 513-519.
- Seeger, E.M., Kusch, P., Fazekas, H., Grathwohl, P. and Kaestner, M. (2011) Bioremediation of benzene-, MTBE- and ammonia-contaminated groundwater with pilot-scale constructed wetlands. *Environ. Pollut.* 159(12), 3769-3776.
- Seeger, E.M., Maier, U., Grathwohl, P., Kusch, P. and Kaestner, M. (2013) Performance evaluation of different horizontal subsurface flow wetland types by characterization of flow behavior, mass removal and depth-dependent contaminant load. *Water Res.* 47(2), 769-780.
- Seifert, J., Taubert, M., Jehmlich, N., Schmidt, F., Volker, U., Vogt, C., Richnow, H.H. and von Bergen, M. (2012) Protein-based stable isotope probing (protein-SIP) in functional metaproteomics. *Mass Spectrom. Rev.* 31(6), 683-697.
- Song, G.D., Liu, S.M., Marchant, H., Kuypers, M.M.M. and Lavik, G. (2013a) Anammox, denitrification and dissimilatory nitrate reduction to ammonium in the East China Sea sediment. *Biogeosciences* 10(11), 6851-6864.
- Song, Y., Ishii, S., Rathnayake, L., Ito, T., Satoh, H. and Okabe, S. (2013b) Development and characterization of the partial nitrification aerobic granules in a sequencing batch airlift reactor. *Bioresour. Technol.* 139, 285-291.
- Sotres, A., Cerrillo, M., Viñas, M. and Bonmatí A. (2016) Nitrogen removal in a two-chambered microbial fuel cell: Establishment of a nitrifying–denitrifying microbial community on an intermittent aerated cathode. *Chemical Engineering Journal* 284, 905-916.
- Sovik, A.K. and Morkved, P.T. (2008) Use of stable nitrogen isotope fractionation to estimate denitrification in small constructed wetlands treating agricultural runoff. *Sci. Total. Environ.* 392(1), 157-165.
- Stahl, D.A. and de la Torre, J.R. (2012) Physiology and diversity of ammonia-oxidizing archaea. *Annu. Rev. Microbiol.* 66, 83-101.
- Starke, R., Keller, A., Jehmlich, N., Vogt, C., Richnow, H.H., Kleinstüber, S., von Bergen, M. and Seifert, J. (2016) Pulsed (13)C<sub>2</sub>-acetate protein-SIP unveils epsilonproteobacteria as dominant

- acetate utilizers in a sulfate-reducing microbial community mineralizing benzene. *Microb. Ecol.* 71(4), 901-911.
- Stein, L.Y. (2011) Heterotrophic nitrification and nitrifier denitrification. *Nitrification*, 95-114.
- Streit, W.R. and Schmitz, R.A. (2004) Metagenomics-the key to the uncultured microbes. *Curr. Opin. Microbiol.* 7(5), 492-498.
- Su, Q., Ma, C., Domingo-Felez, C., Kiil, A.S., Thamdrup, B., Jensen, M.M. and Smets, B.F. (2017) Low nitrous oxide production through nitrifier-denitrification in intermittent-feed high-rate nitrification reactors. *Water Res.* 123, 429-438.
- Taubert, M., Jehmlich, N., Vogt, C., Richnow, H.H., Schmidt, F., von Bergen, M. and Seifert, J. (2011) Time resolved protein-based stable isotope probing (Protein-SIP) analysis allows quantification of induced proteins in substrate shift experiments. *Proteomics* 11(11), 2265-2274.
- Taubert, M., Vogt, C., Wubet, T., Kleinstaub, S., Tarkka, M.T., Harms, H., Buscot, F., Richnow, H.H., von Bergen, M. and Seifert, J. (2012) Protein-SIP enables time-resolved analysis of the carbon flux in a sulfate-reducing, benzene-degrading microbial consortium. *ISME J.* 6(12), 2291-2301.
- Thamdrup, B. and Dalsgaard, T. (2002) Production of N<sub>2</sub> through anaerobic ammonium oxidation coupled to nitrate reduction in marine sediments. *Appl. Environ. Microb.* 68(3), 1312-1318.
- Truu, J., Nurk, K., Juhanson, J. and Mander, U. (2005) Variation of microbiological parameters within planted soil filter for domestic wastewater treatment. *J. Environ. Sci. Heal. A* 40(6-7), 1191-1200.
- Truu, M., Juhanson, J. and Truu, J. (2009) Microbial biomass, activity and community composition in constructed wetlands. *Sci. Total Environ.* 407(13), 3958-3971.
- Tu, Y.T., Chiang, P.C., Yang, J., Chen, S.H. and Kao, C.M. (2014) Application of a constructed wetland system for polluted stream remediation. *J. Hydrol.* 510, 70-78.
- Vaillancourt, F.H., Bolin, J.T. and Eltis, L.D. (2006) The ins and outs of ring-cleaving dioxygenases. *Crit. Rev. Biochem. Mol. Biol.* 41(4), 241-267.
- van Afferden, M., Rahman, K.Z., Mosig, P., De Biase, C., Thullner, M., Oswald, S.E. and Muller, R.A. (2011) Remediation of groundwater contaminated with MTBE and benzene: the potential of vertical-flow soil filter systems. *Water Res.* 45(16), 5063-5074.
- van der Waals, M.J., Atashgahi, S., da Rocha, U.N., van der Zaan, B.M., Smidt, H. and Gerritse, J. (2017) Benzene degradation in a denitrifying biofilm reactor: activity and microbial community composition. *Appl. Microb. Biot.* 101(12), 5175-5188.
- van der Zaan, B.M., Saia, F.T., Stams, A.J., Plugge, C.M., de Vos, W.M., Smidt, H., Langenhoff, A.A. and Gerritse, J. (2012) Anaerobic benzene degradation under denitrifying conditions:

- Peptococcaceae as dominant benzene degraders and evidence for a syntrophic process. *Environ. Microbiol.* 14(5), 1171-1181.
- van Kessel, M.A., Speth, D.R., Albertsen, M., Nielsen, P.H., Op den Camp, H.J., Kartal, B., Jetten, M.S. and Lucker, S. (2015) Complete nitrification by a single microorganism. *Nature* 528(7583), 555-559.
- Verhagen, F.J.M. and Laanbroek, H.J. (1991) Competition for ammonium between nitrifying and heterotrophic bacteria in dual energy-limited chemostats. *Appl. Environ. Microb.* 57(11), 3255-3263.
- Villasenor, J., Capilla, P., Rodrigo, M.A., Canizares, P. and Fernandez, F.J. (2013) Operation of a horizontal subsurface flow constructed wetland--microbial fuel cell treating wastewater under different organic loading rates. *Water Res.* 47(17), 6731-6738.
- Viridis, B., Rabaey, K., Rozendal, R.A., Yuan, Z. and Keller, J. (2010) Simultaneous nitrification, denitrification and carbon removal in microbial fuel cells. *Water Res.* 44(9), 2970-2980.
- Viridis, B., Rabaey, K., Yuan, Z. and Keller, J. (2008) Microbial fuel cells for simultaneous carbon and nitrogen removal. *Water Res.* 42(12), 3013-3024.
- Viridis, B., Read, S.T., Rabaey, K., Rozendal, R.A., Yuan, Z. and Keller, J. (2011) Biofilm stratification during simultaneous nitrification and denitrification (SND) at a biocathode. *Bioresour. Technol.* 102(1), 334-341.
- Vogt, C., Kleinstuber, S. and Richnow, H.H. (2011) Anaerobic benzene degradation by bacteria. *Microb. Biotechnol.* 4(6), 710-724.
- Vogt, C., Lueders, T., Richnow, H.H., Kruger, M., von Bergen, M. and Seifert, J. (2016) Stable Isotope Probing Approaches to Study Anaerobic Hydrocarbon Degradation and Degradation. *J. Mol. Microbiol. Biotechnol.* 26(1-3), 195-210.
- von Bergen, M., Jehmlich, N., Taubert, M., Vogt, C., Bastida, F., Herbst, F.A., Schmidt, F., Richnow, H.H. and Seifert, J. (2013) Insights from quantitative metaproteomics and protein-stable isotope probing into microbial ecology. *ISME J.* 7(10), 1877-1885.
- Voyevoda, M., Geyer, W., Mosig, P., Seeger, E.M. and Mothes, S. (2012) Evaluation of the effectiveness of different methods for the remediation of contaminated groundwater by determining the petroleum hydrocarbon content. *CLEAN - Soil, Air, Water* 40(8), 817-822.
- Vymazal, J. (2007) Removal of nutrients in various types of constructed wetlands. *Sci. Total Environ.* 380(1-3), 48-65.
- Vymazal, J. (2013) The use of hybrid constructed wetlands for wastewater treatment with special attention to nitrogen removal: a review of a recent development. *Water Res.* 47(14), 4795-4811.

- Vymazal, J. (2014) Constructed wetlands for treatment of industrial wastewaters: A review. *Ecol. Eng.* 73, 724-751.
- Wang, H. and Ren, Z.J. (2013) A comprehensive review of microbial electrochemical systems as a platform technology. *Biotechnol Adv.* 31(8), 1796-1807.
- Wang, H.B., Zhang, Z.X., Li, H., He, H.B., Fang, C.X., Zhang, A.J., Li, Q.S., Chen, R.S., Guo, X.K., Lin, H.F., Wu, L.K., Lin, S., Chen, T., Lin, R.Y., Peng, X.X. and Lin, W.X. (2011) Characterization of metaproteomics in crop rhizospheric soil. *J. Proteome Res.* 10(3), 932-940.
- Wang, X., Cai, Z., Zhou, Q., Zhang, Z. and Chen, C. (2012) Bioelectrochemical stimulation of petroleum hydrocarbon degradation in saline soil using U-tube microbial fuel cells. *Biotechnol. Bioeng.* 109(2), 426-433.
- Wang, Y., Zhao, Y., Xu, L., Wang, W., Doherty, L., Tang, C., Ren, B. and Zhao, J. (2017) Constructed wetland integrated microbial fuel cell system: looking back, moving forward. *Water Sci. Technol.* 76(2), 471-477.
- Weelink, S.A., Tan, N.C., Ten Broeke, H., van Doesburg, W., Langenhoff, A.A., Gerritse, J. and Stams, A.J. (2007) Physiological and phylogenetic characterization of a stable benzene-degrading, chlorate-reducing microbial community. *FEMS Microbiol Ecol.* 60(2), 312-321.
- Wei, M., Harnisch, F., Vogt, C. and Richnow, H.H. (2015a) Harvesting electricity from benzene and ammonium-contaminated groundwater using a microbial fuel cell with an aerated cathode. *RSC Adv.* 5, 5321-5330.
- Wei, M., Rakoczy, J., Vogt, C., Harnisch, F., Schumann, R. and Richnow, H.H. (2015b) Enhancement and monitoring of pollutant removal in a constructed wetland by microbial electrochemical technology. *Bioresour. Technol.* 196, 490-499.
- Weiner, J.M. and Lovley, D.R. (1998) Rapid benzene degradation in methanogenic sediments from a petroleum-contaminated aquifer. *Appl. Environ. Microb.* 64(5), 1937-1939.
- Wen, X., Gong, B., Zhou, J., He, Q. and Qing, X. (2017) Efficient simultaneous partial nitrification, anammox and denitrification (SNAD) system equipped with a real-time dissolved oxygen (DO) intelligent control system and microbial community shifts of different substrate concentrations. *Water Res.* 119, 201-211.
- World Health Organization (2003a) Ammonia in drinking-water, WHO, Geneva.
- World Health Organization (2003b) Nitrate and nitrite in drinking-water.
- Wrage, N., Velthof, G.L., Van Beusichem, M.L. and Oenema, O. (2001) Role of nitrifier denitrification in the production of nitrous oxide. *Soil Biol. Biochem.* 33(12), 1723-1732.
- Wrighton, K.C. and Coates, J.D. (2009) Microbial fuel cells: plug-in and power-on microbiology. *Microbe.* 4(6), 281-287.

- Wu, C.H., Lai, C.Y., Lin, C.W. and Kao, M.H. (2013) Generation of power by microbial fuel cell with ferricyanide in biodegradation of benzene. *CLEAN - Soil Air Water* 41(4), 390-395.
- Wu, D., Yang, L., Gan, L., Chen, Q., Li, L., Chen, X., Wang, X., Guo, L. and Miao, A. (2015a) Potential of novel wastewater treatment system featuring microbial fuel cell to generate electricity and remove pollutants. *Ecol. Eng.* 84, 624-631.
- Wu, S., Kuschik, P., Brix, H., Vymazal, J. and Dong, R. (2014) Development of constructed wetlands in performance intensifications for wastewater treatment: a nitrogen and organic matter targeted review. *Water Res.* 57, 40-55.
- Wu, S., Wallace, S., Brix, H., Kuschik, P., Kirui, W.K., Masi, F. and Dong, R. (2015b) Treatment of industrial effluents in constructed wetlands: Challenges, operational strategies and overall performance. *Environ. Pollut.* 201, 107-120.
- Xie, S., Liang, P., Chen, Y., Xia, X. and Huang, X. (2011) Simultaneous carbon and nitrogen removal using an oxic/anoxic-biocathode microbial fuel cells coupled system. *Bioresour. Technol.* 102(1), 348-354.
- Yadav, A.K., Dash, P., Mohanty, A., Abbassi, R. and Mishra, B.K. (2012) Performance assessment of innovative constructed wetland-microbial fuel cell for electricity production and dye removal. *Ecol. Eng.* 47, 126-131.
- Yan, H. and Regan, J.M. (2013) Enhanced nitrogen removal in single-chamber microbial fuel cells with increased gas diffusion areas. *Biotechnol. Bioeng.* 110(3), 785-791.
- Yan, H., Saito, T. and Regan, J.M. (2012) Nitrogen removal in a single-chamber microbial fuel cell with nitrifying biofilm enriched at the air cathode. *Water Res.* 46(7), 2215-2224.
- Yao, S., Ni, J., Ma, T. and Li, C. (2013) Heterotrophic nitrification and aerobic denitrification at low temperature by a newly isolated bacterium, *Acinetobacter* sp. HA2. *Bioresour. Technol.* 139, 80-86.
- Yerushalmi, L., Lascourreges, J.F. and Guiot, S.R. (2002) Kinetics of benzene biotransformation under microaerophilic and oxygen-limited conditions. *Biotechnol. Bioeng.* 79(3), 347-355.
- Yerushalmi, L., Lascourreges, J.F., Rhofir, C. and Guiot, S.R. (2001) Detection of intermediate metabolites of benzene biodegradation under microaerophilic conditions. *Biodegradation* 12(6), 379-391.
- You, S.J., Ren, N.Q., Zhao, Q.L., Kiely, P.D., Wang, J.Y., Yang, F.L., Fu, L. and Peng, L. (2009) Improving phosphate buffer-free cathode performance of microbial fuel cell based on biological nitrification. *Biosens. Bioelectron.* 24(12), 3698-3701.
- Yu, C.P., Liang, Z., Das, A. and Hu, Z. (2011) Nitrogen removal from wastewater using membrane aerated microbial fuel cell techniques. *Water Res.* 45(3), 1157-1164.

- Zaki, S. (2006) Detection of meta- and ortho-cleavage dioxygenases in bacterial phenol-degraders. *J. Appl. Sci. Environ. Mgt.* September 10(3), 75-81.
- Zhang, D.Q., Jinadasa, K.B., Gersberg, R.M., Liu, Y., Ng, W.J. and Tan, S.K. (2014) Application of constructed wetlands for wastewater treatment in developing countries--a review of recent developments (2000-2013). *J. Environ. Manage.* 141, 116-131.
- Zhang, F., Ge, Z., Grimaud, J., Hurst, J. and He, Z. (2013a) Long-term performance of liter-scale microbial fuel cells treating primary effluent installed in a municipal wastewater treatment facility. *Environ. Sci. Technol.* 47(9), 4941-4948.
- Zhang, F. and He, Z. (2012a) Integrated organic and nitrogen removal with electricity generation in a tubular dual-cathode microbial fuel cell. *Process Biochem.* 47(12), 2146-2151.
- Zhang, F. and He, Z. (2012b) Simultaneous nitrification and denitrification with electricity generation in dual-cathode microbial fuel cells. *J. Chem. Tech. Biotech.* 87(1), 153-159.
- Zhang, J., Müller, C. and Cai, Z. (2015) Heterotrophic nitrification of organic N and its contribution to nitrous oxide emissions in soils. *Soil Biol. Biochem.* 84, 199-209.
- Zhang, L., Altabet, M.A.W., T. and Hadas, O. (2007) Sensitive measurement of  $\text{NH}_4^+ \text{}^{15}\text{N}/\text{}^{14}\text{N}$  ( $\delta^{15}\text{NH}_4^+$ ) at natural abundance levels in fresh and saltwaters. *Anal. chem.* 79(14), 5297-5303.
- Zhang, L., Xia, X., Zhao, Y., Xi, B., Yan, Y., Guo, X., Xiong, Y. and Zhan, J. (2011) The ammonium nitrogen oxidation process in horizontal subsurface flow constructed wetlands. *Ecol. Eng.* 37(11), 1614-1619.
- Zhang, T., Gannon, S.M., Nevin, K.P., Franks, A.E. and Lovley, D.R. (2010) Stimulating the anaerobic degradation of aromatic hydrocarbons in contaminated sediments by providing an electrode as the electron acceptor. *Environ. Microbiol.* 12(4), 1011-1120.
- Zhang, T., Tremblay, P.L., Chaurasia, A.K., Smith, J.A., Bain, T.S. and Lovley, D.R. (2013b) Anaerobic Benzene Oxidation via Phenol in *Geobacter metallireducens*. *Appl. Environ. Microb.* 79(24), 7800-7806.
- Zhang, Y. and Angelidaki, I. (2016) Microbial electrochemical systems and technologies: it is time to report the capital costs. *Environ. Sci. Technol.* 50(11), 5432-5433.
- Zhao, Y., Collum, S., Phelan, M., Goodbody, T., Doherty, L. and Hu, Y. (2013) Preliminary investigation of constructed wetland incorporating microbial fuel cell: Batch and continuous flow trials. *Chem. Eng. J.* 229, 364-370.
- Zhu, G., Wang, S., Feng, X., Fan, G., Jetten, M.S. and Yin, C. (2011) Anammox bacterial abundance, biodiversity and activity in a constructed wetland. *Environ. Sci. Technol.* 45(23), 9951-9958.

- Zhu, X., Burger M, Doane T A and Horwath, W.R. (2013) Ammonia oxidation pathways and nitrifier denitrification are significant sources of N<sub>2</sub>O and NO under low oxygen availability. *Proceedings of the National Academy of Sciences of the United States of America* 110(16), 6328-6333.
- Zhuang, L., Zheng, Y., Zhou, S., Yuan, Y., Yuan, H. and Chen, Y. (2012) Scalable microbial fuel cell (MFC) stack for continuous real wastewater treatment. *Bioresour. Technol.* 106, 82-88.

## ACKNOWLEDGEMENTS

First of all, I would like to extend my sincere gratitude to Dr. Hans Hermann Richnow for giving me the opportunity to work on “Compartment Transfer-CoTra” project in department of isotope biogeochemistry, Helmholtz-Centre for Environmental Research in Leipzig. I also would like to thank Jun.-Prof. Dr. Jana Seifert for the good cooperation and for giving me the chance to submit and defend my thesis at Faculty of Natural Sciences, Hohenheim University.

My deepest gratitude goes to my supervisor, Dr. Carsten Vogt, for his instructive advice and valuable guidance on my PhD work. He has spent much time helping me to finish the experiment and writing work. Without his patient instruction, insightful encouragement and expert guidance, the completion of this thesis would be not possible.

Special thanks are given to Nico Jehmlich and Vanessa Lünsmann, who helped me to finish the work on protein identification and analysis. Thanks to Jörg Ahlheim for his help to transfer contaminated groundwater from the Leuna sites.

Further, I want to express my gratitude to all the people from the Department of isotope biogeochemistry, especially to Stephanie Hinke, Steffen Kümmel, Petra Bombach, Andreas Hardy Keller, Xi Wei for their encouragement and inspiring suggestions.

Last but not the least, my gratitude also extends to my family, who have been assisting, supporting and caring for me, even though I was living so far away and did not spend enough time with them. Thanks to my friends at the UFZ who shared the coffee breaks and lunch breaks with me and supported me with their understanding and encouragements.

## LIST OF PUBLICATIONS

**Manman Wei**, Jana Rakoczy, Carsten Vogt, Falk Harnisch, Rainer Schumann, Hans H. Richnow. Enhancement and monitoring of pollutant removal in a constructed wetland by microbial electrochemical technology. *Bioresource Technology*, 2015, 196: 490-499.

**Manman Wei**, Falk Harnisch, Carsten Vogt, Jörg Ahlheim, Thomas R. Neu and Hans H. Richnow. Harvesting electricity from benzene and ammonium-contaminated groundwater using a microbial fuel cell with an aerated cathode. *RSC Advances*, 2015, 5: 5321-5330.

**Manman Wei**, Carsten Vogt, Vanessa Lünsmann, Naomi Susan Wells, Jana Seifert, Nico Jehmlich, Kay Knöller, Hans H. Richnow. Isotopic and proteomic evidence for microbial nitrogen transformation process in a microbial electrochemical technology-constructed wetland (MET-CW) treating contaminated groundwater. In preparation

**Manman Wei**, Furong Tan, Hong Zhu, Kai Cheng, Xiao Wu, Jinbin Wang, Kai Zhao, Xueming Tang. Impact of Bt-transgenic rice (SHK601) on soil ecosystems in the rhizosphere during crop development. *Plant, Soil and Environment*, 2012, 58 (5): 217-223.

**Manman Wei**, Rubing Zhang, Yuguang Wang, Houguo Ji, Jia Zheng, Xinhua Chen, Hongbo Zhou. Microbial community structure and diversity in deep-sea hydrothermal vent sediments along the Eastern Lau Spreading Centre. *Acta Oceanologica Sinica*, 2013, 32 (4): 42-51.



Annex 2 to the University of Hohenheim doctoral degree regulations for Dr. rer. nat.

**Affidavit according to Sec. 7(7) of the University of Hohenheim doctoral degree regulations for Dr. rer. nat.**

1. For the dissertation submitted on the topic

Treatment of benzene and ammonium contaminated groundwater using microbial electrochemical technology and constructed wetlands

I hereby declare that I independently completed the work.

2. I only used the sources and aids documented and only made use of permissible assistance by third parties. In particular, I properly documented any contents which I used - either by directly quoting or paraphrasing - from other works.
3. I did not accept any assistance from a commercial doctoral agency or consulting firm.
4. I am aware of the meaning of this affidavit and the criminal penalties of an incorrect or incomplete affidavit.

I hereby confirm the correctness of the above declaration: I hereby affirm in lieu of oath that I have, to the best of my knowledge, declared nothing but the truth and have not omitted any information.

---

Place and Date

---

Signature